AN EVALUATION OF THE IMPACTS OF AGING ON SKELETAL MUSCLE PERFORMANCE IN SEVERAL MAMMALIAN DIVERS

A Dissertation

by

ALLYSON GAYLE HINDLE

Submitted to the Office of Graduate Studies of
Texas A&M University
in partial fulfillment of the requirements for the degree of

DOCTOR OF PHILOSOPHY

December 2007

Major Subject: Wildlife and Fisheries Sciences

AN EVALUATION OF THE IMPACTS OF AGING ON SKELETAL MUSCLE PERFORMANCE IN SEVERAL MAMMALIAN DIVERS

A Dissertation

by

ALLYSON GAYLE HINDLE

Submitted to the Office of Graduate Studies of
Texas A&M University
in partial fulfillment of the requirements for the degree of

DOCTOR OF PHILOSOPHY

Approved by:

Co-Chairs of Committee,	M. Horning
	R.W. Davis
Committee Members,	W.H. Neill
	D.S. MacKenzie
	J.M. Lawler
Head of Department,	T.E. Lacher

December 2007

Major Subject: Wildlife and Fisheries Sciences

ABSTRACT

An Evaluation of the Impacts of Aging on Skeletal Muscle Performance in Several Mammalian Divers. (December 2007)

Allyson Gayle Hindle, B.S., University of Manitoba;

M.S. University of Manitoba

Co-Chairs of Advisory Committee: Dr. M. Horning
Dr. R. Davis

Based on the 'free radical theory of aging,' I hypothesized that hypoxia caused by the mammalian dive response induces free radical production which could modulate or accelerate cellular aging. On the other hand, to prevent free radical "stress" (pro-/antioxidant imbalance), divers could display elevated protective mechanisms. Additionally, the unusual connection between diving physiology and foraging ecology implies that aging physiology is significant to our understanding of ecology for divers. This study examines three aspects of aging in representative diving mammals.

First, gracilis muscle morphology was analyzed for old/young shrews (water shrew, *Sorex palustris* (diver); short-tailed shrew, *Blarina brevicauda* (non-diver)). Extracellular space was elevated in old animals (10% diver, ~70% non-diver; P=0.021), which corresponded to a larger extracellular collagen component of old muscle (~60%; P=0.008). Muscle was dominated by Type I collagen, and the ratio of collagen Type I: III more than doubled with age (P=0.001).

Second, oxidative stress markers, protective antioxidant enzymes and apoptosis were examined in muscle of the two shrew species. The activities of antioxidant

enzymes catalase and glutathione peroxidase were statistically identical at each age in both species. The Cu,Zn superoxide dismutase isoform was, however, elevated in older animals (115% diver, 83% non-diver, P=0.054). Only one indicator of oxidative stress (lipid peroxidation) increased with age (P=0.009), whereas the other markers declined (4-hydroxynonenal content, P=0.008, dihydroethidium oxidation, P=0.025). Apoptosis occurred in <1% of myocytes, and did not change with age. On balance, diving water shrews did not have adaptations to combat oxidative stress, yet they do not display excessive oxidative tissue damage. Apoptosis was similar between species.

The third study component was the development of a predictive simulation model for the energetics of old/young foraging Weddell seals, *Leptonychotes weddellii*. With advancing age, the model predicts declining net energy gain associated with a decrease in muscle contractile efficiency. The effects of age are exacerbated when good prey patches are scarce. In such cases, declines in old seal energy gain caused by increased buoyancy and decreased aerobic dive limit become apparent. The model also addresses the idea that behavioral plasticity may allow older animals to compensate for age-related performance constraints.

NOMENCLATURE

4-HNE	4-hydroxynonenal
A_{dive}	Respiratory costs of diving
ADL	Aerobic dive limit
A_{fecal}	(A_f) fecal production cost; energy not assimilated
$A_{myocyte}$	Average myocyte cross-sectional area
$A_{respiratory}$	(A_r) total respiratory cost
$A_{surface}$	Respiratory costs at the surface
A_{total}	Total area of section
$A_{urinary}$	(A_u) cost of urinary production; energy not assimilated
A_{waste}	(A_w) total cost of waste production
BMR	Basal metabolic rate
BSA	Bovine serum albumin
cADL	Calculated aerobic dive limit
CAT	Catalase
CS	Citrate synthase
DD	Dive duration
DHE	Dihydroethidium
D:S	Dive: surface duration ratio
ECM	Extracellular matrix
ECS	Extracellular space
EDL	Extensor digitorum longus

$E_{expended}$	Simulated daily energy expenditure
E_{gained}	Simulated daily energy intake
FOX	Ferrous oxide xylenol orange assay
GPx	Glutathione peroxidase
GSH	Reduced glutathione
HIF	Heat increment of feeding
IGF-1	Insulin-like growth factor 1
K_m	Substrate concentration at ½ Vmax
LDH	Lactate dehydrogenase
MHC	Myosin heavy chain
MMP	Matrix metalloprotease
MR	Metabolic rate
$NO^{\cdot}$	Nitric oxide
$O_2^{\cdot -}$	Superoxide radical
$ONOO^-$	Peroxynitrite
P	Environmental prey density
PBS	Phosphate buffered saline
PDST	Post-dive surface time
$\rho_{myocyte}$	Myocyte density in area
$P_{threshold}$	Prey threshold for bout diving
ROS	Reactive oxygen species
RNS	Reactive nitrogen species

SOD	Superoxide dismutase
STS	Short-tailed shrew
TBS	Tris buffered saline
TUNEL	Terminal transferase dUTP nick-end labeling
V_{max}	Maximum velocity of an enzyme-catalyzed reaction
VO_2	Volume of oxygen consumed
VO_{2max}	Maximum volume of oxygen which can be consumed
WS	Water shrew

TABLE OF CONTENTS

Page

Page

Page

LIST OF TABLES

LIST OF FIGURES

FIGURE Page

FIGURE Page

FIGURE Page

1. INTRODUCTION

Literature Review

Skeletal Muscle Aging

In the wider scope of aging research, one can argue that skeletal muscle health and function has significance on par with life-saving disciplines such as cardiology and internal medicine. In the human forum, muscle functionality is key to preventing injury, maintaining mobility and independence, and therefore has tremendous potential to improve quality of life. In wild animals, it is even easier to see how maintaining muscle performance can be the difference between life and death. Foraging ability and elusion of predators relies on both the power and the endurance output of skeletal muscle.

Classic signs of aging in humans and laboratory animals include a loss of muscle endurance, which can occur through decreased oxygen transport across a thickening capillary basement membrane (Tomonaga 1977), and declines in certain enzyme activities with age (Klitgaard et al. 1989*a*). Aging is also accompanied by a loss of force generating capacity (Tomonaga 1977), as well as a reduction in contraction and recovery speeds (Klitgaard et al. 1989*b*). This decline of muscle mass, strength and quality with advancing age is termed 'sarcopenia'. In humans, sarcopenia is observed even among physically healthy adults. While the mechanisms for this occurrence have not entirely been elucidated, it may be caused by apoptosis (Dirks and Leeuwenburgh 2002; Pollack et al. 2002), mitochondrial DNA mutations (Herbst et al. 2007), or can be hormone driven, corresponding to declines in anabolic hormone levels (growth hormone and sex

---

This thesis follows the style of *Journal of Experimental Biology*.

steroid hormones for examples; Marcell 2003). Denervation is also a major cause of skeletal muscle loss. Removal of a-motor neuron input can trigger the loss of the entire motor unit. Reinnervation via axonal sprouting from adjacent motor neurons can preserve some fibers by incorporating them into a new motor unit, however this generally compensates incompletely for fiber loss. Older muscle has a disproportional denervation and loss of Type II muscle fibers (Brooks and Faulkner 1994), which can then be reinnervated and taken up into Type I motor units. This causes an overall "slowing" of skeletal muscle with aging (Brooks and Faulkner 1994), which can result in weakness and loss of fine movement.

Reduced cross-sectional area will reduce muscle force-generating capacity. In addition to the loss of performance resulting from declines in muscle mass and area with age, a loss of specific force (force per unit cross-sectional area), has also been documented (Brooks and Faulkner 1994; Thompson 1999). This suggests that impairment of excitation-contraction coupling is of concern in aging skeletal muscle. In intact fibers collected from the muscles of laboratory rodents, a change in the ratio of dihydropyridine to ryanodine receptors has been advanced as a cause for excitation-contraction 'uncoupling' in aging muscle (Payne and Delbono 2004). No change in the number of dihydropyridine receptors was seen, however, a drastic reduction in ryanodine receptors occurs. This reduction would impair signal transduction from the surface depolarization to the release of Ca^{2+} from the sarcoplasmic reticulum. This issue does not seem a universal one, however, since intact preparations of human skeletal muscle fibers do not display such shifts in receptor density with age (Ryan and Ohlendieck

2004). Despite the difference between the composition and behavior of intact human and animal muscle fibers, individual preparations of permeabilized fibers behave similarly across species (Larsson et al. 1997; Krivickas et al 2001; Lowe et al. 2001; 2004). These cases show that the intrinsic reduction in force generation of aging muscle is caused in part by alterations in the conformation of the myosin head. In preparations of old muscle fibers, less myosin heads were found in the 'strong' actin-binding site during contraction. Additionally, the V_{max} and K_m of the enzyme actomyosin ATPase are reduced in older muscle fibers (Prochniewitz et al. 2005). The V_{max} decline is caused primarily by the conformational changes in myosin noted above. Age-related alterations in both actin and myosin (and their interaction) appear to cause K_m decline.

Reactive Oxygen Species in Mammalian Skeletal Muscle

The 'free radical theory of aging' (Harman 1994) posits that maximum longevity and aging are driven by free radicals, such as reactive oxygen species. Reactive oxygen species (ROS) are defined as compounds containing an unpaired outer valence electron, and are produced via sequential steps of oxygen reduction. In skeletal muscle, the mitochondrial electron transport chain accounts for virtually all (ca. 96%) direct ROS production, chiefly in the form of superoxide anion ($O_2\cdot^-$) (Boveris and Cadenas 2000). Both enzymatic and non-enzymatic systems then convert the superoxide product into other ROS (*e.g.*, H_2O_2, $H_2O\cdot$, $^1O_2$, $OH\cdot$). Examples of such systems in skeletal muscle are superoxide dismutases (SOD, mitochondrial) glutathione reduction systems (GSH, cytosolic) and catalase (in peroxisomes) (Boveris and Cadenas 2000). It is a shift in the

balance between these pro-oxidative mechanisms and their scavenger counterparts that creates oxidative stress, which can be defined as the pro-/antioxidant imbalance itself, or the potential or actual cellular damage caused by such a shift. More recently, Harman's 'free radical' theory has evolved into the 'oxidative stress theory of aging' (Sohal and Weindruch 1996). It states that *"A chronic state of oxidative stress exists in cells of aerobic organisms even under normal physiological conditions because of an imbalance of proxidants and antioxidants. This imbalance results in a steady-state accumulation of oxidative damage in a variety of macromolecules. Oxidative damage increases during aging, which results in a progressive loss in the functional efficiency of various cellular processes"*. Oxidative stress can result from a decrease in antioxidant capacity or an increase in ROS production individually, or in combination. Intracellular glutathione depletion typically precedes macromolecule oxidation (Robertson et al. 2001), and past this point, oxidative stress can be directly measured by concentration within, or outflow from the muscle bed of certain oxidized substances.

The pathophysiology of oxidative stress can be severe (Robertson et al. 2001). In general, it appears that moderate oxidative stress is important in signaling apoptotic events. Oxidants can indirectly induce apoptosis by altering the cell's internal environment to facilitate the release of cytochrome c from mitochondria – which can be a pre-apoptotic step in vertebrates (Pollack et al. 2002). On the other hand, severe oxidative stress is associated with cell necrosis. ROS produce cell damage by oxidizing macromolecules, such as proteins, lipids, and nucleic acids (Robertson et al. 2001). Thus, afflicted cells may suffer simultaneous damage to enzyme systems, phospholipid

membranes, and DNA. Mitochondrial DNA is particularly susceptible to oxidative damage, since mitochondria are an initial ROS production site. With respect to nuclear DNA, mitochondrial DNA is also less protected, due to the absence of histones and reduced DNA repair pathways (Bohr and Anson 1999).

The high metabolic rates of muscle, relative to other tissues, elevate ROS production in this location. Muscle contraction is associated with production of ROS (Reid et al. 1992) as well as nitric oxide (NO), which is significant in cellular nitrosative stress via peroxynitrate formation (Kobzik et al. 1994). However, skeletal muscle also appears to have high stress resistance (e.g., Renault et al. 2002). A component of this resistance is likely antioxidants, which are known to increase muscle force production during fatigue (Mohanraj et al. 1997) and to have increased activities as a result of muscle conditioning (see Clanton et al. 1999 for review). ROS production increases with age (Bejma and Ji 1999), due to a presumed reduction in antioxidant defensive capacity or presumed increase in oxidant production via the respiratory chain. Because mitochondria are the main source of ROS production during aerobic metabolism, they also become the primary target of ROS damage. Such damage can lead to an increase in free radical outflow from mitochondria, which generates a positive feedback cycle of oxidative stress that can lead to apoptosis (Barja and Herrero 2000; Sastre et al. 2000). Damaged mitochondria may also suffer from decreased respiratory capacity with age, which results in whole-body declines in maximum aerobic capacity seen with age (Lee and Wei 2001). In fact, cellular oxidative damage has been clearly demonstrated to

increase in aged human muscle (Mecocci et al. 1999). Accumulation of ROS is also a likely trigger for sarcopenia (see Fulle et al. 2004 for review).

The link between ROS and skeletal muscle aging has been widely discussed, and its specifics remain poorly understood (see reviews by Fulle et al. 2004; Zhong et al. 2007). Free radical stress is important in modulating several sites of excitation-contraction coupling. In aging, this modification may have negative effects, compromising both excitation/contraction coupling rates, and specific force generation. For example, ROS-induced modification of cysteine and tyrosine residues in the protein Ca-ATPase appears to impair its function (Viner et al. 1999; Sharov et al. 2006). Since Ca-ATPase is responsible for the re-uptake of Ca^{2+} into the sarcoplasmic reticulum, it controls muscle relaxation. On the other hand, anti-apoptotic factor IGF-1 (insulin-like growth factor) prevents an age-related decline in specific force in vitro (González et al. 2003).

Aging in Wild Populations

Aging theories can be applied to populations to determine the likelihood of the observable senescence in that population. Several currently recognized evolutionary theories for aging (see Kirkwood and Austad 2000; Troen 2003 for review) suggest that the root of senescence is a reduction in the force of natural selection with advancing age, either through reproductive selection (animals have a reduced reproductive contribution to the next generation as they age) or survival selection (selection is reduced with probability of survival to a given age). In very few cases do these theories predict age-

related senescence to occur in wild populations, since mortality typically occurs first (*e.g.*, Kirkwood and Austad 2000; Parsons 2002).

However, in wild populations it is more appropriate to predict maximal longevity to be associated with low-stress environments (Parsons 2002). From the perspective that oxidants are important in signaling apoptotic events, this would correspond to environments with minimal oxidant exposure. Low oxidant exposure is regulated internally in birds (Herrero and Barja 1997; 1998) and bats (Brunet-Rossini and Austad 2004), resulting in maximum longevities for these species which far exceed those of similarly sized mammals, despite their high mass-specific metabolic rates. In all cases examined, this is the result of low mitochondrial H_2O_2 release into the cytosol stemming from reduced ROS generation at respiratory chain complexes I and III (Herrero and Barja 1998). For example, this occurs in parakeets (Herrero and Barja 1998) simply through reduced mass-specific mitochondrial oxygen consumption. Other birds such as the canary, however, rely more heavily on mitochondria that are less "leaky" to free radicals, or H_2O_2 to achieve the same end (Herrero and Barja 1998). Pigeons, as a third example, employ both strategies to reduce H_2O_2 outflow from mitochondria (Herrero and Barja 1997).

In considering level of oxidant exposure, one can argue that diving mammals exist in high stress environments, as their behavior subjects them to periodically high levels of oxidative stress. Because foraging and other activities take place during periods of underwater breath-holding, the organs and tissues are exposed to changing levels of oxygen availability. Weddell seals, at least, do not display the typical clearance

(smooth multiexponential washout kinetics) of metabolites during voluntary diving that is characteristic of exercising terrestrial animals, and the authors suggest this to be related to perfusion adjustments during diving and after surfacing (Guppy et al. 1986). This supports the suggestion that flux through the respiratory chain may also be more highly variable than for the daily exercise range of a terrestrial animal, since divers operate under conditions of low aerobic metabolic rates (under hypoxia) as well as the occasional absence of aerobic metabolism altogether (anaerobiosis), followed by normoxia at the water surface. Hypoxia itself, as well as metabolic shifts such as reperfusion of hypoxic regions, may spur the production of harmful oxygen radicals, possibly overwhelming antioxidant defenses (e.g., Gottlieb 2003; Hermes-Lima and Zenteno-Savín 2002; Elsner et al. 1998; see text below for mechanisms). Therefore, for diving mammals we might expect an earlier display of senescence. Since the life spans of such animals are not shorter than predicted by allometry, observable senescence may occur in older animals (rather than death occurring first). However, given that diving mammals should be well-adapted to their environments, and that aerobic diving is assumed to not compromise physiological homeostasis, some provision should be made to deal with any ROS exposure associated with diving. This could occur as a reduction in ROS release, as seen in birds. It could also occur through elevated antioxidant levels. If stress resistance genes, specifically with respect to energy production, are important in longevity, diving mammals represent a new model system that will offer unique insights into mammalian aging.

Reactive Oxygen Species and Senescence in Diving Mammals

The goal of the typical mammalian dive response is to conserve oxygen. A "classic" dive response is accomplished via apnea, bradycardia, and peripheral vasoconstriction to non-essential vascular beds (see Butler and Jones 1997 for review). While an intense dive response is observed occasionally in nature, in association with anaerobic diving, it also occurs in lesser form even during voluntary, aerobic dives. In the latter case, the dive response appears to control local hypoxia in tissues, resulting in a maximal aerobic dive limit (Davis and Kanatous 1999; Davis et al. 2004). The dive response likely has consequences for the production of ROS through either tissue hypoxia or, ischemia with its subsequent reperfusion. Although aerobic metabolism is generally maintained in primary locomotory muscles, severe local hypoxia may develop during the dive or by dive termination. However, non-essential skeletal muscle (i.e., non-swimming) and skin and certain visceral tissue (Davis et al. 1983), on the other hand, may be subject to greater vasoconstriction (i.e., ischemia) during routine diving. This occurrence has been demonstrated directly in a small diver (Tufted duck, *Aythya fuligula*; Bevan and Butler 1992), and to date can also be hypothesized (to a much lesser degree) in larger, less active divers (Butler and Jones 1997). Despite the likelihood that lifelong diving preconditions tissues to hypoxia, and that prior exposure to ischemic stress, at least, often attenuates the effects of future exposure, this does suggest that divers are exposed to a chronic ROS onslaught much greater than in non-divers.

Even without age-related impairments, skeletal muscle in mammalian divers may be subjected to ROS-mediated damage in two ways: local hypoxia and post-dive

reperfusion. Massive reperfusion injury occurs in tissues following complete ischemia (Flaherty and Weisfeldt 1988), and such mechanisms would impact diving animals surfacing into an oxygen-rich environment following an anaerobic dive. Mechanisms driving ROS production in reperfused tissue are many, but can include: 1) ischemic conversion of xanthine dehydrogenase to xanthine oxidase, which drives purine oxidation reactions producing $O_2\cdot^-$; 2) rapid rise in electron flux through the respiratory chain (intrinsic mitochondrial production); 3) accumulation of activated white blood cells (such as neutrophils) which generate ROS; 4) oxidation of accumulated catecholamines or prostaglandins via P450 monooxygenases. In mammalian divers, for which the majority of diving is within the ADL, significant (chronic) damage via this pathway is unlikely, since vasoconstriction during submergence does not near the point of complete ischemia. However, this is certainly possible within an animal's lifetime (e.g., with a fright-induced maximum dive response).

Hypoxia is likely to be a more chronic contributor of ROS to skeletal muscle in divers (see Clanton et al. 1999 for review). At present, hypoxia's influence in skeletal muscle is unknown; although in vitro studies of hypoxic hepatocytes (Dawson et al. 1993) and cardiomyocytes (3-4 Torr; Vanden Hoek et al. 1997*a*) indicate that hypoxia itself is sufficient to significantly increase the production of superoxide radicals. This occurrence is defended against in the hearts of diving turtles through elevated levels of heat shock protein 60 (Chang et al. 2000). A similar situation may be present in the skeletal muscle of mammalian divers, where end-dive muscle PO_2 (in seals) is known to decline to considerably less than 5 Torr, even when muscles remain at rest (Guyton et al.

1995). In the hypoxic chick cardiomyocyte model, the primary ROS-generating mechanism is mitochondrial production of $O_2^{\cdot -}$. These migrate via anion channels into the cytosol, where Cu,Zn-SOD converts them to H_2O_2 (Vanden Hoek et al. 1997*b*; 1998). The respiratory chain develops a highly reduced redox state under hypoxia (i.e., too many reducing equivalents drives the single-electron reduction of O_2). Therefore, the maintenance of aerobic metabolism under such conditions increases the relative rate of ROS production (Vanden Hoek et al. 1997*b*). The degree of ROS production during hypoxia is directly dependent on residual O_2 available in tissues (Becker et al. 1999; Berrizbeitia et al. 2002). Thus, O_2 access through myoglobin or exposure to neighboring cells has an exacerbating effect.

This model system becomes especially interesting when the possible benefits of ROS preconditioning are considered. Experimentally, low-level ROS exposure confers benefit for future higher-level exposure, by reducing the detectable damage to exposed cells (Vanden Hoek et al. 1998; Kukreja 2001). The diving mammal model, therefore, is that of a species subject to lifelong preconditioning, but also lifelong exposure, to severe ROS-generating conditions.

The only aging data for diving animals currently available exists for seals. Surprisingly, senescence has not been readily demonstrated in these animals (Crocker et al. 2001; Pistorius and Bester 2002). This may be linked to elevated natural antioxidant levels, which have been recorded in ringed seals, *Phoca hispida* (Zenteno-Savín et al. 2002). Such findings may simply be an artifact of the high oxidative capacity of pinniped muscles (due to high proportions of slow twitch/oxidative fibers; e.g., Watson

et al. 2003), resulting in above-average antioxidant but also oxidant potential (e.g., Pansarasa et al. 2002). This view also does not consider how this uniquely adapted system might respond to aging pressures. Aging theories suggest little or no selection for adaptation to aging (i.e., different phenotypes between old and young groups) as this would likely be at the cost of the individual's inclusive fitness (Troen 2003). Nonetheless, the ability of these animals to avoid senescence when several lines of reasoning suggest them to be excellent candidates for the display of early senescence is remarkable. This observation gives rise to two questions: 1) what specific physiological and morphological changes occur in skeletal muscle with advancing age in divers? And 2) what specific protective mechanisms exist in these animals to combat such changes? By addressing these questions, we will increase our knowledge of mammalian aging and provide insight into unique challenges faced by aging populations in nature. Additionally, the question can be asked how these small scale (proximal) changes can be expected to play out at the whole animal level.

Study Objectives

This study was intended to quantify certain effects of aging on the exercise physiology of diving mammals. Specifically, muscle samples from the smallest species of diving mammal were examined for indicators of apoptosis, as well as oxidant and antioxidant potential. The impacts of aging on skeletal muscle were addressed by comparison of biochemistry and myocyte anatomy between a diving and terrestrial species within the family Soricidae. Additionally, a simulated energy budget model was

developed to allow the refinement of future field studies for a broad range of divers by highlighting components of exercise physiology which are most likely to impact foraging ecology and their possible changes with age. The model was also intended to examine the extent to which behavioral plasticity might compensate for any age-related reduction in performance, which could go a long way toward explaining why – despite the fact that divers can be considered 'good candidates' for aging – elevated senescence at the organismal or reproductive level is not detected.

Because of knowledge and resource constraints in these areas, it was impossible for the two project objectives to be considered in the same species. Each deals with a separate end of the physiological spectrum of aging for diving mammals: skeletal muscle physiology and physiological ecology. The most appropriate species for each objective were selected for this study – the shrew, because it was possible to obtain the age class sample sizes required for statistical comparison between a diving and non-diving species occupying similar habitat, and the Weddell seal, for which the most physiological data is available for use in parameterizing a simulation model.

2. AGE EFFECTS ON DIVE BEHAVIOR AND THE ENERGY BUDGET OF A SIMULATED WEDDELL SEAL

Introduction

Aging in Marine Mammals

Compared to knowledge of ontogeny and early adulthood, little is known about aging in most marine mammal species. Age-related senescence is generally not predicted for wild populations, since classic aging theory suggests mortality should occur first (e.g., Kirkwood and Austad 2000; Parsons 2002). Any observations of senescence in non-domesticated species typically occur during captivity. Large-bodied mammals are one exception to this rule, however. Naturally long-lived, individual senescence is not only conceivable for this group but largely acknowledged. Aging theory directed specifically towards wild populations suggests that maximal longevity is associated with low stress environments (Parsons 2002). Based on this theory, and in the absence of superior protective adaptations in tissues, one would hypothesize that diving mammals might display early senescence, as their daily bouts of breath-hold exercise create a physiologically high-stress environment. Because daily exercise (i.e., foraging, travel, socialization) is associated with repeating cycles of hypoxia-reoxygenation, energy production in many tissues operates on a time-partitioned schedule (Elsner et al. 1998; Hermes-Lima and Zenteno-Savín 2002). Alterations in flux through the respiratory chain, such as would accompany the maintenance of aerobic metabolism during submergence hypoxia and surface normoxia make the system more variable than that of a terrestrial vertebrate. These metabolic shifts may result in

oxidative stress in the mitochondria, and the ensuing production of harmful oxygen radicals (e.g., Gottlieb 2003). High oxidative stress leads to mitochondrial dysfunction, lipid, protein and DNA damage, and ultimately cellular apoptosis and senescence (Robertson et al. 2001). These occurrences can constitute cellular oxidative stress, and should correlate with a more rapid aging or lifespan expressed per metabolic rate or animal mass.

Proof of such individual senescence has been inconsistently collected for pinnipeds, however. It is a testament to the difficulty of conducting such investigations on long-lived and relatively inaccessible animal populations that individual senescence has been addressed in few studies, and appears to occur in a species-dependant manner (Crocker et al. 2001; Pistorius and Bester 2002; Beauplet et al. 2006). Undetectable senescence (or the absence of its consistent occurrence) may be the result, in part, of opportunistic approaches to investigating the topic in marine mammals. It could be the result of elevated tissue protective mechanisms to combat oxidative stress, allowing tissues to maintain physiological homeostasis during diving.

It also suggests, however, that pinnipeds may be capable of a degree of physiological or behavioral compensation to the aging process, thus attenuating its effects on foraging or even reproductive decline.

While there is a need to investigate the effects of aging on dive and foraging performance in pinnipeds, this can be a formidable task in either the lab or the field. I have therefore developed a simulation model based on the daily energy budget of a Weddell seal (*Leptonychotes weddellii*) – one of the best studied pinnipeds, to predict

the impact of physiological aging on the foraging ecology and performance of a model diver. A number of approaches have been taken to describe the submergence behavior of individual marine predators. The majority of these approaches base predictions on marginal value theorem, seeking to maximize the animal's foraging time with respect to oxygen use and recovery time (e.g., Kramer 1988; Houston and Carbone 1992). Recently however, the constraints imposed on an individual predator by prey availability and distribution (e.g., Thompson and Fedak 2001; Cornick and Horning 2003) have been addressed also. This model defines a foraging strategy based on predator-prey interaction in a patchy environment and, within the context of a daily energy budget, tests the success of this strategy over varying predator age. This model also considers behavioral variables that can likely be adjusted in a compensatory manner, providing a model input for behavioral plasticity. Thus, this is an individual behavioral response-based foraging energetics model, where the environment determines behavioral response within the individual's behavioral plasticity, as delimited by physiological constraints

Model Background

The daily energy budget can be balanced between energy intake and output with the surplus or deficit energy allotted to, or subtracted from, body mass each day. For the species in question, the Weddell seal, much is known regarding the basic physiology and foraging ecology which would comprise this energy throughput (Kooyman et al. 1980; Hill et al. 1987; Castellini et al. 1992; Ponganis et al. 1993; Hindell et al. 2002; Williams et al. 2004). Although the vast majority of this information is available only for pups,

juveniles and young adults (e.g., Kooyman et al. 1983; Burns and Castellini 1996; Burns 1999), many physiological parameters can be estimated with confidence for older individuals, as these functions tend to scale with body mass to the ¾ power. For example, basal metabolic rate ($mLO_2 \cdot kg^{-1} \cdot min^{-1}$) can be expressed in mass-specific terms as $9.98M^{-0.25}$, where M is body mass, in kg (Kleiber 1975).

Energy intake is a product of fish caught and their caloric value. Weddell seals prey primarily on the 15 – 25 cm long Antarctic silverfish (*Pleuragramma antarcticum*; Burns et al. 1998), and will eat anywhere from 1 to ~20 individuals per successful dive (Fuiman et al. 2002). Seals also prey on the 1 – 2 m Antarctic toothfish, *Dissostichus mawsoni* (Davis et al. 1999), although far less frequently. This model describes foraging only on the smaller *Pleuragramma*.

Exercise Physiology and Aging

The structure and enzyme capacity of the skeletal muscles of most diving mammals support the belief that underwater metabolism remains primarily aerobic (e.g., Kanatous et al. 1999, 2002). Thus, oxygen storage and supply, and how they might change with advancing age, become significant considerations for exercise physiology in mammalian divers.

Myoglobin concentrations do not decrease with aging in humans (Folkow and Svanborg 1993). Although diving animals of advanced age have not been studied, myoglobin concentrations in adult divers also do not appear to decline (Dolar et al. 1999; MacArthur et al. 2001). Lean muscle mass, however, is reduced with aging in

laboratory animals and humans, even athletes (Folkow and Svanborg 1993). Total mass-specific myoglobin content should therefore be reduced in older cohorts.

Existing data on mammalian aging with respect to hematology are not consistent. Aging humans and rats demonstrate decreases in blood volume due to a decline in plasma and erythrocyte volumes, while blood composition, hematocrit, and hemoglobin concentrations remain relatively constant (Folkow and Svanborg 1993). If pinnipeds continue to grow throughout their lifetime, aging should be associated with an overall increase in blood volume; however it is unknown whether mass-specific blood volume is altered with age. Galápagos fur seals, *Arctocephalus galapagoensis*, demonstrate a modest reduction in red blood cell count with age, but corresponding declines in hematocrit and hemoglobin concentrations are negligible (Horning and Trillmich 1997). A decrease in red blood cell count, with the maintenance of hematocrit suggests a concomitant decrease in plasma volume with age. Any age-related compromise of muscle oxygen storage or circulatory oxygen delivery (without concurrent reduction in metabolic rate) will compromise $V_{O_2}max$, as well as the aerobic dive limit (ADL) in divers. For specifically those reasons, human athletes demonstrate a significant reduction in $V_{O_2}max$ with aging (Julius et al. 1967). Senescence in muscle causes reduction of performance through the progressive loss of, among other things, strength and mass (Evans 1995). Muscle senescence is also associated with increased muscle stiffening and decreased elasticity (Mays et al. 1988; Kovanen and Suominen 1989; Gosselin et al. 1998), both of which could contribute to loss of muscle efficiency by increasing internal work required for a given force output.

These potential impacts of aging on anatomy and physiology of a simulated Weddell seal will impact the daily energy budget. This occurs through several avenues, including respiratory costs and foraging efficiency. The purpose of this model is therefore to: a) estimate/predict the extent to which certain age-related changes may be detectable in behavioral, physiological, and performance assessments; b) determine which assessments are likely to be most sensitive to aging, and c) estimate the extent to which a hypothesized decrease in performance-related parameters with advancing age may be accommodated by behavioral plasticity. The results will ultimately be geared toward refining future field efforts, which will make the difficult study of marine mammal ecology and physiology more effective.

Materials and Methods

Conceptual Model Overview and Assumptions

This model represents a daily energy budget for individual adult Weddell seals foraging on *Pleuragramma*. Energy gained each day is a function of fish eaten and the associated assimilated caloric value of prey. Energy expenditures are described by the respiratory costs of basal metabolism, locomotion and digestion. Growth (or loss of mass) is a function of the difference between daily energy gains and expenditures. This model also describes diving behavior on a per-dive basis. Prey availability divides simulated dives into feeding bout, and shorter searching patterns.

The simulations operate under several assumptions. Many of these assumptions may be more or less limited in their applicability to free-ranging Weddell seals. However, the level of applicability should not affect age-related comparisons within the model. The primary framework of this model is that of a 12-h foraging period followed by 12 h of surface rest. Clearly this framework is not strictly realistic; in fact, Williams et al. (2001) suggest that Weddell seals rest at the water surface for up to 6 h only. However, this assumption is designed to approximate a general ratio of foraging and surface resting over a two-week period. Attempting to duplicate the diving and resting habits of Weddell seals on a finer time scale would add needless variability to the simulation, and was also unnecessary in the context of the objectives to measure age-related differences. For example, an extended surface period might be expected following a dive bout. I think these additional periods of surface resting are accounted for in the 12-h daily rest period.

Certain, more peripheral, energetic costs are also excluded from the simulation, when there is no a priori reason to expect them to change with age. For example, thermoregulation is included in the model only via the heat increment of feeding (HIF), which is a part of the equations used to describe the energetics of foraging. Both old and young adult seals must operate in the same thermal environment, thus the energetic costs of defending body temperature outside of the thermal neutral zone are ignored.

Despite the limited framework provided by the assumptions, it is important to remember that both simulated old and young adult seals must operate under identical limitations. In fact, such limitations support the objectives by reducing variability in the simulation and allowing a more direct look at the variables of interest in the aging process.

Mechanistic Overview

This model is stochastic with a dt of 1 minute, run over a total of 14 days (20160 time steps). Temporal dynamics of central model variables are represented as follows:

$$\text{Daily Energy}_{(t+1)} = \text{Daily Energy}_{(t)} + E_{gained} - E_{expended} \quad (1);$$

$$(E_{gained}\ (\text{kJ}) - E_{expended}\ (\text{kJ}))/1000 = \text{Growth (kg)} \quad (2);$$

$$\text{Mass}_{(t+1)} = \text{Mass}_{(t)} + \text{Growth} \quad (3).$$

An overview of thew key model features is as follows:

Physiology

- Energy budget = $E_{gained} - E_{expended}$, with excess energy diverted to growth

  = (caloric value of prey × fish per day) – ($A_{respiartion} + A_{waste}$)

- Dive costs described by MR, dive min, flipper stroking
- MR scales allometrically

Behavior

- Foraging activity is represented by searching dives and feeding bouts
- Search dives are 2-6 min
- Successful search dive starts feeding bout and is extended to ADL, when observed prey density exceeds a given threshold
- Subsequent prey encounter chances are elevated, reflecting patchy prey distribution.

Aging Paradigms

- Young adult seal
- Old – ADL, 10% decline in ADL
- Old – muscle, 10% decline in contractile function (relates to flipper stroking)
- Old – buoyancy, 5% decline (relates to dive: surface ratio)
- Old – all, combination of above

Daily Energy Budget

Daily energy intake (E_{gained}, kJ) is represented as number of fish eaten × caloric value of prey at the conclusion of each day (minutes = 1440). The average caloric value of one Antarctic silverfish used here was 325 kJ (R.W. Davis, Unpubl. Obs.). In this simulation, daily energy intake is capped if the energy derived from foraging success exceeds an allometric maximum of a 5% body energy intake per day (this equation was parameterized based on a 5% increase for a 450 kg animal). Daily energy expenditures ($E_{expended}$, kcal), also evaluated at day's end, are represented as A_r (respiratory costs) + A_w (costs of waste or digestion). While digestive costs are predominantly functions of ingested energy, respiratory costs are functions of locomotion, heat increment of feeding, and mass-specific respiration, as described below.

$$A_{respiration} = (A_{dive}*5.09 + A_{surface}*5.09)/1000 \quad (4),$$

describes the conversion of respiratory costs in mLO_2 (VO_2) into kcal per day. A_{dive} (mLO_2), is the daily metabolic cost of diving, which incorporates metabolic rate (MR) or basal metabolic rate (BMR) associated with diving and recovery, and HIF if applicable, multiplied by the total minutes of feeding and non-feeding dives per day (Parameterized from Williams et al., 2004). The equations are given by:

Fed VO_2 plus recovery: (MR)*dive length + transport

$$= 16.19 + ((12.08M^{-0.25} * \text{successful dive min}) + 0.05*\text{strokes})*M \quad (5);$$

Non-Feeding VO_2 plus recovery: BMR*dive length + transport

$= ((9.98M^{-0.25} * \text{unsuccessful dive min}) + 0.04*\text{strokes})*M$ (6);

with the variable 'strokes' described below. $A_{surface}$ (mLO_2), is the metabolic cost of surface minutes per day, assuming a thermoneutral environment (Kleiber 1975).

BMR ($mLO_2 \cdot kg^{-1} \cdot min^{-1}$)*surface min = $9.98*M^{-0.75}$*daily surface min (7).

Digestion costs (A_{waste}) are represented as:

A_{waste} (kJ) = $A_{urinary}$ + A_{fecal} (8),

where A_{waste} is total digestion cost, $A_{urinary}$ is the energy lost via urinary output, and A_{fecal} is the energy lost through fecal waste. The components of digestion are calculated by:

$A_{urinary}$ (kJ) = Max (5% ingested energy, 5% $A_{respiration}$) (9);

A_{fecal} (kJ) = 15% ingested energy (10).

As seen above, respiratory cost equations are based, amongst other things, on dive length and cost of transport. The latter is described in this simulation via number of flipper strokes taken per min (per Williams et al. 2004). This model relates flipper

stroking rates to buoyancy, which is described by body fat index, and is parameterized following Sato et al. (2003).

Index of fatness = (22.5 + % blubber)/67.4 = axillary girth/standard length (11),

Strokes (strokes/min): IF Index of fatness < 0.78,

THEN 50*Daily dive min*contractile properties,

ELSE 60*Daily dive min*contractile properties (12).

Contractile properties of the swimming muscle are also a constant affecting cost of transport. It is set to an index of 1 for the normal state, and any decline in contractile capacity can be expressed as a normalized value. Aging in mammalian skeletal muscle is associated with an increase in total collagen content (Mays et al. 1988; Kovanen and Suominen 1989; Gosselin et al. 1998). Connective tissue is part of both the series and parallel elastic elements of muscle contraction (see Brooks et al. 2000 for review), implying that higher levels of collagen correlates with increased muscle stiffness. This correlation occurs because the force generated by contractile tissue must work against the resistance of the elastic components to generate movement. More collagen equals more internal resistance to a muscle contraction of a given size. While age-related deposition of collagen in skeletal muscle is not predicted to negatively affect fatigue resistance (Kovanen 2002), is has been suggested to impair burst force generation. This could relate to the locomotory patterns of seals during the initial descent phase of dives, or during prey pursuit.

Dive Predictions and Prey Encounter

Behaviorally and physiologically relevant dives for seals in this model were considered to be dives less than 23 min long. Behaviorally, less than 2% of natural dives exceed this range and, physiologically, this is considered a threshold beyond which anaerobic metabolism is required to sustain underwater activity (Kooyman et al. 1980). This results in substantial lactate buildup in blood, and subsequently longer surface recovery intervals, and reduced energetic efficiency of dives (Fedak and Thompson 1993).

The default dive pattern is a short, searching dive between 2 and 6 minutes. The probability (P), or per-minute rate, of encountering prey on a given dive is stochastically drawn from an exponential prey distribution (filtered to be between 0 and 1) once per dive (Fig. 1). For a successful dive: P × dive minutes = fish caught. This approach is a hybrid of the prey availability options outlined by Thompson and Fedak (2001), that prey is uniformly distributed, or widely scattered. Our goal was to hold prey at a uniform density throughout a given dive, but to generate variability similar to dispersed prey patches between dives.

Each simulation is influenced by a prey threshold ($P_{threshold}$). A super-threshold prey encounter rate (i.e., $P = P_{threshold}$) lengthens a searching dive to the ADL (23 min, per Williams et al. 2004). The animal's ability to detect prey is heightened subsequent to successful dives, permitting a simulated dive bout up to four dives in length. This allows continued successful dives even if prey level is falling (e.g., when the animal is exploiting a diminishing food patch). In the case of bout diving, P declines to 90% of

the previous dive's P, to simulate returning to the same prey patch but facing prey loss due to dispersion or consumption. If at any time calculated P declines below $P_{threshold}$, the bout is terminated and P is drawn again from the exponential distribution. Real-world predators must re-revaluate prey density each foraging trip, and do not assume a given prey density during a diving bout (Krebs et al. 1974). Therefore, a super-threshold value for P must accompany all bout diving. Although prey detection is enhanced by success, this model does not allow continued ADL-length dives throughout a bout. Dive lengths diminish during a dive bout, each falling to 90% of the previous dive and stabilizing at 50% of ADL. Bouts may contain a maximum of four dives, provided that P remains above $P_{threshold}$. If at any point P fails to exceed $P_{threshold}$, searching behavior begins again.

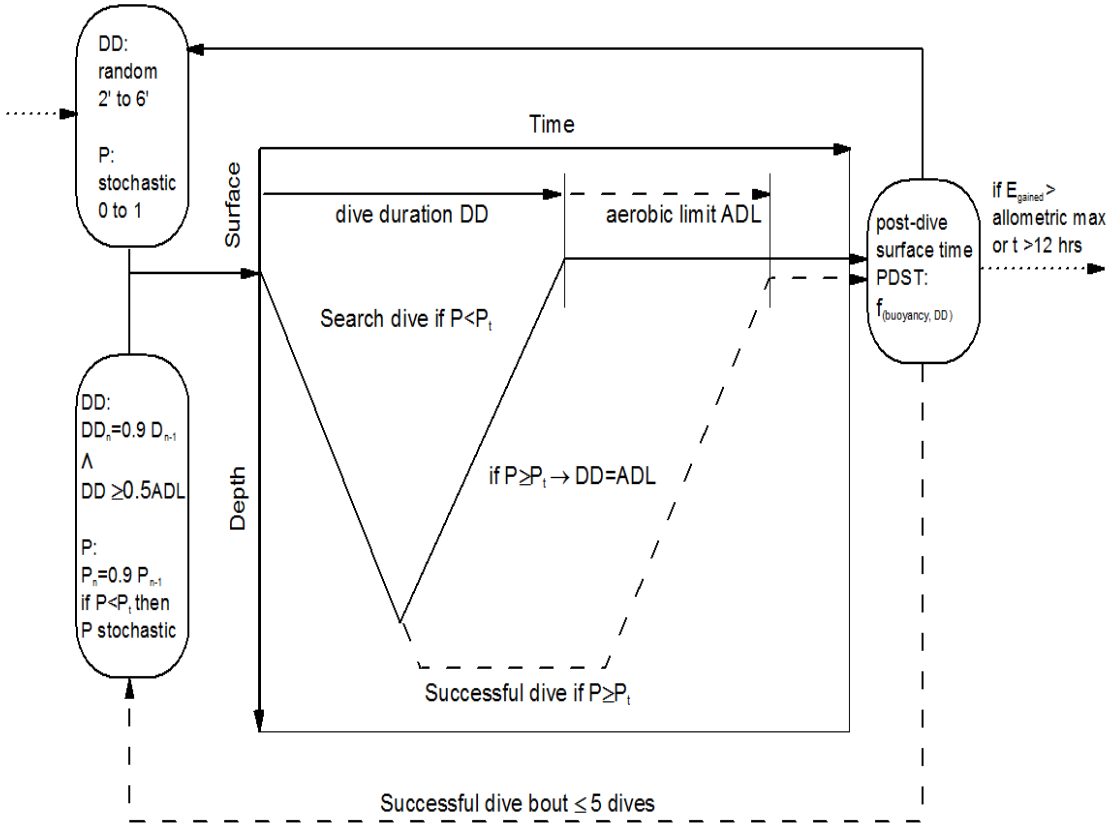

Fig. 1**.** Diagrammatic representation of the time partitioning of diving for the model**.**

Surface intervals are predicted based on previous dive length and the animal's buoyancy. Extended post-dive surface intervals have been associated with stroke-and-glide, versus prolonged gliding locomotion styles in Weddell seals (Williams et al. 2000; Sato et al. 2003). Individuals with higher body fat composition employ more stroke-and-glide diving (Sato et al.2003). Based on the data of Sato et al. (2003), dive: surface ratio (D:S, Y axis) follows a sigmoidal relationship with buoyancy (or index of fatness, X axis). The relationship ranges from X: 0.65, Y: 4.2 to X: 0.9, Y: 1.54, with a median around X: 0.78, Y: 3. Surface interval lengths are also attenuated within a dive bout. This is described by: If P*50/dive number in bout > D:S then that will replace the D:S ratio for that dive within the bout.

The dive/surface status of the seal is represented by the state variables 'surface' and 'submerge', with the seal being shuttled back and forth between the two states according to dive and surface lengths. The animal begins 'diving' when accumulated surface minutes exceed the predicted surface interval. Likewise, surfacing occurs when accumulated dive minutes exceed the predicted dive length.

Age-Related Changes

Three parameters were selected for specific consideration in the aging seal model. First, the contractile ability of swimming muscle in 'Old' adult seals was reduced by 10% ('Old – muscle'; Equation 12). This describes the reduction in sprint capacity and general force production from older muscle. Skeletal muscle contraction and half relaxation times are typically prolonged in old age (Edström and Larsson 1987),

a feature related to the increased proportion of slow twitch fibers observed with advancing age. In Weddell seal muscle biopsies, significant increases in total collagen deposits, as well as a shift from Type III to Type I collagen with aging have also been observed (Hindle et al. 2007 - Abstract). Increased total collagen deposits, as well as higher amounts of the stiffer Type I collagen will increase the passive resistance in muscle that must first be overcome by contraction before force can be generated (Brooks et al. 2000; see next Section). In the second paradigm, ADL was reduced by 10% in 'Old' seals ('Old – ADL'). Based on the possibility of both increased energy expenditure underwater (see previous), as well as that of reduced oxygen stores (i.e., myoglobin as well as blood oxygen stores) and the reduced peripheral vasoconstriction described in other mammals (e.g., Folkow and Svanborg 1993; Dinenno *et al.* 2000), it is reasonable to consider the possibility of a decline in ADL with advancing age. Third, an increase in buoyancy (percent body blubber) of 5% with age ('Old – blubber') was tested (Equations 11; 12).

Any allometric equations contained in this model (e.g., respiratory costs) will yield changing mass-specific rates as the simulated seal gains or losses mass during the two week run. Because an initial mass difference between the groups could result in considerable differences in energy flux over a two week period, mass was held constant between the age paradigms. Although increasing mass with age is expected for Weddell seals (e.g., Fujise et al. 1985), this trend appears to be attenuated once seals reach prime reproductive age. Past age nine for instance, no significant increase in body mass in these animals was noted (Unpubl. Obs.). Rather than consider different initial masses

for the age paradigms, all simulations were run from initial masses of 350 and 400kg for both 'Young' and 'Old' adult seals.

Available Model Outputs

The primary model output used in these analyses was mass. Percent mass change over the two week simulation was calculated for replicates of each scenario. Other components of the energy budget (e.g., E_{gained}, $E_{expended}$, various respiratory costs) are also generated by the model on a daily basis and could be examined over a two week simulation. Additional daily variables generated that may be suitable for analyses are measures of dive behavior and foraging efficiency, including: dive minutes; successful dive minutes; fish eaten; average dive length; and average dives per bout.

Objectives

The overall objective of this simulation was to reasonably quantify age-related changes in a daily energy budget for Weddell seals, for a behavioral response-based foraging strategy. The age effects modeled suggest changes in cost of transport and to

the physiological limits of behavioral plasticity. Initially, the model outputs were validated against existing data for the opposite end of the age spectrum – ontogeny. Specifically, published values for oxygen stores and ADL were applied to the model to determine if growth outputs were reasonable.

Subsequently, 'Young' adults were compared to 'Old' adults of a similar mass. Physiological and anatomical paradigms of aging (see above) were examined individually and in combination in simulated 'Old' adults. First, percent mass change over the two week simulation was examined for each paradigm over a range of exponential prey encounter rate distribution means. Second, each paradigm was also examined over a range of prey encounter thresholds ($P_{threshold}$) for bout dive initiation. In this analysis, the distribution mean for prey encounter rate was held constant at 0.3 fish·min^{-1}. Finally, I assessed whether optimum search dive duration differs between the simulated groups of Weddell seals. This was considered over a range of $P_{threshold}$ values, with the prey encounter distribution mean again held constant at 0.3 fish·min^{-1}.

Results

Evaluation of Simulation System Dynamics with Respect to Natural System

Overall, the model appears to behave appropriately, with the inherent stochasticity generating independent dive sequences (e.g., Fig. 2 as an example of a dive bout), as well as independent energy flux each day (Fig. 3). Trends in number of fish eaten per day are similar to those of E_{gained} (Fig. 4A), indicating that prey consumption is a primary driving variable for that half of the energy budget. Trends in $E_{expended}$ on the other hand, are closely tracked by dive min per day (Fig 4B), indicating that respiratory costs of exercise are a primary component of energy expenditure.

The endpoint output for this model is body mass. Because the logistics of daily handling of Weddell seals are difficult, there are no data available on natural weight fluctuations in adults over the time interval in question. However, mass output data seem reasonable, with daily gains and losses typically between 0.5 and 1% of initial body mass. Energy flux (i.e., E_{gained} and $E_{expended}$) also appears reasonable across a two-week run (Fig. 3). It is important to note that under initial model conditions a simulated adult Weddell seal tends to gain mass each day (i.e., $E_{gained} > E_{expended}$). This occurrence is not absolute, however, since daily mass loss is occasionally observed (Fig. 3). In the event of zero capture success and continuous searching behavior by the seal, mass drops precipitously at a rate of ~2.5% per day.

To further validate this model, its outputs were also considered for the case of a juvenile predator, given dive behavior parameters collected from the literature and slightly reduced prey encounter efficiencies from adults (Table 1). According to those

Table 1. Simulated mass change for adult, juvenile and weaned pup Weddell seals, given assumed ADLs and prey encounter rates.

	Adult (350 kg)	Adult (400 kg)	Adult (450 kg)	Juvenile (132 kg)	Weaned Pup (96.5 kg)
ADL (min)[a]	23	23	23	12	8
Prey distribution mean (fish·min^{-1})	0.3	0.3	0.3	0.15	0.15
Prey threshold (fish·min^{-1})	0.3	0.3	0.3	0.15	0.15
Mass change (%)	9.92 ± 0.13	6.62 ± 0.15	2.68 ± 0.15	10.70 ± 0.20	6.20 ± 0.18

[a] cADLs which correspond to juvenile and weaned pup average mass were taken from Burns (1999). ADL for adult Weddell seals from Williams et al. (2004).

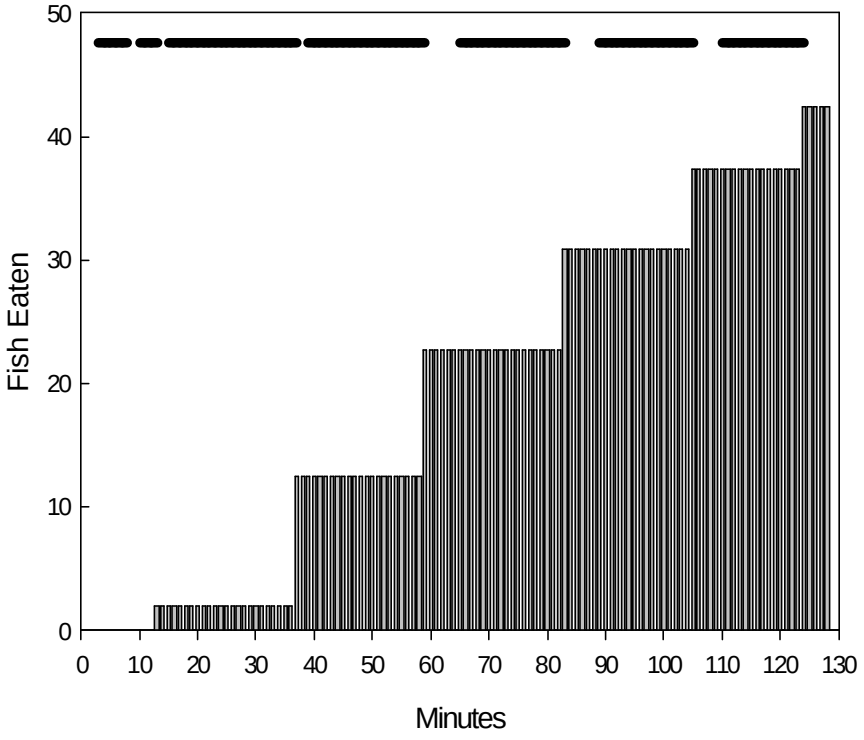

Fig. 2. Representative outputs from a 130 min simulated bout of diving in a prey patch by a 350 kg seal. Bars indicate the cumulative number of fish caught during the bout, and the top discontinuous line indicates times of submergence. Fish caught during a dive are added to the cumulative total in the last minute of submergence.

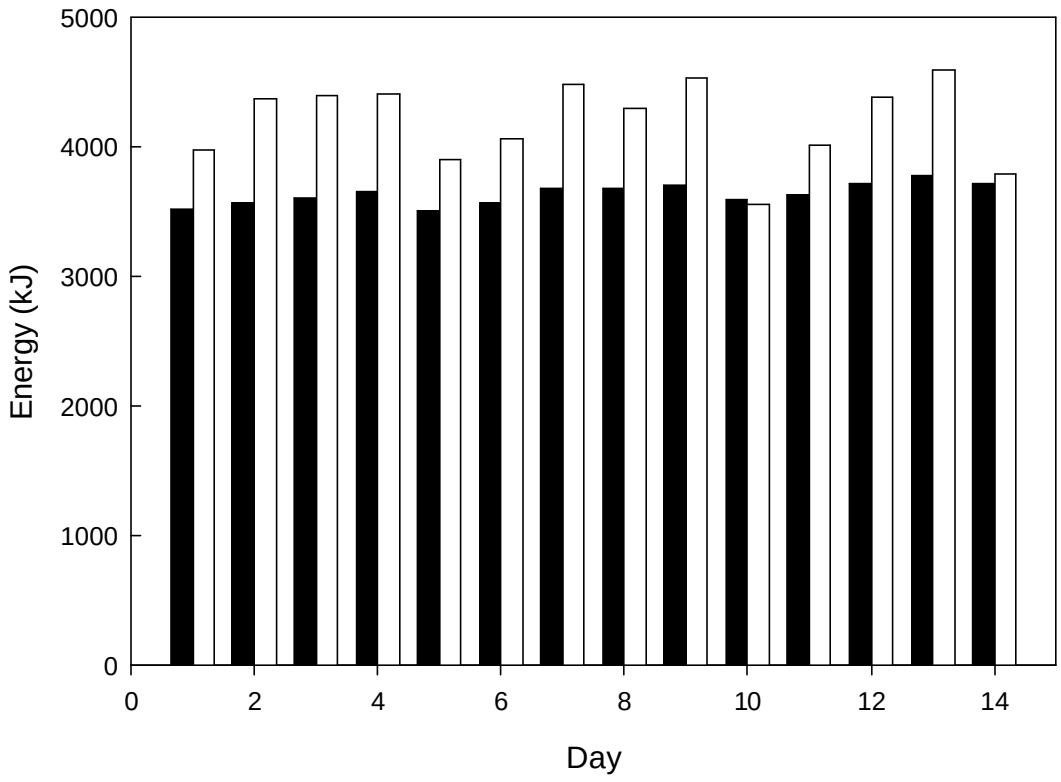

Fig. 3. Daily energy expenditures (filled bars) and gains (unfilled bars) over a representative two week simulation for a 350 kg seal.

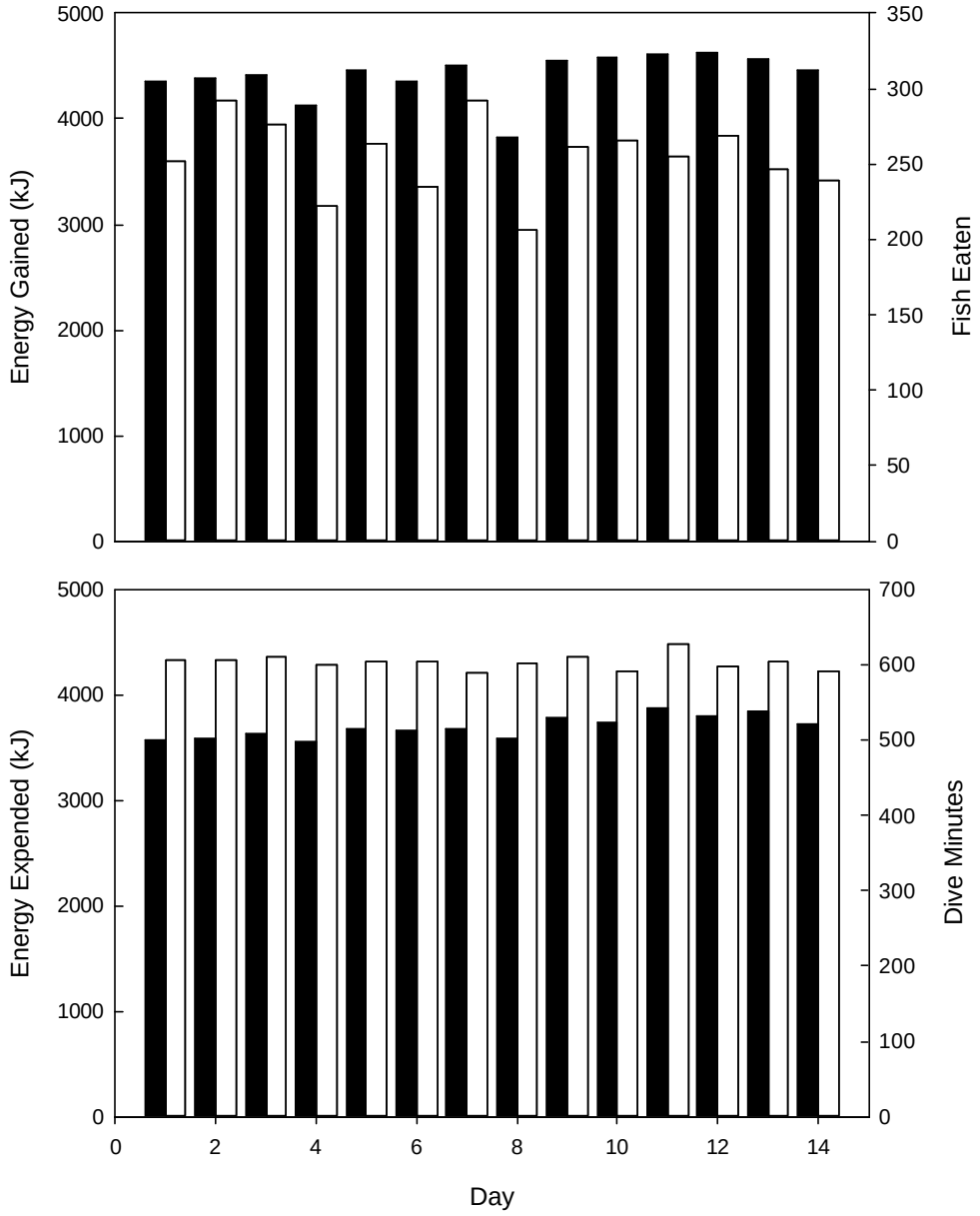

Fig. 4. Daily energy outputs and primary driving variables over a two week representative simulation for a 350 kg seal. (A) Energy gained (filled bars) is compared to fish eaten (unfilled bars) each day. (B) Energy expended (filled bars) is compared to dive minutes (unfilled bars) each day.

simulations, juvenile Weddell seals are capable of similar growth to young adult seals (10.7 versus 9.9% mass increase over two weeks; Table 1). Weaned pups, on the other hand, were capable of slightly less growth than were juveniles, based on their dive behavior (6.2% mass increase over two weeks; Table 1).

Sensitivity Analysis

The per-dive prey encounter rate (P) was the model's only stochastic variable. Because this value is a central driving variable for this model, a deterministic sensitivity analyses was not attempted. Rather, replicates of a stochastic sensitivity analysis were averaged. Because variability was observed to stabilize following 50 replicates (Fig. 5), 50 simulations were run to generate the sensitivity analysis as well as results for all objectives.

The response of mass at the end of the 14-day trial was generally greatest for those variables having direct influence on the energy budget (Table 2). The most significant variable in the sensitivity analysis was respiratory energy costs ($A_{respiratory}$), causing a greater than 8% difference in mass change for a ±10% initial value of this variable (Table 2). Sensitivity analysis also revealed that initial mass is a key parameter (>5% difference between ±10% initial values; Table 2). Both caloric value of prey (5.9%) and fish caught per dive (5.7%) contribute to daily E_{gained} and figure prominently in the sensitivity analysis. The threshold of prey encounter ($P_{threshold}$) at which dive behavior changes was more important than prey encounter rate (P) itself (3.5 versus 2.0%). The only variable which did not generate a significant difference in mass

Table 2. Sensitivity analysis for model variables. Each variable is manipulated ± 10% and the difference in outputs compared.

Variable	Output (% mass change)		Difference	$F_{1,98}$	P
	+ 10 %	– 10 %	(%)		
$A_{urinary}$	6.40 ± 0.15	6.90 ± 0.14	0.5	6.055	0.016
A_{fecal}	5.68 ± 0.15	7.52 ± 0.15	1.84	68.789	<0.001
A_{waste}	5.23 ± 0.13	7.63 ± 0.14	2.4	173.014	<0.001
$A_{respiratory}$	2.60 ± 0.14	10.69 ± 0.14	8.09	1654.193	<0.001
$A_{surface}$	5.29 ± 0.15	7.58 ± 0.14	2.29	122.795	<0.001
Mass	3.93 ± 0.15	9.17 ± 0.12	5.24	294.202[a]	<0.001
E_{gain} cap	7.37 ± 0.16	4.13 ± 0.11	-3.24	277.981[a]	<0.001
Fish caloric value	8.72 ± 0.12	2.83 ± 0.14	-5.89	1187.956	<0.001
A_{dive} (feeding)	4.75 ± 0.13	8.07 ± 0.14	3.32	327.234	<0.001
A_{dive} (non-feeding)	5.69 ± 0.14	7.61 ± 0.14	1.92	94.560	<0.001
A_{dive} (overall)	3.55 ± 0.14	9.14 ± 0.15	5.59	740.643	<0.001
Muscle contraction	4.72 ± 0.14	8.26 ± 0.15	3.54	280.640	<0.001
% Blubber	5.92 ± 0.15	6.16 ± 0.15	0.24	1.277	0.261
Prey dist. Mean	7.54 ± 0.14	5.53 ± 0.15	-2.01	94.593	<0.001
$P_{threshold}$	7.94 ± 0.13	4.49 ± 0.15	-3.45	264.781[a]	<0.001
ADL	7.26 ± 0.13	7.00 ± 0.15	-0.26	20.474	<0.001
Dive: Surface	6.75 ± 0.13	6.37 ± 0.14	-0.38	4.230	0.042
Fish per dive	8.64 ± 0.12	2.93 ± 0.16	-5.71	294.188[a]	<0.001

[a] Non-parametric ANOVA was employed.

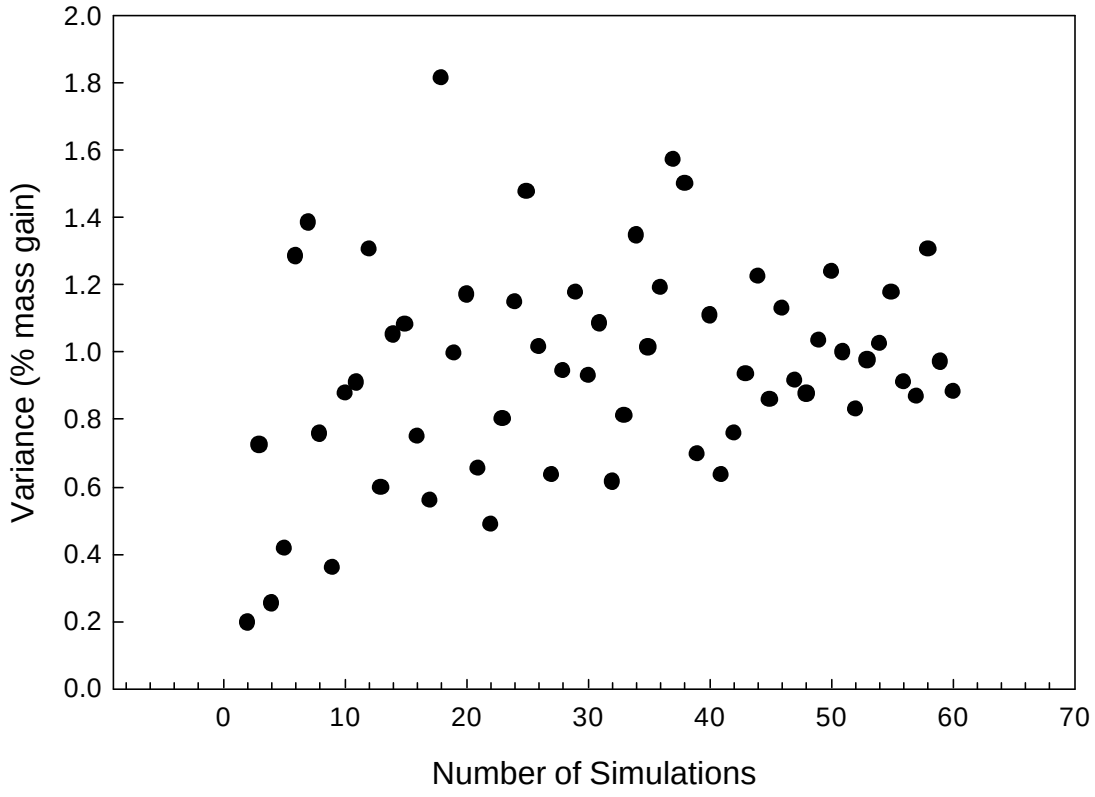

Fig. 5. Variance in the model output (% mass gain) begins to stabilize after approximately 50 repetitions of the simulation.

output from ±10% initial starting values was percent body blubber (Table 2).

Variables were generally more significant to the sensitivity analysis when they were the product of other significant variables. For example, the respiratory costs of diving, $A_{dive\ feeding}$ and $A_{dive\ non\text{-}feeding}$ were 3.3 and 1.9%, respectively, while $A_{dive\ total}$ was 5.6% (Table 2). This group of significant variables is a component of the calculation for $A_{respiratory}$, which may account for its high value.

Effect of Simulated Aging on Diving and the Energy Budget

Percent mass change increased in all age paradigms with an increase in the mean of the exponential distribution for prey encounter rate. In these simulations, seals were unable to exhibit positive growth if this distribution mean fell below 1.5-2 fish·min^{-1} (Fig. 6). Conditions of higher prey encounter rates (distribution means greater than ~0.4 fish·min^{-1}) resulted in maximal growth for each paradigm individually (Fig.6).

The 'Young' adult seal, along with the 'Old – ADL' and 'Old – buoyancy' paradigms demonstrated the highest levels of positive growth. In other words, there were no obvious differences between the growth curves of 'Young' adult seals and those with increased buoyancy or a decreased ADL over a range of prey encounter rates (Fig. 6). There was a clear reduction, on the other hand, in positive growth for 'Old – muscle' and 'Old – All' versus 'Young' seals (Fig. 6). The reduced growth observed in seals with limited swimming muscle contractile properties was similar to that observed for the 'Old' seal with all three physiological/anatomical adjustments (Fig. 6).

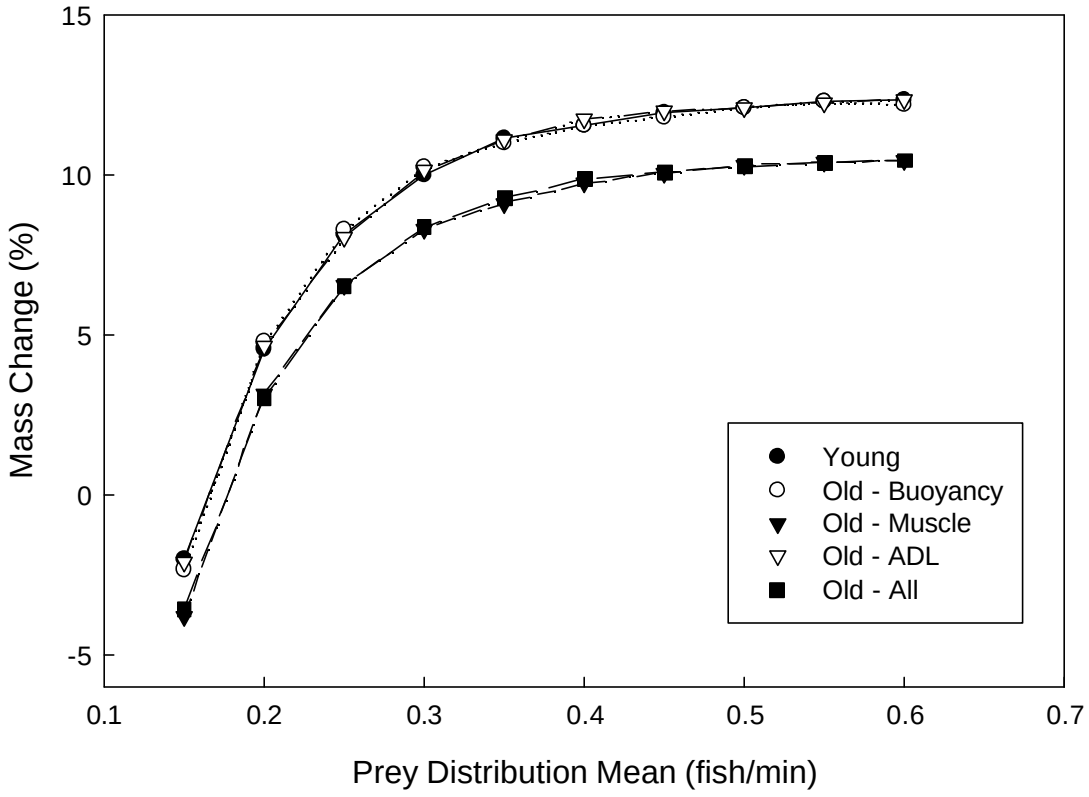

Fig. 6. Percent mass change over a simulated two week foraging period for a 350 kg seal. Outputs for 'Young' versus 'Old' seal paradigms were compared across a range of exponential prey distribution means. 'Old' adult seals were modified from the simulated 'Young' adult by adjusting percent body blubber (5% increase), contractile function of muscle (10% reduction), ADL (10% reduction), or a combination of all.

As with prey encounter rate distribution mean, percent mass change increased in all age paradigms with a higher prey encounter rate threshold for the adjustment of dive behavior (Fig. 7). With a constant P of 0.3 fish·min^{-1}, growth did not become negative until $P_{threshold}$ declined below 0.2 fish·min^{-1} (Fig. 7). Percent mass change appeared to level off for all groups above 0.35-0.4 fish·min^{-1}, which were thresholds slightly higher than the mean prey encounter rate (Fig. 7). Also as with Fig. 1-6, percent growth was highest for, and was similar between the 'Young' and the 'Old – buoyancy' and 'Old – ADL' paradigms (Fig. 7). Reduced growth rates were observed for the 'Old – muscle' and the 'Old – all' paradigms, and again these were similar to each other (Fig. 7).

Increased length of search dives was correlated to reduced positive growth in all cases examined here (Fig. 8). The correlation was stronger as $P_{threshold}$ was reduced (i.e., a higher $P_{threshold}$ compensated for longer search dives; Fig. 8A versus Fig. 8D, for

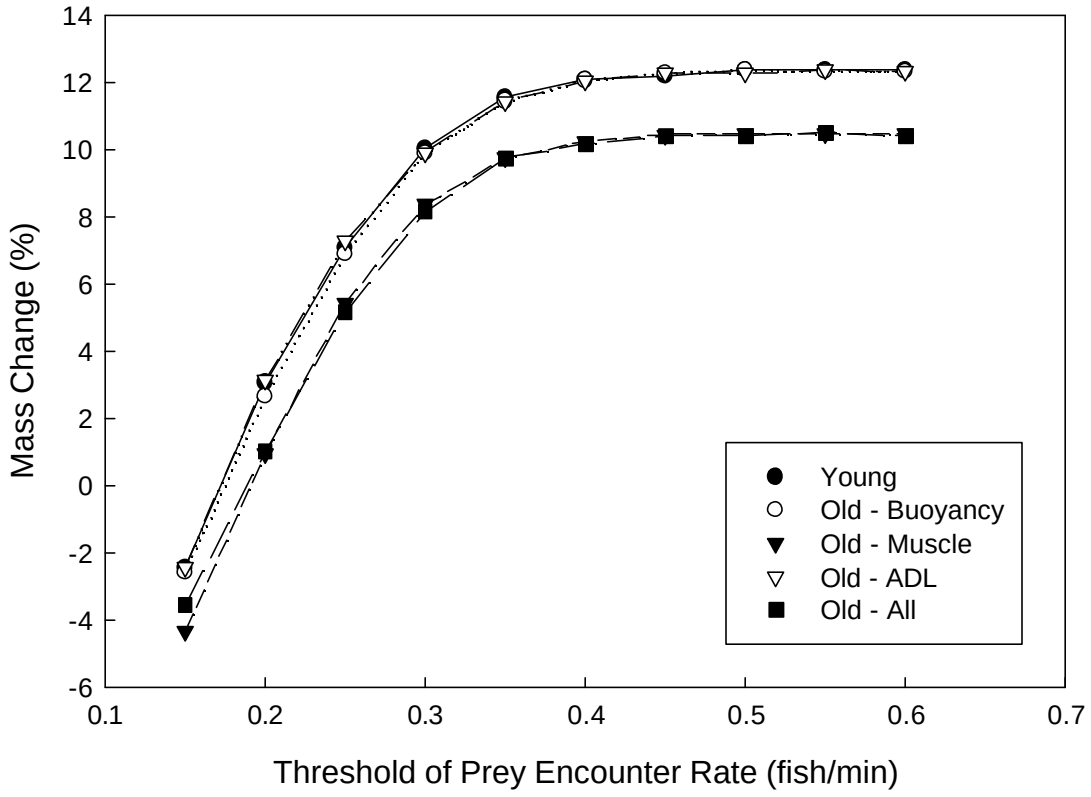

Fig. 7. Percent mass change over a simulated two week foraging period for a 350 kg seal. Outputs for 'Young' versus 'Old' seal paradigms were compared across a range of prey thresholds required to initiate a dive bout. Exponential prey distribution mean was held constant at 0.3 fish/min for all simulations. 'Old' adult seals were modified from the simulated 'Young' adult by adjusting percent body blubber (5% increase), contractile function of muscle (10% reduction), ADL (10% reduction), or a combination of all.

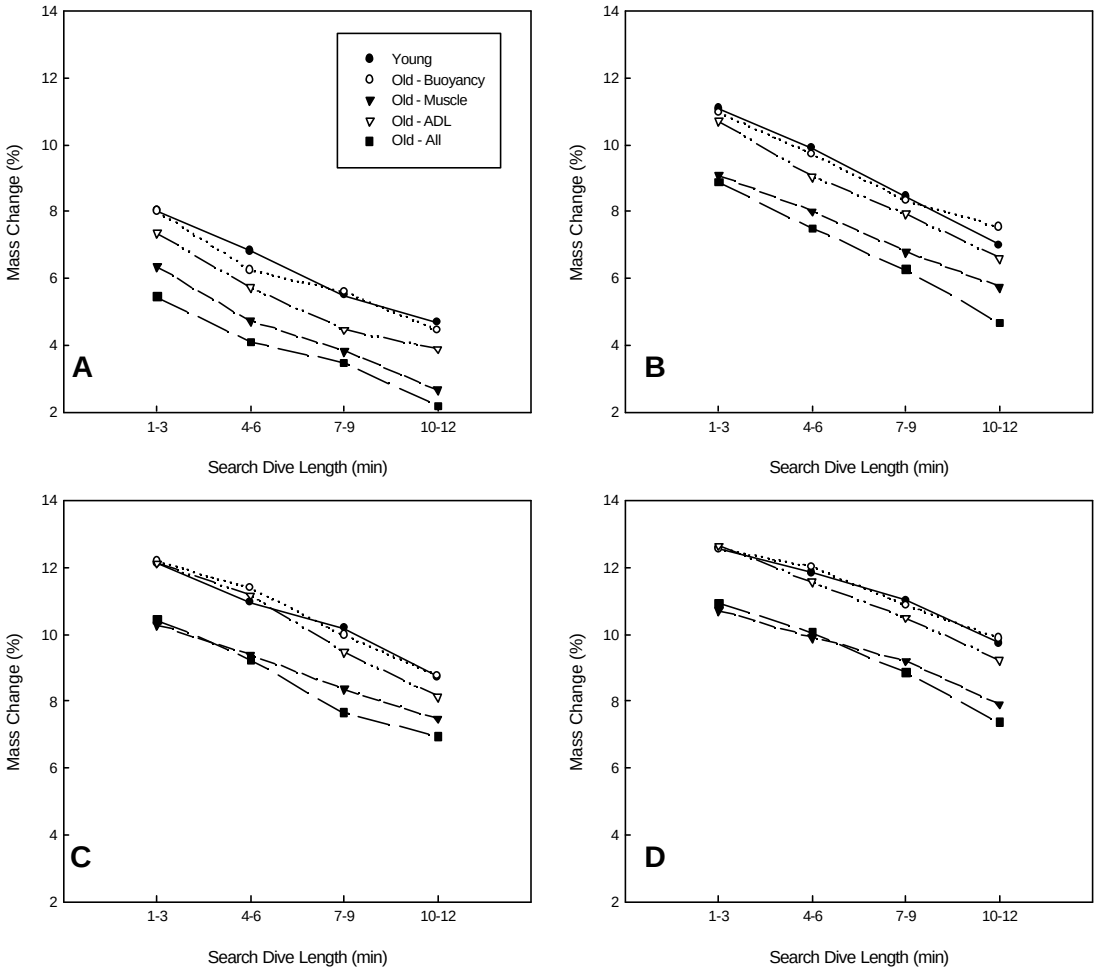

Fig. 8. Percent mass change over a simulated two week foraging period for a 350 kg seal. Outputs for 'Young' versus 'Old' seal paradigms were compared across a range of search dive lengths. $P_{threshold}$ required to enter a dive bout was also varied (A: 0.25; B: 0.3; C: 0.35; D: 0.40 fish·min^{-1}), while the exponential prey distribution mean was held at 0.3 fish·min^{-1}. 'Old' adult seals were modified from the simulated 'Young' adult by adjusting percent body blubber (5% increase), contractile function of muscle (10% reduction), ADL (10% reduction), or a combination of all.

example). At the highest $P_{thresholds}$ examined (Fig. 8C, D), the differences in results between the five age paradigms was similar to those described for Figs. 6 and 7, namely that 'Young', 'Old – buoyancy' and 'Old – ADL' were similar to each other, and were markedly higher than those for 'Old – muscle' and 'Old – all', which were also similar to each other. These differences become less obvious at lower $P_{thresholds}$, where a separation between the mass output for the different paradigms becomes more clear (Fig. 8A, B). In these cases the 'Young' adult is still most similar to 'Old – buoyancy', however simulated seals with increased percent blubber appear to have slightly reduced growth compared to 'Young' adults. At a $P_{threshold}$ of 0.25 fish·min^{-1} min (Fig. 8A) there is a clear separation between 'Old – ADL' and the previous two paradigms, as well as between 'Old – Muscle' and 'Old – All'. The lowest percent growth is observed for the simulated 'Old' adult seal having all three physiological/anatomical adjustments related to aging (Fig. 8A).

Discussion

Applicability of the Model

A number of approaches have been taken to describe the submergence and foraging behaviors of individual marine predators. The majority of these approaches base predictions on the application of the 'marginal value theorem' to respiratory or energetic constraints, and seek to optimize an animal's foraging time with respect to oxygen use and recovery (Kramer 1988) as well as energy (Houston and Carbone 1992). This has largely involved dive behavior predictions based upon oxygen loading at the surface, and depletion of those reserves at depth (i.e., Kramer 1988). Similar arguments have also been made for the control of dive: surface behavior by levels of carbon dioxide (Stephenson 2005). The early versions of these models tended to deal exclusively with energy production by aerobic pathways (Kramer 1988; Houston and Carbone 1992). More recent contributions, however, have suggested that the use of anaerobic metabolism may be a significant component of foraging in selected diving species (Ydenberg and Clark 1989; Carbone and Houston 1996; Carbone et al. 1996; Mori 1998), serving to increase accessibility to prey patches in the environment, and to allow the maximal exploitation of unpredictably variable food patches. Models which rely heavily on a simulated animal's use of anaerobiosis are typically parameterized for diving birds, although dives beyond the ADL certainly do occur in some marine mammal species. Because it seems, however, that exploratory dives (versus feeding dives) are those likely to exceed the ADL in less than five percent of Weddell seal dives

(e.g., Kooyman et al. 1980; Hindell et al. 2002; Williams et al. 2004), this model does not simulate foraging dives fueled by anaerobic metabolism.

A more recent approach has been to impose physiological constraints on behavioral options (Thompson and Fedak 2001; Cornick and Horning 2003), and to drive a predators behavior largely in response to a patchy, but unpredictable prey distribution. These approaches, however, do not allow fine-scale behavioral foraging adjustments for individual dives based on actual physiological mechanisms. Instead, recent approaches are behavioral response models, where the behavior of the predator operates within given limits, and is adjusted mainly in response to prey distribution. For the presented here, physiology determines the limits of behavioral plasticity, but fine scale behavior is largely driven by prey distribution. Since physiology may in turn be influenced by behavior (Gilmour et al. 2005), modeled variations in prey density force behavioral adjustments within a predator's plasticity, and from this control, physiological costs can be inferred.

Functionality of the Model

Overall, the model appears to behave appropriately, with the inherent stochasticity generating independent dive sequences, as well as independent energy flux each day. Special care was taken to parameterize the parts of the model which have the largest effects on the energy budget based on sensitivity analyses. The large body of literature available on the physiology of Weddell seals was drawn upon to parameterize the model. E_{gained}, for example, was driven by fish eaten per day. Fish per day was a

product of average fish per dive, which was based on the direct measurements, via video footage, of successful dives collected by Fuiman, Davis and Williams (2002) for Weddell seals foraging in McMurdo Sound, Antarctica. Trends in $E_{expended}$ on the other hand, are closely tracked by dive min per day. The output for this value is within the expected range based on individual and daily dive data collected for this species (e.g., Kooyman et al. 1980, Williams et al. 2004).

The sensitivity analysis was also used as a tool to highlight variables which had a large effect on the model outcome. The response of mass at the end of the 14-day trial was generally greatest for those variables having direct influence on the energy budget, such as respiratory costs. Those values were taken from direct field measurements, via respirometry, for adult Weddell seals (Williams et al. 2004). Caloric value of prey (i.e., the average caloric value of an individual prey item) has been directly measured by calorimetry (R.W. Davis Unpubl. Obs.). This value falls well within the range of other published values for *Pleuragramma*, such as 5.2±0.16 kcal·g^{-1} prey (n=4; Ainley et al. 2003), where maximum prey size would be 200 g. This corresponds to an average prey size consumed by seals of 62.5 g. Initial mass was held constant for all adult seal paradigms, despite the fact that the sensitivity analyses revealed this variable to be important. Although it is generally held that phocid mass increases with age towards, and throughout adulthood, (e.g., Fujise et al., 1985), this may not universally be true for comparisons over a narrower age range. Data collected from adult Weddell seals in Erebus Bay (Unpubl. Obs.), showed no significant correlation between age and mass for males and non-lactating females past the age of nine (n=17, r^2=0.10, P=0.12). This

finding supports the decision to remove initial mass as a dynamic variable for adult seals in this model.

Due to the importance of initial mass in the model outputs however, it was necessary to confirm that the model behaved appropriately across a range of body mass. Thus the model was parameterized for juvenile Weddell seals with respect to their observed prey density and threshold and their ADL (per Burns 1999). In addition to decreased ADL, this was accomplished by reducing realized prey density and the threshold of that density required for bout diving. This corresponds to reduced dive depths of juveniles and pups relative to adults (Burns 1999), likely limiting available prey patches and therefore realized prey densities (Mori 2002). The model operated well at lower initial body mass, such that simulated juvenile and weaned pup Weddell seals showed similar potential for growth with successful foraging in this model (juveniles were nearly on par with the growth potential of young adults, while pups were slightly lower). Modeling a higher growth potential for juveniles or weaned pups could easily be accommodated by increasing their realized prey density and thresholds.

Effect of Prey Condition and Simulated Aging on Diving and the Energy Budget

Following the predictions for foraging success made by other models and experiments (e.g., Cornick and Horning 2003), percent mass change increased in all age paradigms with an increase in the mean of the exponential distribution for prey encounter rate (i.e., growth potential increases with prey density). In these simulations, seals were unable to exhibit positive growth if prey distribution means fell below 1.5-2

fish·min^{-1}, which holds with the prediction that below a given prey density, foraging cost outweighs benefit (Cornick and Horning 2003). There also existed a prey encounter rate (distribution means greater than ~0.4 fish·min^{-1}) which resulted in maximal growth for each paradigm. Although the model does not deal specifically with the cessation of foraging at a given degree of satiation, there is a physiological limit in the number of fish that can be assimilated each day. The model describes this limit as a cap in mass gain.

There were no obvious differences between the growth curves of 'Young' adult seals and those with increased buoyancy or a decreased ADL over a range of prey encounter rates (Fig. 6). This is not surprising in the case of increased buoyancy, given that this was the single variable tested in the sensitivity analyses that did not result in significant mass change. Buoyancy results in increased energy costs during descent via increased stroking, but also reduced stroking upon ascent, relative to slimmer animals (Sato et al. 2003). Since the latter recoups some of the cost of descent, it is difficult to predict what the actual effects on the energy budget might be. While ADL in the sensitivity analysis does result in significant mass change, in this scenario (Fig. 6), and over the prey densities examined, it appears to effect little change with age. It does indicate that the relative length of bout dives versus searching dives correlates with sufficiently higher prey consumption such that a slightly reduced maximum foraging dive duration makes little difference in a prey patch. This suggests that the behavioral response foraging strategy modeled here, encompasses a sufficient degree of plasticity to allow an animal to compensate for increased physiological constraints, in this case with age. There was a clear reduction, on the other hand, in positive growth for 'Old –

muscle' and 'Old – All' versus 'Young' seals and the degree of this reduction was similar in both groups. This implies that any reduction in the contractile ability of swimming muscle has a significant impact on the energy budget for foraging, beyond the ability of animals to make behavioral adjustments. For this model, contractile properties stand to have a major impact on the energy budget since it affects the cost of all dives. From laboratory analyses, marked increases in collagen deposition within senescent muscle in seals has been documented (Hindle et al. 2007, Abstract). Unfortunately, the degree to which such age-related changes impact the functionality of muscle remains unclear. The increased muscle collagen levels, and the possibility for this observation to be the cause of reduced muscle function, however, could be a mechanism for the significance of the 'contractile properties' variable in the model.

As with prey encounter rate, growth increased in all age paradigms with a higher threshold of encounter at which bout dives commenced (Fig. 7). This follows well from the previous scenario, which demonstrated an increased benefit with increased prey density. These data imply avoiding commitment to long, more energetically expensive, bout dives until a threshold at, or above, the actual prey density in the environment is beneficial. In other words, it is wasted energy to assume the energetic costs of bout diving if the prey density is low. This is essentially the same as the 'giving up rule' proposed by Thompson and Fedak (2001), which predicts that predators should gain a net benefit from giving up on a dive bout when no prey is encountered early in searching. This is also supported by Fig. 8, which demonstrates that mass gains are substantially higher for shorter typical search dive durations. Although prey density

thresholds beyond the range of realistic prey densities were not examined, growth is expected to eventually decline from its optimal value, since behavior would become entirely searching. As seen with Fig. 6, growth reaches a maximum asymptotic value; in this experiment this value is slightly higher than the true prey density. This result is intuitive when considering that a forager should chose to expend the energy involved in a long feeding dive only in above-par prey conditions. With a constant distribution mean for prey encounter rate of 0.3 fish·min^{-1}, growth did not become negative until $P_{threshold}$ declined below 0.2 fish·min^{-1} (Fig. 7). This highlights the idea that it is not beneficial for predators to expend energy pursuing a sub-standard prey patch, but rather to continue searching. The scenario explored in this case (adjusting $P_{threshold}$ when all other variables remain the same), resulted in similar differences to Fig. 6 in the net energy gain for the five age paradigms.

Increased search dive length was more costly to simulated foraging seals, which is expected since the small number of fish consumed in searching dives would not likely overcome the cost of diving itself. At reduced threshold levels for prey encounter rate, and during longer search times, the differences between the growth potential in the five age paradigms became clearer. Young adults maintained the highest growth potential, and growth potential decreased in order for old adults with increased buoyancy, decreased ADL, decreased contractile properties of swimming muscle and all of the above. It seems that in conditions of prey surplus, there is sufficient plasticity in the dive behavior of older seals, as modeled, to almost completely compensate for the physiological and anatomical limits of age. As observed in the previous experiments,

and in conditions with either higher behavioral $P_{thresholds}$ or shorter searching dives, changes in buoyancy and even changes in ADL are not sufficient to reduce growth potential. In the conditions of lower $P_{threshold}$, the model suggests that the limit of behavioral plasticity has been attained, and past this point a reduction in net energy gain becomes evident.

Model Predictions and Conclusions

The model offers the following predictions: (1) foraging efficiency increases with increasing prey encounter rate to a point, and becomes asymptotic at a point when no further prey can be assimilated; (2) there exists a level of prey encounter rate at which net energy balance is negative; (3) the optimal behavioral threshold for prey encounter rate is slightly higher than the mean prey encounter rate in the environment, (4) thresholds too far below optimal result in negative energy balance; (5) net energy gain declines with physiological age paradigms in the following order: Young > Old-Buoyancy > Old-ADL > Old- Muscle > Old-All; (6) net energy gain differences with tested age paradigms are exacerbated when good prey patches are scarce (i.e., when search dives must be extended, or when sub-standard prey patches are pursued due to a lowering of $P_{threshold}$), (7) behavioral plasticity may allow older animals to compensate for certain age related performance constraints.

The concept of behavioral plasticity in aging pinnipeds is an interesting one. We know relatively little about their foraging behavior, compared to terrestrial predators, simply because so much of their range is out of our view. Several studies of Weddell

seals in recent years have made real strides forward in our understanding of this topic, including three-dimensional spatial use (Hindell et al. 2002) and seal-mounted video observations (Davis et al. 1999). The demonstration in this model that plausible physiological and anatomical adjustments with age might have large effect on foraging success, especially in areas of low prey density, is equally interesting. Weddell seals occupying breeding colonies in Erebus Bay, forage from limited tidal cracks within and around breeding colonies (Hindell et al. 2002). Because the colonies are located on steep slopes, foraging dives are constrained in direction. This means that the seals must forage in the same general areas, likely within a mile of the tidal crack (Hindell et al. 2002 found that the mean distance traveled from the colony by lactating females for foraging was 616.6 ± 222.2 m). This has been speculated to causes regional prey depletion and increased interspecific foraging competition (Hindell et al. 2002). Examinations of Weddell seals foraging in McMurdo Sound versus those foraging around White Island reveal that White Island seals are fatter (Castellini et al. 1984), which may suggest that either prey depletion or increased competition occurs in McMurdo Sound. Any decline in net energy gain as a result of aging, which is expected to become more obvious in conditions of low prey density, may be readily apparent in this environment. However, the possibility of compensation through behavioral plasticity might explain the lack of apparent senescence in a species expected to be a prime candidate for such effects.

3. HISTOLOGICAL CHANGES IN AGING MUSCLE IN TWO SPECIES OF SHREW

Introduction

Skeletal muscle form and function relies heavily on both contractile and connective tissue components. The extracellular matrix (ECM) provides an overall three-dimensional framework for muscle, and also creates the connections between individual myofibers. Its principle component is fibrillar collagen, existing in skeletal muscle mainly in Type I and Type III isoforms. Type I collagen tends to be associated with tissue stiffness, while Type III is associated with tissue compliance (Burgeson 1987). Type IV collagen is the other major isoform present in skeletal muscle, comprising a large component of basement membranes. The ECM is important in defining both the passive and active mechanical properties of skeletal muscle (e.g., Kovanen et al. 1984). Connective tissue is part of both the series and parallel elastic elements of muscle contraction (see Brooks et al. 2000 for review). This implies that higher collagen levels are correlated with increased muscle stiffness. This occurs because the force generated by contractile tissue must work against the resistance of the elastic components to generate movement. More collagen equals more internal resistance to a muscle contraction of a given size.

Remodeling of the ECM can have a significant influence on muscle function. Some type of ECM adjustment is observed with virtually all examples of muscle stress; including exercise, injury and disease. As happens in many cases following exposure to stress, collagen remodeling following high-force eccentric contraction occurred in

conjunction with loss of maximal force (Mackey et al. 2004). Hindlimb unloading in rat soleus caused a collagen isoform shift from Type I to Type III, corresponding to contractile remodeling (slow-fast myofiber transformation; Miller et al. 2001). Prolonged muscle stretch due to surgical limb lengthening increases total intramuscular collagen, which in turn reduces range joint movement in rabbits (Williams et al. 1999). Muscular dystrophy models such as the *mdx* mouse develop higher collagen levels in muscle compared to age-matched controls (Marshall et al. 1989).

As skeletal muscle ages, adjustments are made in both the density and the composition of the ECM. Generally, an increase in total collagen content is observed in older muscle (Mays et al. 1988; Kovanen and Suominen 1989; Gosselin et al. 1998), and it becomes more resistant to collagen degrading enzymes (Mohan and Radha 1980). An increase in the ratio between Type I and Type III collagen is also documented (Mays et al. 1988; Kovanen and Suominen 1989). These changes will ameliorate the decline in skeletal muscle contractile function seen with advancing age resulting from sarcopenia. The loss of force generating capacity seen with aging is the result of decline in muscle cross-sectional area, along with myofiber loss. Apoptosis has been suggested to contribute to fiber loss with age, although its exact role is not well-established (Dirks and Leeuwenburgh 2002; Pollack et al. 2002). In large part the decline in overall muscle cross-sectional area occurs as a consequence of denervation and loss of 'fast' type II motor units (Brooks and Faulkner 1994). This myofiber loss is attenuated in part by reinnervation by neighboring 'slow' motor units. While this does preserve some cross-sectional area and therefore force generating capacity of the muscle, it causes an overall

'slowing' of skeletal muscle with aging (Brooks and Faulkner 1994), which can affect contractile function.

All of the evidence previously mentioned has been collected from laboratory animals. Are similar trends expected in the wild? Not only must we assume some degree of 'exercise-training' adaptations to be present in wild animals since they cannot lead a sedentary existence, but also, aging theories applied to wild populations do not generally predict observable senescence to occur, but rather that death will occur first (Kirkwood and Austad 2000; Parsons 2002). Exercise training studies conducted in rats show that activity modifies ECM remodeling with age. While it does not affect the increase in total collagen present in old muscle (Kovanen and Suominen 1989), it does reduce overall muscle stiffness (Gosselin et al. 1998). Aging at the level of myofiber type has been analyzed in some wild species (Savolainen and Vornanen 1995*a*), and do appear to follow the 'slowing' trend documented for humans and laboratory animals. But to date remodeling of the ECM with age has not been considered in wild animals.

The purpose of this experiment was to quantify the morphology of a selected skeletal muscle in two species of wild-caught shrew. Both the contractile as well as the connective tissue components were considered in old and young field-caught shrews to determine if anatomical muscle aging, as we understand it for humans and domesticated species, also occurs in wild populations.

Materials and Methods

Capture, Animal Care and Sampling

Two species of red-toothed shrew (Family: Soricidae) of similar mass and occupying similar habitat, were selected for this study. The primary distinction in life-history between theses species is that the North American water shrew (*Sorex palustris*, Richardson 1828) is adapted to aquatic foraging, while the short-tailed shrew (*Blarina brevicauda*, Say 1823) exploits an entirely terrestrial home range. The maximum lifespan for both species in the wild is about 18 months (George et al. 1986; Beneski and Stinson 1987), and both species can breed in the season or year in which they were born (George et al. 1986; Beneski and Stinson 1987). Adult (second summer) and young-of-the-year shrews of both species were captured in Whiteshell and Nopoming Provincial Parks (49°49' N, 95°16' W; 50°67'N, 95°28' W) and at the Fort Whyte Centre, Winnipeg, Manitoba (49°50' N, 97°10' W), during the summers of 2005 and 2006. Animals were transported to the Animal Holding Facility, University of Manitoba. Here they were housed separately in 72-L terraria fitted with screen lids, in a controlled-environment room held at 20±1ºC with a 12L:12D photoperiod, as previously described (Hindle et al., 2003; Gusztak and Campbell, 2004).

A 10-cm deep mixture of sterilized peat moss and potting soil in the bottom of each container provided a substrate for burrowing. Each shrew was provided with a wooden nest box (11 cm×12 cm×10 cm), nesting materials (leaves, grasses and cotton batting) and sections of plastic pipe for additional cover. Holding containers with access to a 30-cm deep aquatic section was provided for water shrews. Animals were

maintained on a mixture of beef heart, beef liver, canned dog food (chicken and beef base) and ground beef enriched with calcium and multivitamin supplements. This diet was supplemented daily with sunflower seeds, live earthworms (*Lumbricus* sp.) and mealworms (*Tenebrio molitor*), and in the case of water shrews with fish, snails or crayfish (*Procambarus clarkii*). Water was provided ad libitum (Hindle et al., 2003; Gusztak and Campbell, 2004). All study animals were captured and cared for in accordance with the principles and guidelines of the Canadian Council on Animal Care (University of Manitoba Animal Use Protocol # F05-014).

Shrews were euthanized with an overdose of isoflurane inhalant anesthetic. The gracilis muscle was removed and frozen in liquid nitrogen-cooled isopentane for subsequent histochemical and immunohistochemical analyses. Following tissue collection, the lower jaws were processed for age determinations. Muscle samples were stored at -80ºC.

Age Determination

Mandibles were cleaned of tissue and placed in a detergent solution at 60ºC for 24 h to remove all remaining skeletal muscle. Following digestion, mandibles were decalcified (RDO, Apex Engineering, Aurora, IL) at room temperature for 1 h in the case of water shrews, and 1.5 h in the case of short-tailed shrews. Decalcified bone was rinsed in PBS (138 mM NaCl, 2.7 mM KCl, pH=7.4) and 20 µm sections were cut on a cryostat at -20ºC. Sections were mounted on glass slides, treated with the general protein stain, hematoxylin (Fisher Scientific, Waltham, MA), and coverslipped. The

presence or absence of a growth ring in the mandible and teeth was diagnostic for the individual's status as young (year 1) or old (year 2; see Fig. 9).

Muscle Morphology

For all histochemical analyses of muscle, cross-sections (7-9 μm) were cut on a cryostat at -20ºC. Transverse orientation was verified using a standard light microscope. Slides were air dried, rinsed in PBS and treated with hematoxylin for analysis of fiber cross-sectional area and myocyte density. Extracellular space (ECS) was also calculated for the analysis region by the following equation:

$$ECS = A_{total} - \rho_{myocyte} * A_{myocyte}, \quad (13)$$

where extracellular space is the difference between the total area analyzed (A_{total}, μm^2) and the area occupied by myocytes, which is the product of myocyte density ($\rho_{myocyte}$, number$\cdot A_{total}^{-1}$) and average myocyte cross-sectional area ($A_{myocyte}$, $\mu m^2 \cdot myocyte^{-1}$).

Fiber Typing

Muscle fiber type distribution was examined with a metachromatic technique which stains myosin ATPase. Because inconsistencies in the reaction of type II subgroup myosin ATPases with these classic stain types has previously been documented for shrews (Savolainen and Vornanen, 1995*b*), this technique was only useful for distinguishing

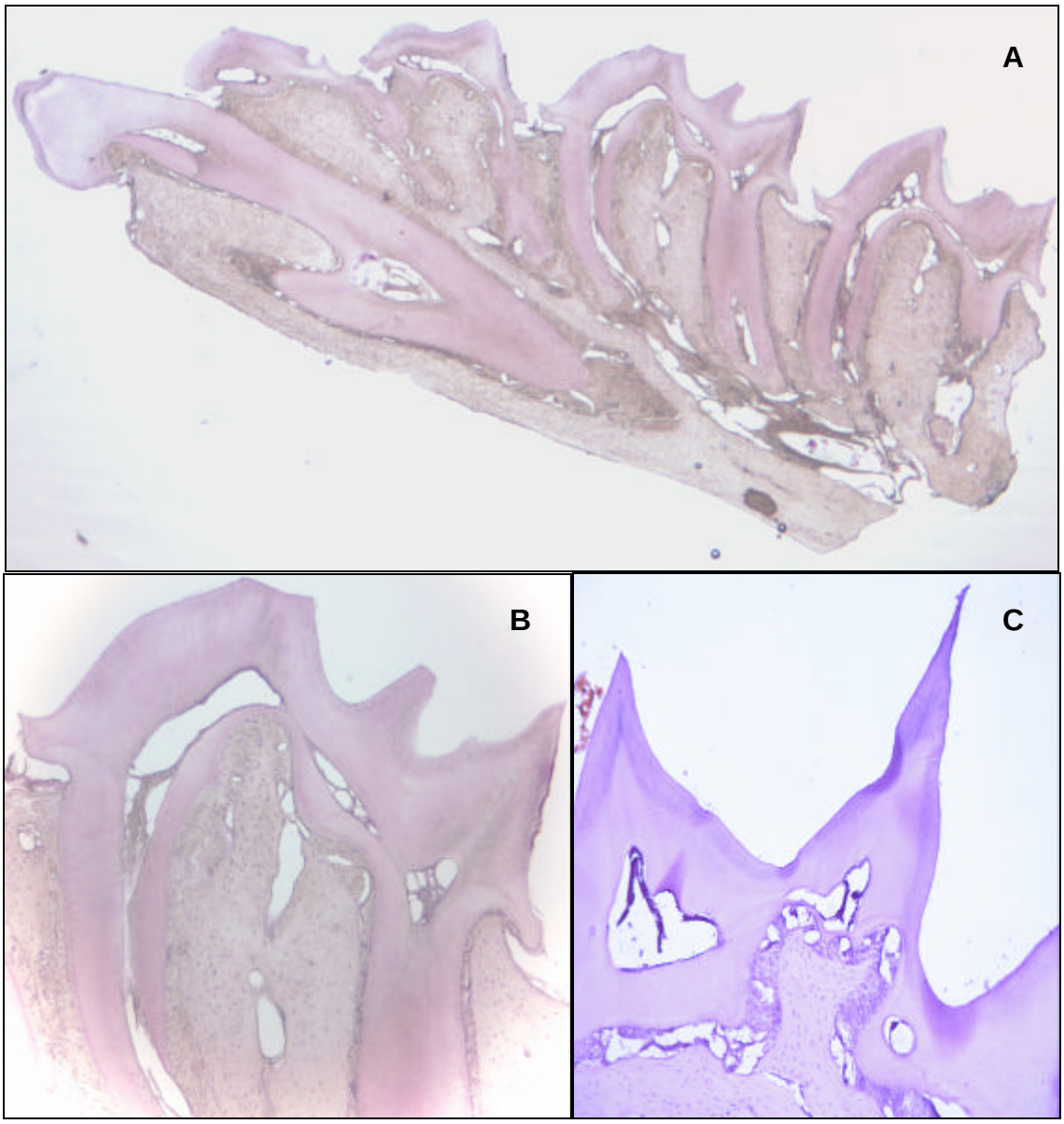

Fig. 9. Sectioned short-tail shrew lower jaws and teeth (20 µm), stained with hematoxylin, were used for age determination. Image A represents an entire jaw (20X magnification) of a young short-tailed shrew. Tooth crowns (100X magnification) were examined for the absence (Fig. B, young) or presence (Fig. C, old) of a growth ring.

between type I and II fibers. The method followed was precisely according to the recommendations of Ogilvie and Feeback (1990) and was carried out entirely at room temperature. This includes a 2-min ATPase preincubation (preincubation solution 2, pH = 4.5), followed by three 2-min Tris rinses (0.1 M, pH = 7.8), then a 25-min ATP incubation (incubation solution 3, pH = 9.4). Slides were rinsed in three changes of 1% calcium chloride solution, counterstained with 0.1% toluidine blue for 90 sec, then dehydrated rapidly (1 × 95%, 2 × 100% ethanol), cleared in xylene and mounted.

Picrosirius Red for Total Collagen

Total collagen was visualized with Picrosirius red histochemical staining (Sweat et al., 1964). The original method was modified by the addition of phosphomolybdic acid treatment, which has been reported to prevent uptake of the picrosirius red stain into the cytoplasm (Dolber and Spach, 1987). Sections were fixed in Bouin's solution (70% aqueous picric acid, 5% glacial acetic acid, 25% formalin) for 30 min. Slides were rinsed (1 min) in distilled water and placed in 0.2% phosphomolybdic acid for 5 min. Sections were then immersed directly in Picrosirius red solution (0.1% F3B Sirius red in saturated aqueous picric acid) for 90 min. Slides were rinsed for 10 s each in acidified H_2O (0.5% glacial acetic acid) and picric alcohol (20% ethanol, 70% dH_2O, 10% picric acid), then dehydrated (1 × 70%, 1 × 95%, 2 × 100% ethanol), cleared in xylene and mounted.

Immunohistochemistry for Collagen Typing

Collagen types I and III were analyzed in muscle cross-sections following the method described by Mackey et al. (2004). Frozen sections were fixed in pre-cooled (-20ºC) acetone, then blocked with 50 µL of 5% goat serum in TBS (50 mM Tris, 150 mM NaCl, pH=7.5) for 60 min at room temperature. Sections were washed (0.5% Tween-20 in TBS) and then incubated with 50 µL rabbit primary antibody (Rockland Immunochemicals, Gilbertsville, PA) for 40 min at room temperature. Primary antibodies were diluted in 1% BSA-TBS in the ratios of 1:75 for Type I collagen, and 1:100 for Type III collagen. Sections were washed again and incubated for 30 min at room temperature in 50 µL peroxidase-labeled goat anti-rabbit secondary antibody (Rockland Immunochemicals, 1:1000 diluted in 1% BSA-TBS). After a final wash, sections were exposed for 5 min to diaminobenzidine substrate-chromogen (DAKO, Carpinteria, CA). Slides were rinsed in dH_2O and then dehydrated, cleared and mounted.

Microscopy and Image Analysis

All images were collected using a Spot Pursuit Slider CCD camera and a Nikon E400 microscope. Images were exported in TIFF format, converted to grayscale, and analyzed using ImageJ image analysis software (version 1.37s, National Institutes of Health, USA). Muscle morphology, such as myocyte densities and cross-sectional areas as well as fiber type distributions were counted or calculated directly from calibrated images using a stage micrometer. A minimum of 50 myocytes were included in the

analyses for each animal, and cells directly adjacent to the edge of the section were excluded.

Total collagen from the sections was identified by positive staining with picrosirius red. ImageJ was used to threshold the images to isolate these stained intercellular regions. The area occupied by collagen (number of pixels^2) as a percentage of total area was calculated and recorded. Regions identified as Type I or Type III collagen from immunohistochemistry were also isolated through the thresholding function of ImageJ. The percent areas of each collagen type were recorded, as well as the Collagen I: Collagen III ratio.

Statistical Analyses

Results were analyzed using SPSS statistical software (version 11.5.1). Data was tested for normality using the Shapiro-Wilkes statistic and homogeneity of variance was confirmed using a modified Levene test. Data were natural log-transformed when necessary to meet assumptions for parametric tests. Results were compared using Nested Linear Mixed Model procedures (i.e., Fixed factor 'AGE' nested within fixed factor 'SPECIES'). Significance was set at the 5% level and means are presented ±1 S.E.M.

Results

Study Animals

A total of 19 water shrews (*Sorex palustris*), and 15 short-tailed shrews (*Blarina brevicauda*) were captured in the summers of 2005 and 2006 (Table 3). The average initial mass of captured water shrews was 14.12±0.29 g, while the average initial mass was 22.36±0.47 g for short-tailed shrews. There was no statistical difference between the initial masses recorded for old (n=9 WS; n=8 STS) versus young (n=10 WS; n=7 STS) animals from either species (t=1.057, df=14 with unequal variances, P=0.308 for water shrews; t=1.317, df=13, P=0.210 for short-tailed shrews).

Myocyte Morphology

Water shrew myocytes in the gracilis muscle were 30% larger in cross-sectional area ($F_{1,26}$=6.335, P=0.018) and occurred at 18% lower number/area ($F_{1,26}$=7.771, P=0.01) than did those of short-tailed shrews (Table 4; Fig. 10). While myocyte cross-sectional area appeared to be markedly different between young and old water shrews (829±5 versus 1036±7; Table 4), the distribution was noticeably right skewed, with two outlying high values for old water shrews. These data were natural log-transformed to regain a normal distribution, and the subsequent nested analyses did not reveal any age-related differences in cross-sectional area for either species ($F_{2,26}$=2.211, P=0.130). While a stronger statistical trend was apparent, myocyte number/cross-sectional area was likewise not different between age groups for either species ($F_{2,26}$=2.74, P=0.083).

Table 3. Summary of animals sampled during 2005 and 2006 in Manitoba, Canada.

Species	Age	*n*	Average initial mass (g)
Water shrew (*Sorex palustris*)	Old	9	14.49±0.35
	Young	10	13.79±0.45
Short-tailed shrew (*Blarina brevicauda*)	Old	8	23.31±0.67
	Young	7	21.26±0.69

Shrews were considered 'Old' (year 2) if a growth ring was observed in a sectioned and stained tooth from the lower jaw, otherwise, shrews were considered 'Young' (year 1).

Table 4. Morphological characteristics of gracilis sampled from two species of shrew. Muscle was transversely sectioned at 7-9 µm and stained with hematoxylin prior to analyses.

	Water shrew (*Sorex palustris*)		Short-tailed shrew (*Blarina brevicauda*)	
	Old (*n*=9)	Young (*n*=10)	Old (*n*=8)	Young (*n*=7)
Cross-sectional area (μm^2)	1036±7 *	829±5 *	632±5	669±8
Myocyte density (cells/viewing area)	87.9±1.7 *	111.4±1.6 *	121.6±2.7	106.4±3.1
Extracellular space (μm^2)	60236±43	54467±35 **	69225±48	40398±67 **

Myocyte density is presented as the number of myocytes contained within the analysis program's viewing area (143 838 μm^2). The single '*' denotes a significant (a=0.05) difference between species. The double '**' denotes a significant (a=0.05) difference between age classes.

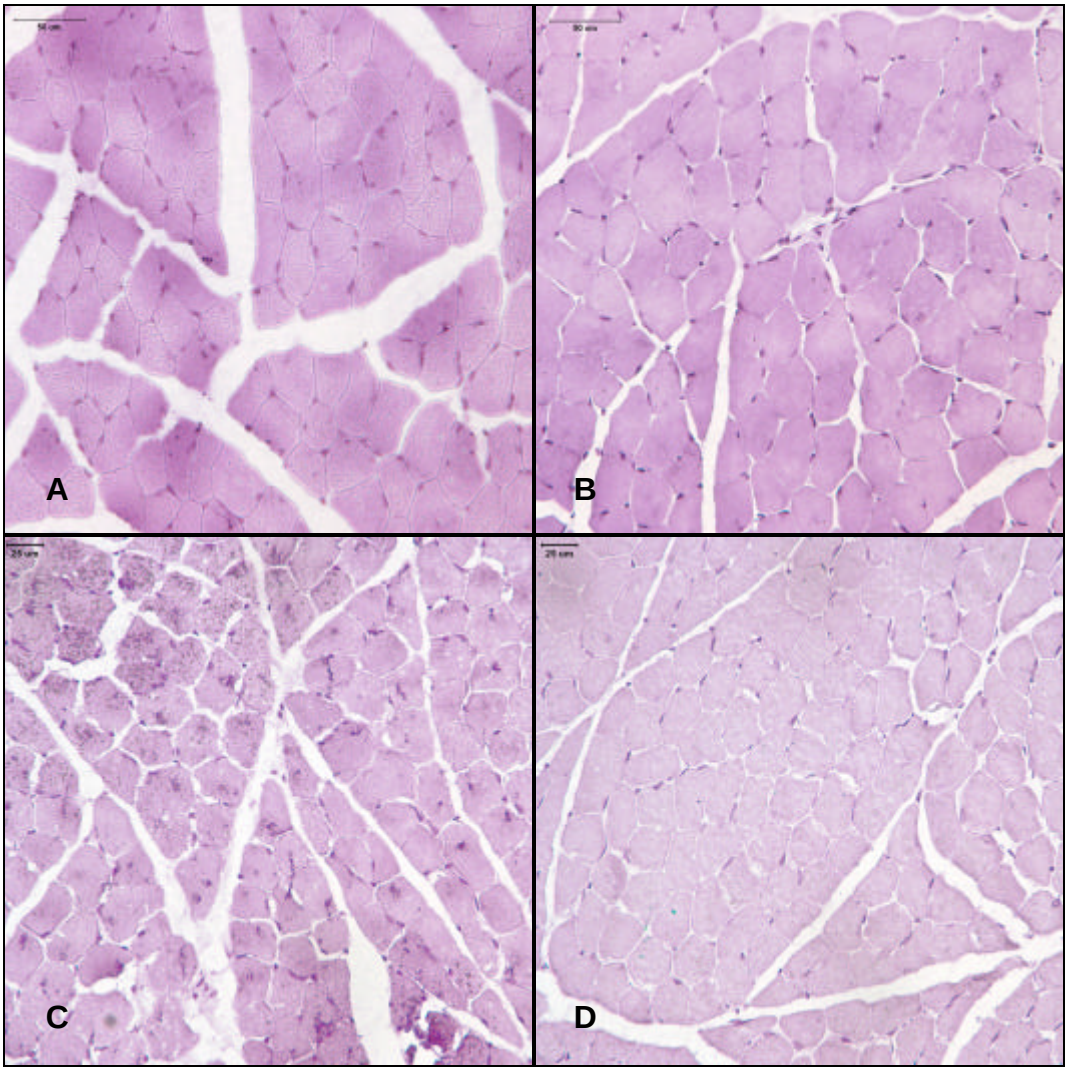

Fig. 10. Gracilis muscle (7-9 µm) stained with hematoxylin for contrast (400X magnification). Samples were collected from water shrews, *Sorex palustris* (A: old; B: young) and short-tailed shrews, *Blarina brevicauda* (C: old; D: young).

Extracellular space, however, the equation for which contains both previous morphological variables, was significantly elevated with age ($F_{2,26}$=4.489, P=0.021), but not different between species overall ($F_{1,26}$=0.029, P=0.867). For the diving species, the increased extracellular space in samples from old animals was 10%, while this difference for the non-diving species was ~70% (Table 4).

Myofiber Type

Metachromatic myosin-ATPase staining for muscle fiber type revealed homogeneous staining within each fiber. This indicates a total absence of fiber type I in both species (Fig. 11). Instead, the homogeneous staining (despite different intensity of coloration) indicates a composition entirely of type II myofibers. This staining pattern suggests that shrew muscle is composed solely of fast twitch fibers. Differentiation into type II subclasses was not possible with the staining method selected in this study, as inconsistent staining response of type II fiber subclasses has previously been documented in shrew species (Salvolainen and Vornanen 1995*b*).

Total Collagen

A considerable increase in intracellular collagen (~60%) was noted in old shrews of both species (20.2±0.9% area versus 12.3±0.7% area in water shrews, for example; $F_{1,26}$=5.816, P=0.008; Table 5; Fig. 12). There was, however, no difference between the

Table 5. Summary of collagen distribution within gracilis muscle (7-9 µm transverse sections) from young and old water shrews and short-tailed shrews.

	Water shrew (*Sorex palustris*)		Short-tailed shrew (*Blarina brevicauda*)	
	Old (*n*=9)	Young (*n*=10)	Old (*n*=8)	Young (*n*=7)
Total collagen (% area)	20.2±0.9	12.3±0.7 **	18.±1.1	11.5±1.2 **
Collagen: Muscle Ratio	899.6±6.8	648.3±4.9 **	1285.4±11.1	609.32±8.5 **
Type I: Type III Collagen Ratio	4.3±0.6	1.9±0.2 **	4.9±0.8	2.0±0.5 **

The double '**' denotes a significant (a=0.05) difference between age classes.

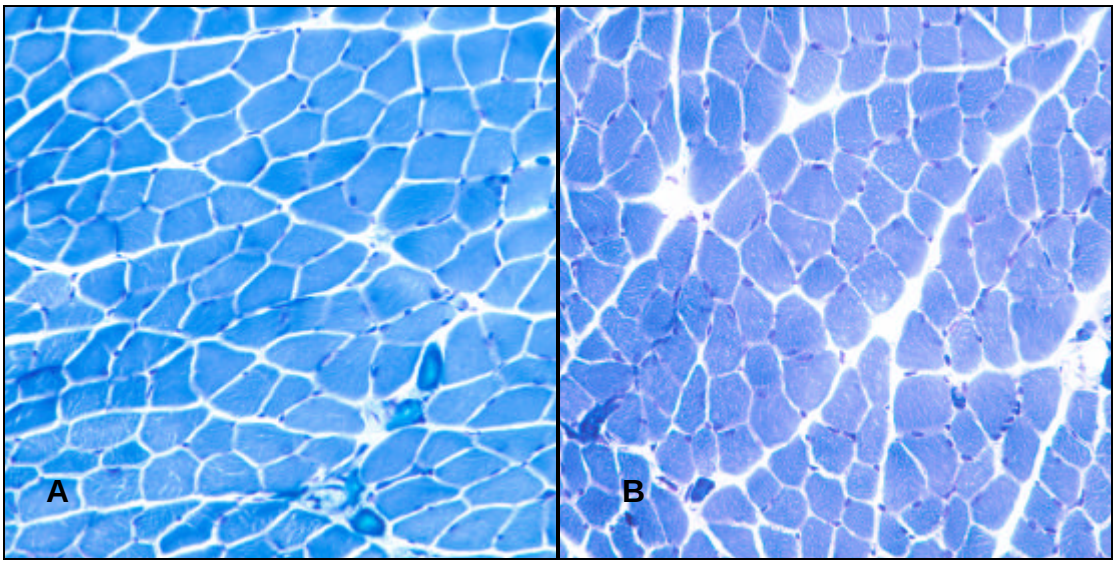

Fig. 11. Sectioned gracilis muscle (7-9 µm; 400X magnification) stained for myosin-ATPase using a metachromatic technique for single sections (Ogilvie and Feeback 1990). 'A' represents a sample of stained water shrew muscle, 'B' represents a similar sample taken from a short-tailed shrew. The homogenous staining in each fiber, with the absence of a denser staining near the myocyte exterior edge identifies all the fibers in these sections as type II (fast twitch).

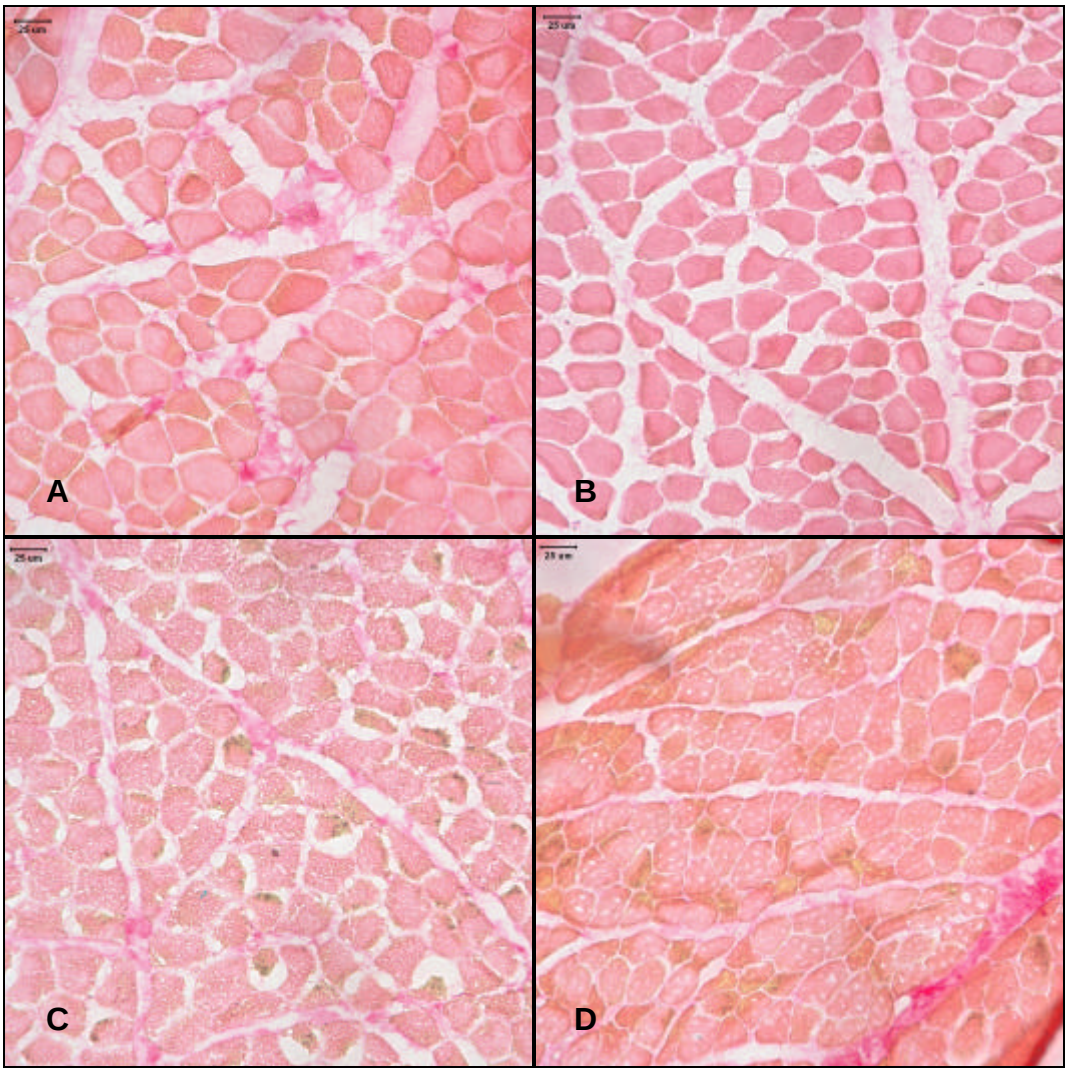

Fig. 12. Gracilis muscle sections (7-9 µm; 400X magnification) stained for total collagen content with picrosirius red. This staining technique labels intracellular collagen bright red in color. The cytoplasm does take on some red color also, but this effect is reduced by pre-treatment with phosphomolybdic acid. Representative sections from water shrews (A: old; B: young) and short-tailed shrews (C: old; D: young) are presented.

diver and the non-diver in this regard ($F_{2,26}$=0.048, P=0.838). The ratio between collagen and muscle area within the sections followed a similar trend (age effect: $F_{2,26}$=5.561, P=0.01). Old water shrews displayed a ~30% increase in this ratio compared to young animals, while this ratio more than doubled for old versus young short-tailed shrews (Table 5). There was not, however, a significant effect of species on this variable ($F_{1,26}$=3.227, P=0.084; Fig. 12).

Collagen Subtypes

Type I was the dominant form of collagen in all samples analyzed (Fig. 13A). While the ratio of collagen Type I: Type III was similar between species (ln-transformed: $F_{1,26}$=0.57, P=0.458), it increased by more than two fold for old shrews of both the diver and the non-diver (ln-transformed: $F_{2,26}$=8.745, P=0.001; Table 2-3; Fig. 13).

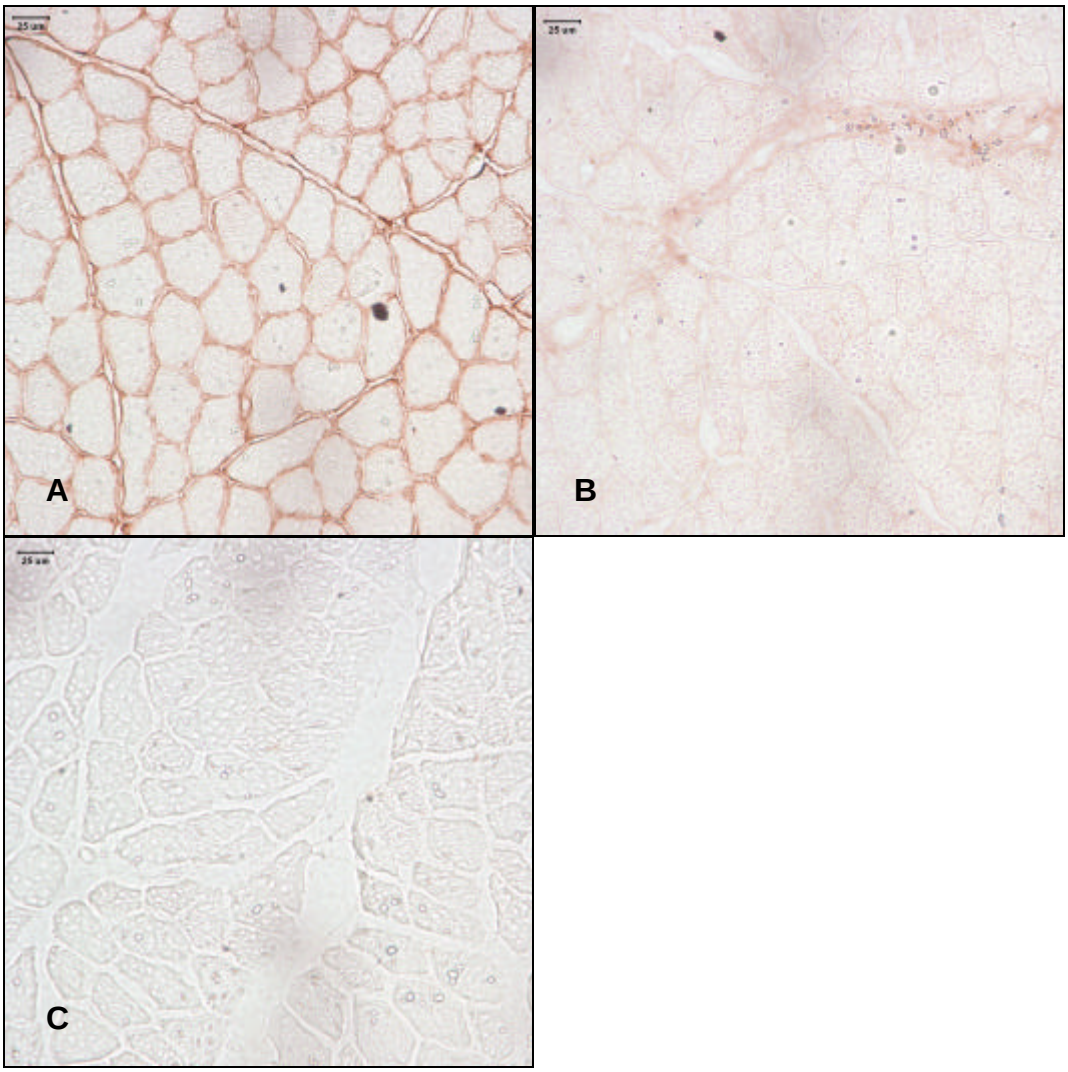

Fig. 13. Immunohistochemical staining for collagen subtypes in water shrew gracilis muscle (7-9 μm; 400X magnification). Type I is shown in A, Type III in B and the negative control in C.

Discussion

Myocyte Dimensions

The average cross-sectional area of gracilis muscle fibers was 923 μm^2 for water shrews and 667 μm^2 for short-tailed shrews. These data are in general consensus with the information previously published for this family, which includes a variety of measurements collected from the 7.9g common shrew (*Sorex araneus*), averaging between approximately 550 and 625 μm^2 (Savolainen and Vornanen 1998). Despite the general trend for a decline in skeletal muscle fiber area with decreasing body size in small flying and non-flying mammals (Pietschmann et al. 1982), the opposite trend is visible here between the 14.1-g water shrew and the 22.4-g short-tailed shrew. This could be nothing more than an example of a group of species which do not conform to the trend. Such an exception has been documented in pectoralis muscle of several small flying mammals (Pietschmann et al. 1982). More likely, however, this difference in fiber size indicates a discrepancy in the degree of use the muscle receives in each species.

The gracilis muscle is superficial and lies on the medial thigh. It functions primarily as a supplemental muscle in motions such as flexion and adduction of the thigh at the hip, and in medial rotation of the flexed knee. It is likely that the whole-body aquatic locomotion of the water shrew involves the gracilis. By contrast, the short-tailed shrew is less likely to require output from gracilis during terrestrial locomotion. As well, fossorial animals, such as moles, rely more heavily on forelimb for digging. This is supported by limb-specific myoglobin values, which are high in forelimb for moles

such and the coast mole and start-nosed mole (McIntyre et al. 2002), and equal between limbs for the water shrew (R.W. Gusztak, Unpubl. Obs.).

The finding of increased fiber volume in the smaller water shrew is interesting, since it would serve to decrease intercapillary distance. This would be a clear drawback for a diving animal relying very heavily on aerobic metabolism underwater, as evidenced by the low buffering capacity of water shrew muscle (R.W. Gusztak, Unpubl. Obs.). This could be countered by the general increase in capillary density with decreasing mass, which has been described in other species (Mathieu-Costello et al.2002; Pietschmann et al. 1982). In those reports however, it is difficult to determine to what degree this change in capillary density is the result of increased capillarization, and what is simply the result of decreased fiber volume.

While cross-sectional area does not change significantly with advancing age, there is a 25% increase in the fiber cross-sectional area of water shrews. This is observed despite no significant mass change between the age groups. It is entirely possible that the lack of significance for this clear trend is the result of insufficient sample size given the decidedly skewed distribution of the data. This trend is also counterintuitive to the typical mammalian response to aging, which describes muscle atrophy, or decreased muscle cross-sectional area and fiber loss, although an age-increase in fiber cross sectional area has been documented in horses (Rivero et al. 1993). As part of skeletal muscle aging in mammals, one major occurrence is denervation, resulting in the removal of fast motor units from the aging muscle. This is a major cause of disuse atrophy, and is seen in humans and laboratory populations (e.g., Kovanen

1989). Since cross-sectional fiber area is an important determinant of force output, this occurrence is interesting when you consider that old versus young shrews, or any wild animal in point of fact would be expected to have similar contractile output requirements for foraging or predation elusion. Prey and predators still move at the same speed. Perhaps the loss of motor units coupled with the sustained requirements of existence in their habitat could cause an exercise-induced hypertrophy of remaining fibers, accounting for the increased size. Considering that younger animals appear to have a better response to exercise- (or stretch-) induced hypertrophy (e.g., Lee and Alway 1996) this is strongly indicative of the use of gracilis muscle in water shrew locomotion. The reduced reliance on this muscle group for short-tailed shrews would explain why a similar increase in fiber area was not seen with age in this species.

What was significant in relation to myocyte morphology and aging was the extracellular space, which was significantly elevated in both shrew species. Short-tailed shrews demonstrated a ~70% increase in this parameter, while water shrew ECS was elevated by no more than 10%. Presumably any increase in myocyte cross-sectional area would be compensatory to increases in ECS. The mechanism for this increase in ECS with age is likely that described above; namely the loss of motor units via apoptosis and denervation, and the incomplete reinnervation by slower neighboring motor neurons. In mammals we observe a disproportional denervation and loss of ‘fast’ muscle fibers (Brooks and Faulkner 1994), which can then be reinnervated and taken up into ‘slow’ motor units. This process has been indirectly documented in other species of shrew. While it is typical for mammals to demonstrate a shift from type II to type I motor units

with advancing age, shrews have not previously been noted to have any type I fibers in their muscle. Thus, the 'slowing' effect of age in shrews has been described as a shift in fast glycolytic IIb to fast oxidative IIa or IIx (Savolainen and Vornanen 1995*a*).

Muscle Fiber Type

Metachromatic myosin-ATPase staining for muscle fiber type revealed homogeneous staining within each fiber. This indicates a total absence of fiber type I in both species, since the presence of a darker band around the fiber periphery is diagnostic of type I fibers with the method used (Ogilvie and Feeback 1990). Instead, the homogeneous staining (despite different intensity of coloration) indicates a composition entirely of type II myofibers. This staining pattern suggests that shrew muscle is composed solely of fast twitch fibers. This observation is in good accord with the literature, as type I myofibers (or myosin heavy chains, MHC) have not previously been documented in any of the common shrew (*Sorex araneus*, Savolainen and Vornanen 1995*a*,*b*), Etruscan shrew (*Suncus etruscus*, Peters et al. 1999; Jürgens 2002) or common European shrew (*Crocidura russula*, Peters et al. 1999). Since stride frequency of animals depends on body mass, higher shortening velocities (i.e., more fast twitch fibers) would be expected in smaller animals.

A shift from MHCIIb (fast glycolytic) to MHCIIx (fast oxidative glycolytic) with advancing age occurred in seven muscle groups studies in the common shrew (Savolainen and Vornanen 1995*a*). This is an interesting adaptation of the 'slowing' trend observed in other mammals, which in larger mammals would entail an increased

percentage of type I groups in senescent muscle. This trend holds even in healthy humans and exercise training models. In fact, exercise training with advancing age in rats not only fails to reverse this shift, but rather accelerates the transition to slower, more fatigue resistant fibers (Kovanen and Suominen 1989). Differentiation into type II subclasses was not possible with the staining method selected in this study, therefore I was unable to document whether a similar slowing shift within type II MHC occurred in the two species examined here. In contrast to rat tissues, identification of type II subclass for shrew fibers was not possible, despite the use of several traditional histochemical techniques (Salvolainen and Vornanen 1995*b*). Differentiation of type II subclasses was possible using the Brooks and Kaiser (1970) method; however the labeling of the subtypes was reversed. To resolve this issue, further staining could be performed to identify SDH-activity (Reichmann and Pette 1984). This technique has been used in shrews to classify 'highly oxidative' and 'less oxidative' type II muscle fibers (Savolainen and Vornanen 1995*b*). The gold standard method for fiber subtype identification in this case would however be MHC immunoblotting.

Collagen

An increase in extracellular collagen component of the endomysium was noted in old shrews of both species. As expected, this was accompanied by an increase in the ratio of collagen: muscle area. Although no age significant age effect was noted (P=0.084), the smaller increase in the ratio noted for water shrews versus short-tailed shrews corresponds to the slight increase in myocyte area noted for old water shrews.

This is the first study to demonstrate these ECM changes in wild-caught animals that are so widely demonstrated in humans, as well as laboratory and sedentary domestic species. Increases in total collagen, collagen stability and cross-linking, and resulting passive muscle stiffness have each been widely documented in human and domestic models (Mohan and Radha 1980; Kovanen and Suominen 1989; Gosselin et al. 1998). Biosynthesis of collagen is not affected with aging, indicating that the build-up of connective tissue in the extracellular space is the product reduced degradation with age (Kovanen and Suominen 1989; Gosselin et al. 1998). Extracellular degradation of collagens is handled by matrix metalloproteases, primarily by the collagenases MMP-1 and MMP-8 (Kovanen 2002). Maturation of collagen in the extracellular space involves the development of hydroxylysylpyridinoline (HP), or non-reducible cross-linking, as well as increased glycation (Kjaer 2004), which serves to increase collagen stability. This not only impedes collagen breakdown and turnover in senescent muscle, but also increases the muscle's passive stiffness. In fact, generally speaking, total muscle collagen is positively correlated to tissue stiffness (Kovanen et al. 1984; Gosselin et al. 1994; 1998). More than that, while different muscle types (i.e. slow versus fast) exhibit different degrees of passive stiffness, or tensile strength, their strength per unit collagen is the same, indicating that collagen is the main determinant of stiffness and tensile strength in muscle (Kovanen et al. 1994).

Exercise training in laboratory models, or the lack thereof (e.g., hindlimb unloading) is able to modulate parts of this collagen response. This is not surprising given that the ECM is known to be dynamic and appears to respond to mechanical stress.

In a classic example, two years of endurance training in rats resulted in an increased proportion of slow muscle, with a corresponding increase in total collagen with age and therefore tensile strength (Kovanen et al. 1984). Conflicting results have also been published in a study involving 10 weeks of endurance training in old rats. The study concludes that training does not affect total collagen content, and that collagen cross-linking and therefore muscle stiffness is also reduced with age (Gosselin et al. 1998). This is suggested to be due to increased rates of collagen turnover.

Type I was the dominant form of collagen in all samples analyzed. While the ratio of collagen Type I: Type III was similar between species, it increased by more than 2X for old shrews of both the diver and the non-diver. While this occurrence has also been well documented in laboratory species (e.g. Kovanen and Suominen 1989), this is also the first demonstration of the widely acknowledged structural change in senescent muscle occurring in a wild population.

Type I collagen tends to occur as parallel fibers, conferring strength and rigidity. Its presence is noted especially in slow type muscles, where it confers much of the rigidity required for isometric contractions, and the storage of elastic energy capturing upon lengthening to increase fatigue resistance (Kovanen 2002). Type III collagen, on the other hand, exists as a loose meshwork, and is generally thinner in structure than Type I. This confers compliance to muscle, and therefore Type III is associated more with fast twitch muscles, where the elasticity of the ECM allows the muscle to change it size and contract more quickly (Kovanen 2002).

Following jump training in rats there was an increase in Type III collagen, which accompanied a fiber type shift in the muscle from slow-fast (Pousson et al. 1991). With hindlimb unloading, a shift from Type I to III collagen was also noted along with the slow-fast transition (Miller et al. 2001). With the opposite stimulus of endurance training, there is a fast-slow shift in muscle, which results in a decrease in Type III collagen (Goubel and Marini 1987). An increase in Type I fibers is also documented in fibers undergoing a 'slow' transformation due to electrical stimulus (Miller et al. 2001).

The combined effect of increased total collagen and increased Type I: III collagen ratio with aging has combined effects on muscle function. On one hand increases in muscle tensile strength confer some benefit for stability and fatigue resistance. On the other hand, stiffness in muscle affects its ability to store and release elastic energy during contraction, this decrease in Type I collagen decreases fatigue resistance. How the interplay of these factors effects muscle function remains a matter of speculation. A decrease in the passive compliance of old muscle makes the muscle more load resistant, but also decreases its ability to adjust to altered loading, which can lead to injury. Additionally, the increase in the muscle's passive tension is due to an increase in the parallel elastic component. The result of this is a greater output of force for a given strength of contraction, since the generated force must first overcome the elastic component.

Does Aging Impact Muscle Function in Shrews?

Increased collagen with age confers stability, which may be beneficial to slower, more postural muscle (type I). In shrews, which rely entirely on type II fibers, this increased stability may occur at the expense of contraction speed and force generation, which may compromise stride frequency, and therefore locomotion. In addition to the potential performance loss due to changes in the ECM, shrews may also suffer from other components of sarcopenia, such as loss of specific force (force per unit cross-sectional area; Brooks and Faulkner 1994; Thompson 1999). Loss of force generation in this manner been causally linked to the impairment of excitation–contraction coupling (Payne and Delbono 2004). This includes alterations in the conformation of the myosin head during contraction (Larsson et al. 1997; Krivickas et al 2001; Lowe et al. 2001; 2004), and changes in the kinetics of the enzyme actomyosin ATPase (Prochniewitz et al. 2005). Any impairment of excitation-contraction coupling or increased deposition of collagen in skeletal muscle might increase the internal work requirement for force generation. If a given force output is required of muscle to maintain stride frequency and locomotory speed, the occurrence of either as a consequence of age could be problematic. Even small-scale changes in force generating capacity would be of particular concern for a small animal such as a shrew, which relies solely on fast twitch muscle contraction.

4. PRO- VERSUS ANTIOXIDANT STATUS WITH AGE IN TWO SPECIES OF SHREW

Introduction

The 'free radical theory of aging' (Harman 1994) posits that maximum longevity and aging are driven by free radicals, such as reactive oxygen species. The production of free radicals is thought to increase with aging in skeletal muscle (e.g., Lass et al. 1998), likely due to accumulating mitochondrial damage with age resulting in increased ROS release (Barja and Herrero 2000; Sastre et al. 2000). One suggestion is that free radicals may adjust the regulation of apoptotic processes in the cell, and that apoptotic dysregulation may be involved in aging (see Higami and Shimokawa 2000 for review of this and alternative interpretations). If free radical exposure may be linked to cellular aging, then diving mammals could prove to be a unique mammalian model for investigating the topic.

The mammalian dive response is designed to conserve oxygen. This is accomplished via apnea, bradycardia, and peripheral vasoconstriction to non-essential vascular beds (Butler and Jones 1997). The dive response also acts to partition metabolic activities in advantageous ways. Oxygen conservation and partitioning together should increase available underwater time. Although aerobic metabolism is generally maintained in mammals in primary locomotory muscles, severe local hypoxia may develop by the end of dive. A paradox of oxidative stress is that a surge of free radicals can be generated in situations where oxygen is in surplus, or in deficit. The respiratory chain develops a highly reduced redox state under hypoxia (i.e., too many

reducing equivalents drives the single-electron reduction of O_2). Hypoxia, therefore, is likely to be a chronic contributor of ROS to skeletal muscle in divers (see Clanton et al. 1999 for review). The maintenance of aerobic metabolism under such conditions increases the relative rate of ROS production (Vanden Hoek et al. 1997*b*), and the degree of ROS production during hypoxia is directly dependent on residual O_2 available in tissues (Becker et al. 1999; Berrizbeitia et al. 2002). Thus O_2 access through myoglobin or exposure to neighboring cells has an exacerbating effect.

At present, hypoxia's influence in skeletal muscle is not well-studied; although in vitro studies of hypoxic (3-4 Torr) cardiomyocytes (Vanden Hoek et al. 1997*a*) indicate that low oxygen itself is sufficient to significantly increase the mitochondrial production of superoxide radicals. A similar situation may be present in the skeletal muscle of divers, where end-dive muscle PO_2 (in seals) is known to decline to considerably less than 5 Torr, even when muscles remain at rest (Guyton et al. 1995).

Diving mammals have been postulated to be "a model for coping with oxidative stress" (Zenteno-Savín et al. 2002). This statement arose from a series of direct and indirect measurements in ringed seals (*Phoca hispida*). The kidneys of seals regained function following ischemia, while those of dogs often did not (Halasz et al. 1973). Seal tissues also contain significantly lower levels of hypoxanthine following ischemia than those of pigs, providing reduced substrate for xanthine oxidase-produced ROS (Elsner et al. 1998). Elevated levels of antioxidants have also been documented in the tissues of ringed seals, which the authors suggest is protective against the oxidative stresses

associated with ischemia and reperfusion during diving and surfacing (Zenteno-Savín et al. 2002).

Closer evaluation of this evidence reveals several inconsistencies in the data. For instance, there is not a clear elevation of seal antioxidant levels in all tissues examined, particularly in muscle (Zenteno-Savín et al. 2002; Vázquez-Medina et al. 2006). A higher generation of superoxide is also noted in conjunction with the elevated antioxidants in seal versus pig tissues (Zenteno-Savín et al. 2002). It is possible that such findings may simply be an artifact of the high oxidative capacity of pinniped muscles (due to high proportions of slow twitch/oxidative fibers; e.g., Watson et al. 2003), resulting in above-average antioxidant but also oxidant potential (e.g., Pansarasa et al. 2002. In addition to the inconsistencies of these data, no consideration has been made of how this uniquely adapted system might respond to aging pressures.

One of the most extreme examples of a diving mammal is the North American water shrew. At 8-18 g (Beneski and Stinson 1987), this is the smallest homeothermic diver. Controlled-dive lengths of 37.9 ± 5.3 sec (SD, n = 6) have been recorded from this species (Calder 1969). One could argue, however, that based on the behavioral ADL recorded for water shrews (~5.2 sec; R.W. Gusztak, Unpubl. Obs.), and the unknown degree to which gas exchange from the lung occurs during submersion, that shrews are less of a 'diver' and more of a 'dipper'. In general, shrew muscle is noted for its extremely high contraction frequency and metabolism (e.g., Jürgens 2002). Such energy requirements should correspond to elevated production of ROS during muscle contraction. Unlike larger divers such as seals, whose muscle infers some antioxidant

protection from a high proportion of slow Type I fibers, shrew muscle will not have such benefit. Measurements of fiber-type patterns, myosin composition, and LDH and CS activities all suggest exclusively fast-type fibers in shrew muscle, with IId (fast oxidative) fibers most abundant (Peters et al. 1999; Savolainen and Vornanen 1995*a*). These measurements were also statistically identical in comparisons of EDL (extensor digitorum longus; typically "fast") and soleus (typically "slow") muscles (Peters et al. 1999). Even with aging, the typical shift towards slow motor units observed in other mammals occurs in shrews as a shift from Type IIb to IId myosin heavy chain isoforms (Savolainen and Vornanen 1995b). Thus, shrews could experience the highest ROS exposure (due to muscle metabolism) of any diver. Furthermore, the exclusive occurrence of Type II fibers in shrews cements this species as an extremely viable aging model, since it is Type II fibers that are targeted by apoptosis and atrophy during aging (Holloszy et al. 1991). The diving shrew therefore presents a novel mammalian system in which to investigate the influence of aging on skeletal muscle physiology.

In this experiment, muscle samples collected from the diving water shrew with similar samples collected from field-caught short-tailed shrews. These species occupy similar habitats, with the exception being the aquatic component of the water shrew's life history. Samples from old and young individuals from both species were compared to analyze differences in antioxidant capacity, oxidative stress markers, and apoptosis.

Materials and Methods

Capture, Animal Care and Sampling

Adult and yearling North American water shrews (*Sorex palustris*) and Northern short-tailed shrews (*Blarina brevicauda*) were captured and held as previously described (see Section 3; Hindle et al., 2003; Gusztak and Campbell, 2004). All study animals were captured and cared for in accordance with the principles and guidelines of the Canadian Council on Animal Care (University of Manitoba Animal Use Protocol # F05-014).

Shrews were euthanized with an overdose of isoflurane inhalant anesthetic. Muscles from the forelimb and hindlimb were dissected quickly and frozen in liquid nitrogen for subsequent biochemical analyses. Following tissue harvest, the lower jaws were collected for age determinations, as previously described (see Section 3). Muscle samples were stored at -80ºC.

Tissue Homogenization

Combined hindlimb and combined forelimb muscles were homogenized on ice in lysis buffer (10mM HEPES, 350mM NaCl, 20% glycerol, 1% Igepal-CA630, 1mM $MgCl_2$, 0.1mM DTT), using a glass-on-glass tissue grinder. Homogenate was centrifuged at 12,000 *g* to remove cellular debris. The supernatant was withdrawn and stored at -80ºC until analyses. Total protein was measured using the Bradford technique. Unless otherwise noted, all enzyme activity assays were conducted at room temperature.

Citrate Synthase Activity

The activity of citrate synthase was measured as an indicator of oxidative potential (modified from Srere, 1969). Citrate synthase acts as a ligase for the substrates acetyl CoA and oxaloacetate, forming CoASH and citrate products. CoASH further reacts in the presence of Ellman's reagent (DTNB) to form mercaptide ion, whose production can be monitored at 412 nm. Reaction cocktail (1.0 mL; 0.1 mM DTNB, 0.07% Triton X-100, 0.1 mM acetyl CoA in 100 mM potassium phosphate buffer with 10 mM EDTA, pH = 7.4) was combined with 10 µL of 1:50 homogenate in a cuvette and incubated for 5 min. The substrate oxaloacetate (50 µL; 0.1 mM in buffer) was added and the reaction was followed from 1-4 min. Enzyme activity was expressed as Units per g wet weight of muscle.

Antioxidant Enzyme Activities

The activity of catalase can be measured directly by the extinction of H_2O_2 at ultraviolet wavelengths. Since the oxidation of H_2O_2 by catalase occurs extremely quickly ($k \sim 10^7$) and does not follow the Michaelis-Menten model, catalase activity was measured by following exponential absorbance change at 240 nm over 90 s. Homogenate (1:50) was incubated 1:10 with ethanol for 30 min on ice, then with 1% Triton-X for 15 min at room temperature. The reaction was started by combining this mixture (500 µL) with 500 µL hydrogen peroxide solution (10 mM) in a cuvette (Aebi, 1984). Catalase activity was expressed as Units per g wet weight of muscle.

Glutathione peroxidase (GPx) activity was assayed according to the method of Flohé and Günzler (1984). The conversion of GSH to GSSG, which is catalyzed by GPx, is coupled with the reverse reaction, catalyzed by glutathione reductase. In the reduction reaction NADPH is used as an electron donor substrate, and its depletion in solution can be followed at 340 nm. One unit of GPx activity is the amount required to oxidize 1 mole of GSH/min (which corresponds to the oxidation of 0.5 mole NADPH/min). Muscle homogenate (1:100 dilution; 100 µL) was combined with 800 µL reaction cocktail (0.3 $U \cdot mL^{-1}$ glutathione reductase, 1.25 mM GSH, 0.1875 mM NADPH in 100 mM potassium phosphate buffer with 10 mM EDTA) in a cuvette. The solution was incubated for 3 min at room temperature. The reaction was initiated by adding 100 µL of 12 mM *t*-butyl hydroperoxide, and was monitored from 0-4 min. A blank contained 0.5% BSA in buffer in lieu of homogenate was also run. GPx activity was expressed as Units per g wet weight of muscle.

Superoxide dismutase (SOD) was assayed using an electrophoresis technique (Beauchamp and Fridovich, 1971). Samples (100 mg protein) were kept on ice and loaded into 10% polyacrylamide gels containing 8M urea. SDS was absent from all gels, sample loading buffer and running buffer. Samples were electrophoresed at 4°C in standard Tris-Glycine buffer (pH = 8.3), then placed in staining dishes and treated at room temperature. Gels were photosensitized by soaking in 2.45×10^{-3} M nitroblue tetrazolium in 0.036 M potassium phosphate buffer, pH = 7.8 for 20 min, then washed briefly. Gels were then immersed for 15 min in the dark in a solution containing 0.028M TEMED and 2.8×10^{-5} M riboflavin in buffer, then washed again. After rinsing in dH_2O,

gels were placed on glass plates and illuminated for 5-15 min. When exposed to light the gel background became blue except at positions containing superoxide dismutase. The staining patterns were then photographed, and the intensity of the superoxide dismutase bands compared to positive controls run with SOD isolated from bovine liver (Sigma).

Oxidative Stress Indicators

The probe dihydroethidium (DHE) is a substrate for the flurometric detection of oxidants, which produces the fluorescent product ethidium upon dehydrogenation. This reaction occurs strongly in the presence of superoxide and peroxynitrite ($ONOO^-$), but weakly with H_2O_2, allowing its use as an indicator of the presence of reactive oxygen species (based on Supinski et al., 1999). The presence of antioxidants at physiologically relevant concentrations will also influence the dehydrogenation (Supinski et al., 1999). The ethidium product has an excitation wavelength of 465 nm and an emission wavelength of 585 nm. Flurometer operation was first confirmed and optimized with a standard curve of ethidium bromide. The reaction was prepared in 100 mM potassium phosphate buffer, pH = 7.4. Muscle homogenate (1:50; 160 µL), 240 µL of 1mM purine in buffer, 400 µL of 44 µM DHE, and 400 µL of methanol were mixed well and incubated for 10 min at 37°C before reading. Methanol was required in the reaction to dissolve DHE. Sample fluorescence was quantified in xanthine oxidase units based on a standard curve.

Lipid peroxidation was quantified based on xylenol orange oxidation (Hermes-Lima et al., 1995). The reaction constituents were prepared in 100 mM potassium phosphate buffer (pH = 7.4), combined in a cuvette and incubated in the dark for 12 hours in the following quantities: 225 µL 1mM $FeSO_4$; 90 µL 0.25M H_2SO_4; 90 µL 1 mM xylenol orange; 468 µL 0.055M H_2SO_4; 180 µL 1:50 homogenate. In acidic solution, hydroperoxides catalyze the reaction of xylenol orange with the iron in ferrous sulfate to yield a spectrophotometrically detectable product. Total hydroperoxides detected after an overnight incubation in the dark were expressed based on a concurrently run *t*-butyl hydroperoxide standard curve.

Western Immunoblot Analyses

Protein content of the oxidative stress indicator 4-hydroxnonenol (4-HNE) as well as the antioxidant enzymes Cu,Zn-SOD and Mn-SOD were determined through Western immunoblotting. Samples were separated on 1-mm thick, 15% polyacrylamide gradient gels containing SDS (NextGel: pH = 8.3, Amresco, Solon, OH), which were polymerized by the addition of TEMED and ammonium persulfate, and cast and run with a Mini-Protean 3 setup (BioRad, Hercules, CA). Thirty µg of protein (after evaporation) were mixed with sample buffer (Tris pH = 6.8, 2% SDS, 60 mM DTT, 25% glycerol) and denatured for 4 min at 90°C. They were then loaded into the wells and electrophoresed for 90 min at 145 V. The gels were then transferred for 90 min at 45 V onto nitrocellulose membranes (BioRad). After confirming the presence of consistent protein transfer to the nitrocellulose with a Ponceau S stain, the gels were rinsed in PBS

and blocked with 5% non-fat milk (in PBS with 0.1% Tween-20) at room temperature for 4 h. Blocked membranes were washed for 5 min three times in PBS and 0.4% Tween-20, then were incubated overnight with specific primary antibodies diluted in PBS. Dilutions for primary antibodies were as follows: 4-HNE adducts, 1:5000 (rabbit polyclonal, Calbiochem, San Diego, CA); Cu,Zn-SOD, 1:500 (rabbit polyclonal, Santa Cruz Biotechnology, Santa Cruz, CA); and Mn-SOD, 1:5000 (rabbit polyclonal, Stressgen, Ann Arbor, MI). Membranes were washed again (three times 5 min) in PBS and 0.4% Tween-20, then incubated at room temperature for 90 min with HRP-conjugated anti-rabbit secondary antibody (Rockland Immunochemical, Gilberstville, PA). Following another set of three washes in PBS and 0.4% Tween-20, protein bands were visualized using enhanced chemiluminescence detection (Supersignal West Pico Chemiluminescent Substrate, Pierce, Rockford, IL).

Images of the blots were captured with a CCD digital camera in a darkroom with the following exposure times: 4-HNE, 30 sec; Cu,Zn-SOD, 30 sec; and Mn-SOD, 10 sec. Images were converted to grayscale and densitometry [area*(density – background for each lane)] was calculated using ImageJ software (version 1.37s, National Institutes of Health, USA).

Markers of Apoptosis

Apoptotic cell death in muscle homogenate was measured with a cell death ELISA kit (Roche #11544675001, Indianapolis, IN). This assay measures the presence of mono- and oligonucleosomes (double-stranded, low molecular weight DNA

fragments) in the cytoplasm, which are diagnostic of the nuclear condensation and DNA cleavage that occurs during apoptosis. It is considered an extremely sensitive technique for quantifying apoptosis (Dirks and Leeuwenburgh, 2002). Results are expressed in arbitrary absorbance units per mg protein.

In addition to the production of double-stranded mono- and oligo-nucleosomes during apoptosis, high molecular weight DNA is often subject to single strand breaks ("nicks"). The free 3'-OH terminal of those strand breaks was directly labeled in sectioned gracilis muscle (please see Section 3 for the description of muscle collection, preparation and sectioning). Labeling was carried out via the TUNEL method (Terminal deoxynucleotidyl transferase-mediated dUTP Nick-End Labeling), which uses the enzyme Terminal deoxynucleotidyl transferase (TdT) to attach a fluorescein label to DNA nick ends. Shrew muscle was triply labeled with DAPI (to identify all nuclei), TUNEL (to identify apoptotic nuclei) and laminin (to delineate the basal lamina/extracellular matrix). This labeling scheme allowed nuclei to be distinguished based on location as satellite cells, which occur outside the basal lamina or myonuclei, which occur within the myocyte.

TUNEL labeling was performed following the directions of an in situ cell death detection kit (#11684795910, Roche). Muscle sections on glass slides were removed from the freezer and dipped in PBS, then fixed for 20 min at room temperature in 2% buffered paraformaldehyde. Slides were washed in PBS (three 5-min washes) and incubated in permeabilzation solution (0.2% sodium citrate, 0.1% Triton-X-100) at room temperature for 5 min. Slides were washed again and positive control slides were treated

for 10 min with DNase solution (#4536282001, Roche). After subsequent washing with PBS sections were incubated with TUNEL labeling solution for 60 min at 37°C in the dark. Slides were kept in the dark from this point in the procedure onward, to prevent quenching of the fluorescent labels. Sections were washed in PBS a final time and then labeled for laminin with an immunohistochemical technique.

Primary anti-laminin antibody was applied to sections for 40 min at room temperature (1:25 dilution in 1% BSA-TBS of rabbit polyclonal, Sigma, St. Louis, MO). Sections were washed (0.5% Tween-20 in TBS) then incubated with 50 µL Cy3-labeled Fab' secondary antibody (Sigma), diluted to 1:200 in 1% BSA-TBS. After a final wash slides were coverslipped with an aqueous mounting medium containing DAPI (Vector Labs, Burlingame, CA).

Monochrome images for each label were collected from a Spot Pursuit Slider CCD camera and a Nikon E400 microscope. DAPI bound to DNA emitted blue fluorescence which was viewed with Nikon filter UV-2E/C. Laminin emitted red fluorescence which was viewed with Nikon filter G-2A. Fluorescein emitted green fluorescence and Nikon filter B-2E/C was selected to view the product as it is a bandpass

green filter which eliminates bleed-through from the red wavelengths. The images from the three channels were overlaid using SPOT software and the locations of apoptotic cells were counted directly from the images. All myocytes were analyzed, with the exception of those directly adjacent to the edge of the section.

Statistics

SPSS statistical software (version 11.5.1) was used for all analyses. Data were tested for normality using the Shapiro-Wilkes statistic and homogeneity of variance was confirmed using a modified Levene test. Data were transformed when necessary to meet the assumptions of parametric tests. Results were compared using nested linear mixed model procedures. Means are presented ±1 S.E.M. In figures, single asterisks (*) are used to denote species differences, and double asterisks (**) are used to denote age class differences.

Results

Muscle Oxidative Capacity

For most biochemical characteristics examined there were no detectable differences between forelimb and hindlimb muscle homogenate. Therefore, with the exception of one oxidative stress indicator (see below), only hindlimb values are reported and compared here. Hindlimb samples were selected for analyses because generally a larger sample could be collected from this area, and hindlimbs are expected to have similar locomotory contributions in both species. Additionally, hindlimb was collected and frozen first following sacrifice.

The concentration of muscle protein was similar in both species examined (8.57 $\mu g \cdot \mu L^{-1}$ for water shrews, 9.32 $\mu g \cdot \mu L^{-1}$ for short-tailed shrews; Fig. 14). Protein concentrations were non-significantly ($F_{2,30}$=1.010, P=0.376), but consistently, lower in older individuals (10% decline with age in water shrews, 20% with short-tailed shrews; Fig. 14).

The activity of the oxidative enzyme citrate synthase was 42.7 $U \cdot gww^{-1}$ in the hindlimb of the non-diving short-tailed shrew. This was a 40% elevation compared to the activity of 30.5 $U \cdot gww^{-1}$ recorded from the diving water shrew ($F_{1,27}$=15.834, P<0.0001; Fig. 15). Similar to protein concentration, there was a small but insignificant decrease in the activity of citrate synthase with age in both species ($F_{2,27}$=2.105, P=0.141; Fig. 15).

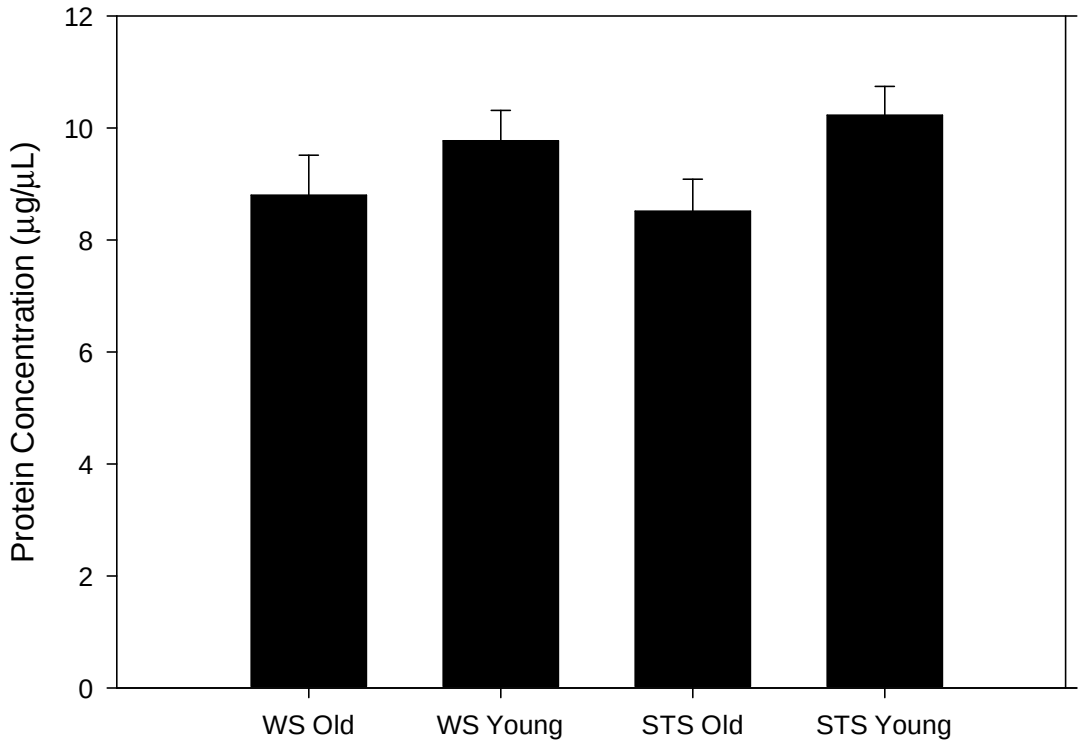

Fig. 14. Comparison of protein concentrations (µg/µL) in skeletal muscle homogenate from two species of shrew. Individuals of both the diving water shrew ('WS') and the terrestrial short-tailed shrew ('STS') were categorized as 'Old' or 'Young' based on the presence of a growth ring in the mandible or dentition (see Section 3). No significant differences were noted.

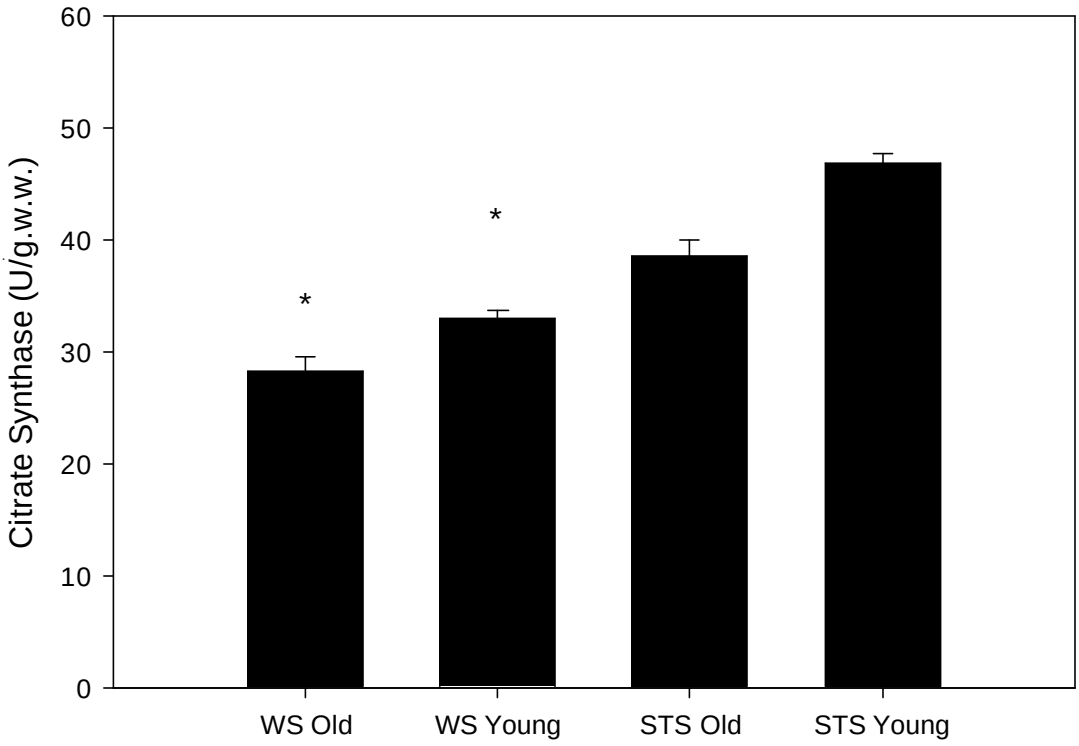

Fig. 15. Comparison of citrate synthase activity (U/g.w.w.) in skeletal muscle homogenate from two species of shrew. Individuals of both the diving water shrew ('WS') and the terrestrial short-tailed shrew ('STS') were categorized as 'Old' or 'Young' as previously described (see Section 3). The single '*' denotes a significant (a=0.05) difference in the activity level of this enzyme between species.

Antioxidant Capacity

Catalase activity levels were elevated 63% in the diver (20.4 $U \cdot gww^{-1}$) compared to the terrestrial shrew (12.5 $U \cdot gww^{-1}$; $F_{1,21}=3.477$, $P=0.076$; Fig. 16). GPx, on the other hand, displayed an opposite trend and was nearly 3X higher in the terrestrial short-tailed shrew (29.3 $U \cdot gww^{-1}$), than the water shrew (8.1 $U \cdot gww^{-1}$; $F_{1,28}=144.335$, $P<0.0001$; Fig. 17). While there was a general trend for antioxidant enzyme activities to increase with age, these changes were not significant for either catalase ($F_{2,21}=1.588$, $P=0.228$; Fig. 16) or glutathione peroxidase ($F_{2,28}=0.484$, $P=0.621$; Fig. 17).

The Cu,Zn and Mn subclasses of superoxide dismutase were assessed in hindlimb via Western immunoblotting. For both enzymes the protein levels were statistically similar between species (Fig. 18; 19). While Mn-SOD showed no differences between age groups in the shrews examined (Fig. 18), Cu,Zn-SOD was elevated in older animals (115% elevation for water shrews, 83% for short-tailed shrews, $F_{2,16}=3.457$, $P=0.054$; Fig. 19).

The gel-based activity assays for both forms of superoxide dismutase did not provide usable results for these species. Because this method requires that the sample remain chilled and un-denatured, the evaporation and concentration of the homogenate, as is typical for western blotting, is not possible. Insufficient amounts of homogenate could be added to the wells in our Western blotting setup to produce consistent results. The faint signal produced in the gel was also insufficient to be able to distinguish between the two isoforms, which should separate slightly upon electrophoresis.

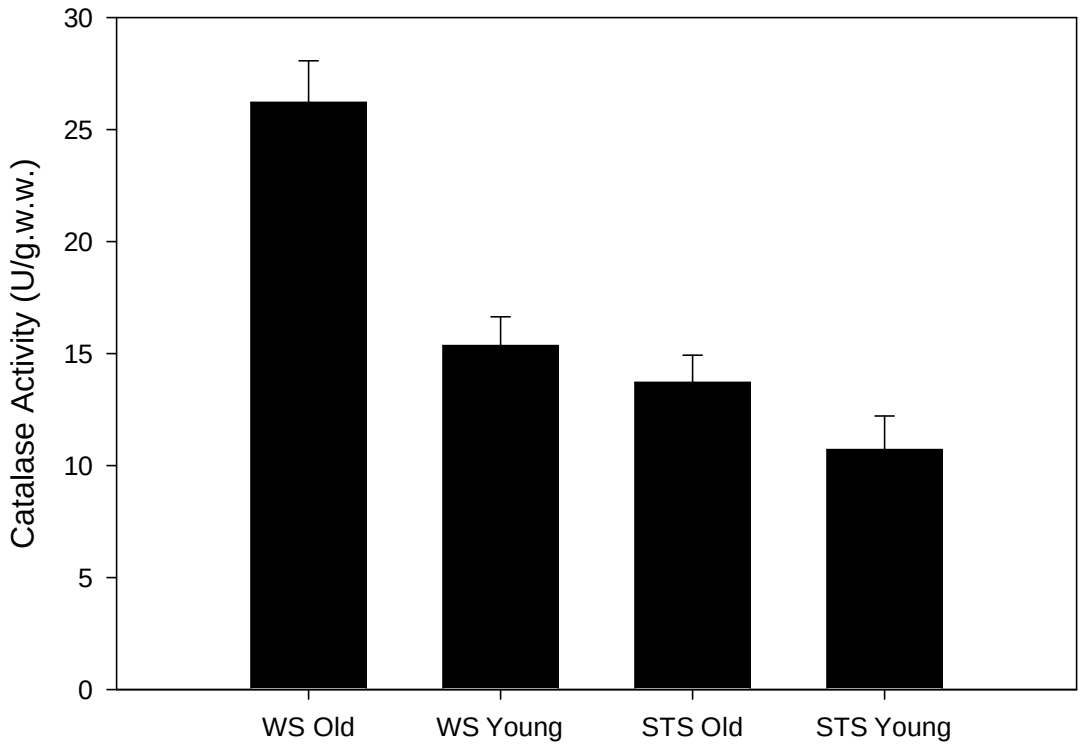

Fig. 16. Comparison of catalase activity (U/g.w.w.) in skeletal muscle homogenate from two species of shrew. Individuals of both the diving water shrew ('WS') and the terrestrial short-tailed shrew ('STS') were categorized as 'Old' or 'Young' as previously described (see Section 3). No significant differences were noted.

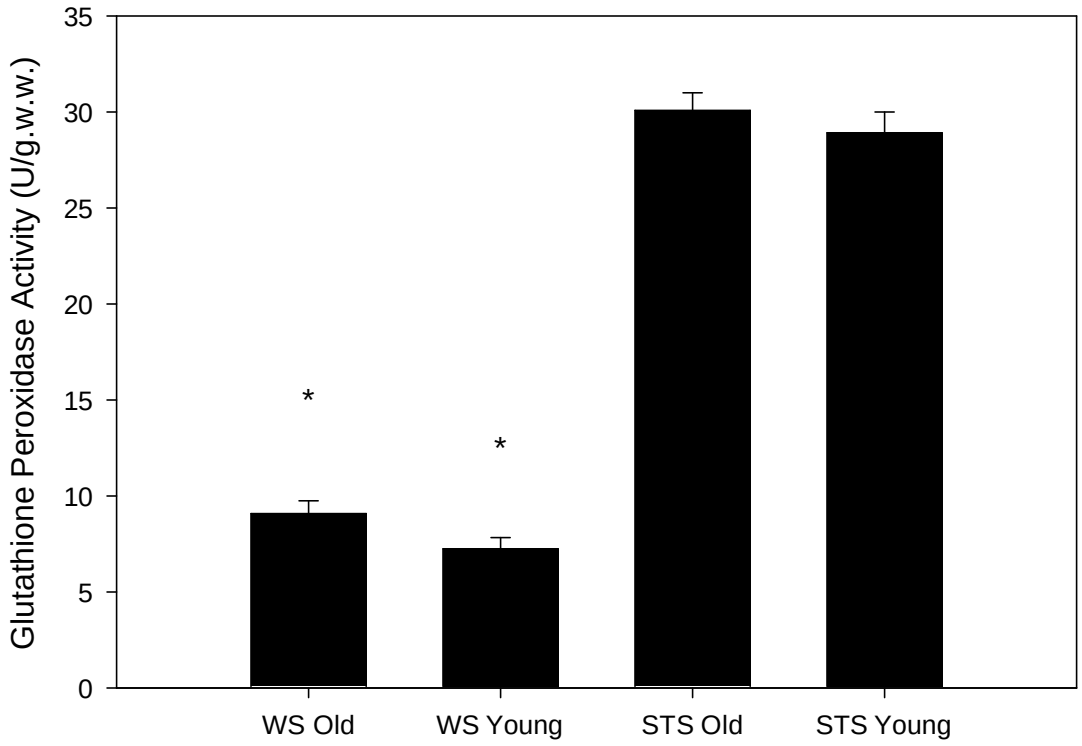

Fig. 17. Comparison of glutathione peroxidase activity (U/g.w.w.) in skeletal muscle homogenate from two species of shrew. Individuals of both the diving water shrew ('WS') and the terrestrial short-tailed shrew ('STS') were categorized as 'Old' or 'Young' as previously described (see Section 3). The single '*' denotes a significant (a=0.05) difference in the activity level of this enzyme between species.

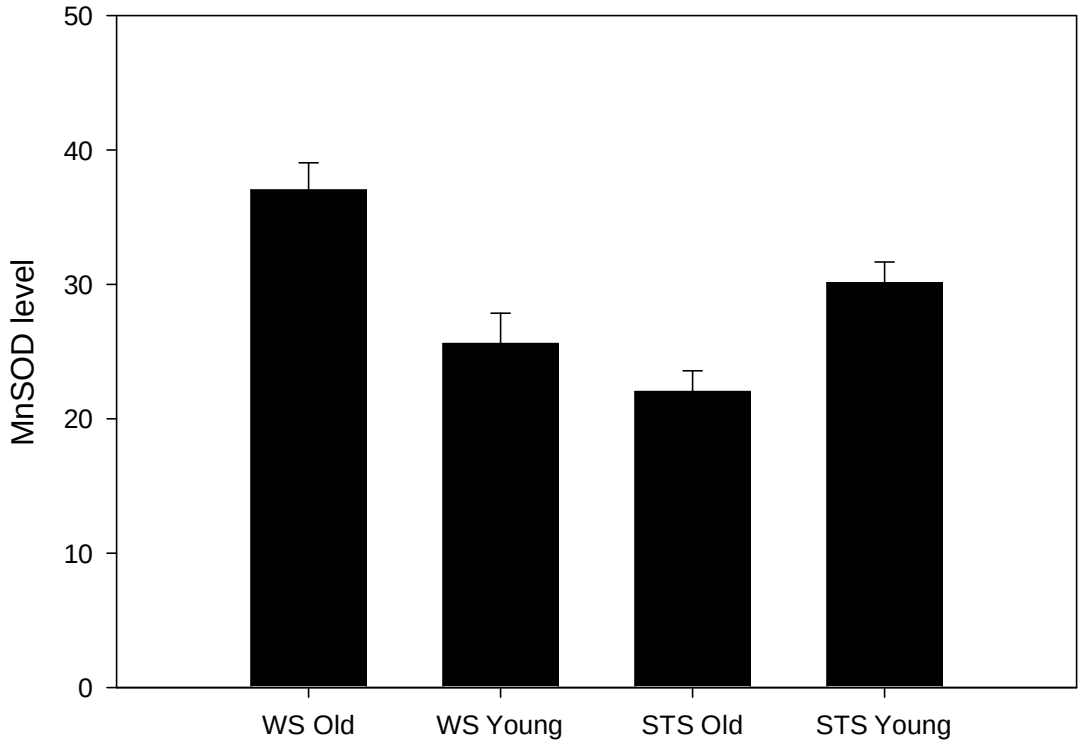

Fig. 18. Comparison of levels of Mn-SOD, expressed in arbitrary units, in skeletal muscle homogenate from two species of shrew. Individuals of both the diving water shrew ('WS') and the terrestrial short-tailed shrew ('STS') were categorized as 'Old' or 'Young' as previously described (see Section 3). No significant differences were noted.

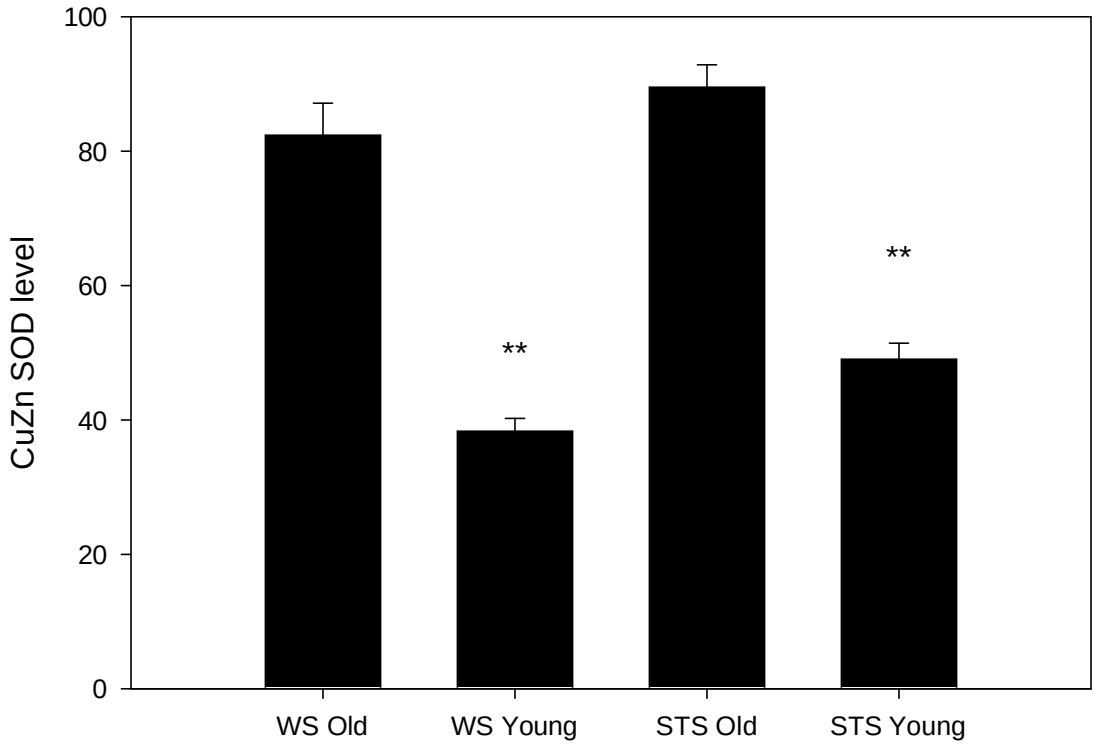

Fig. 19. Comparison of levels of Cu,Zn-SOD, expressed in arbitrary units, in skeletal muscle homogenate from two species of shrew. Individuals of both the diving water shrew ('WS') and the terrestrial short-tailed shrew ('STS') were categorized as 'Old' or 'Young' as previously described (see Section 3). The double '**' denotes a difference (P=0.054) in the activity level of this enzyme between age classes.

Preliminary measurements of total SOD (i.e., measurements taken from the gels of the entire region occupied by both isoforms) do not suggest vast differences in activity between species or age.

Indicators of Oxidative Stress

Lipid peroxidation, measured using a ferrous oxide-xylenol orange assay, varied across species, age and limb (Fig. 20). The non-diver (hindlimb: 16.6 µM *t*-butyl hydroperoxide Eq·gww^{-1}; forelimb: 20.0 µM *t*-but Eq·gww^{-1}) displayed higher levels than the diver (hindlimb: 11.2 µM *t*-but Eq·gww^{-1}; forelimb: 16.7 µM *t*-but Eq·gww^{-1}; $F_{1,62}$=6.607, P=0.013; ln transformed), and in both species old shrews had more lipid peroxidation than did young ($F_{2,62}$=5.120, P=0.009; ln transformed; Fig. 20). This variable was the only measured to be significantly different between muscle groups. In all cases, lipid peroxidation was elevated in the forelimb versus the hindlimb ($F_{2,62}$=3.695, P=0.030; ln transformed; Fig. 20).

Subsequent to lipid peroxidation may be the production of the reactive aldehyde 4-hydroxynonenol. The presence of this reactive species, as measured by western immunoblotting, was also elevated in the terrestrial short-tailed shrew versus the diving water shrew by 35% ($F_{1,25}$=11.596 P=0.002; ln transformed; Fig. 21). Despite the increase in lipid peroxidation with advancing age in both species of shrew, a significant reduction in the presence of 4-HNE was observed with age (~35% decline for both species; $F_{2,25}$=5.949, P=0.008; ln transformed; Fig. 21). No differences were detectable between forelimb and hindlimb.

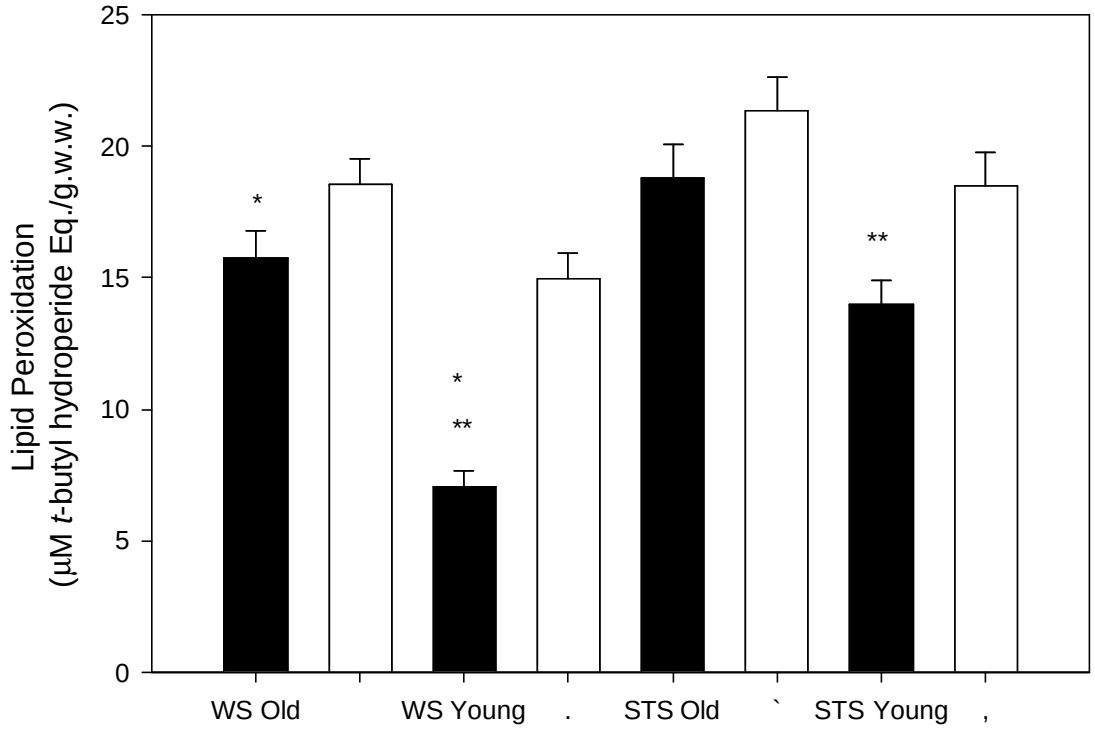

Fig. 20. Comparison of lipid peroxidation (µM *t*-butyl hydroperoxide Eq./g.w.w.) in skeletal muscle homogenate from two species of shrew. Individuals of both the diving water shrew ('WS') and the terrestrial short-tailed shrew ('STS') were categorized as 'Old' or 'Young' as previously described (see Section 3). Black bars indicate the hindlimb measurement for the given group, white bars indicate the corresponding measurement for forelimb. This variable was found to be significantly distinct (a=0.05) between the two shrew species, between age classes for each species and between samples collected from hindlimb and forelimb muscles.

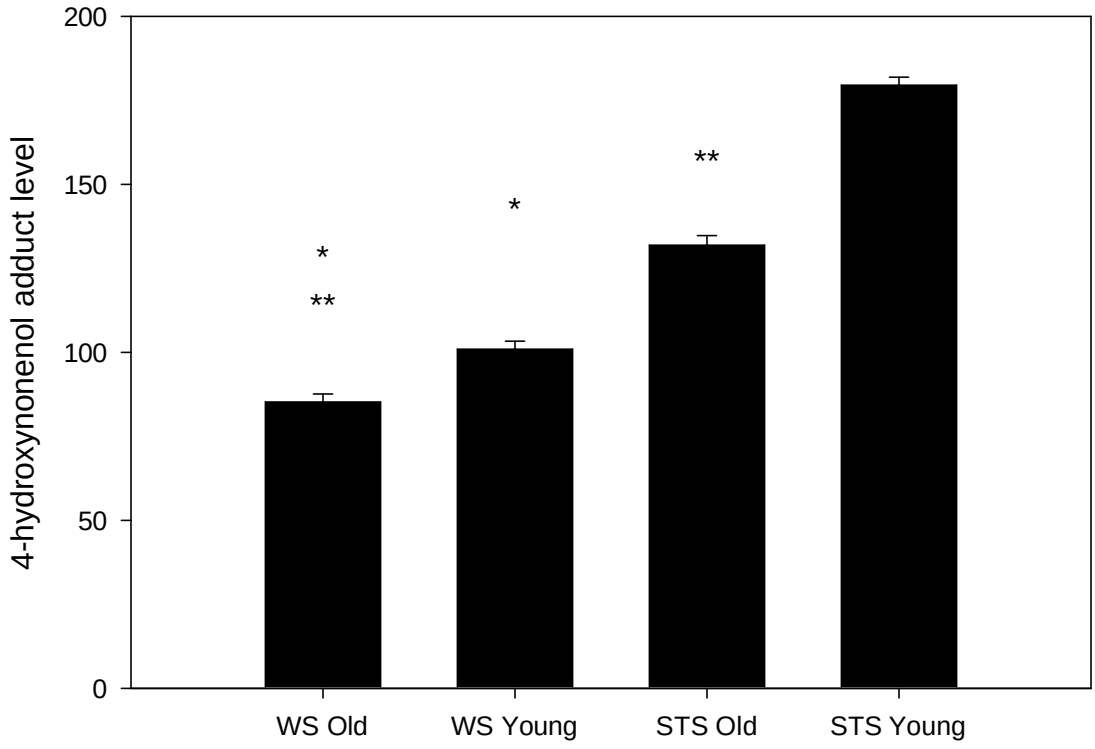

Fig. 21. Comparison of the level of 4-hyroxynonenol adducts, in arbitrary units, in skeletal muscle homogenate from two species of shrew. Individuals of both the diving water shrew ('WS') and the terrestrial short-tailed shrew ('STS') were categorized as 'Old' or 'Young' as previously described (see Section 3). The single '*' denotes a significant (a=0.05) difference in the activity level of this enzyme between species, whereas the double '**' denotes a significant difference between age classes.

Dihydroethidium conversion to its oxidized form, ethidium, in the presence of superoxide anion was also assayed in muscle homogenate. This measurement was also higher in the non-diver (140.1 U xanthine oxidase Eq·gww^{-1}) compared to the diving shrew (95.2 U XO Eq·gww^{-1}; $F_{1,20}$=27.313, P<0.0001; Fig. 22). DHE displayed comparable trends to 4-HNE, rather than lipid peroxidation, and was lower in older versus younger shrews (27% decline for short-tailed shrews; 16% for water shrews; $F_{2,20}$=4.468, P=0.025; Fig. 22).

Apoptosis

Apoptosis was quantified in hindlimb using a cell death detection ELISA method. There were no significant differences observed between the presence of mono- and oligonucleosomes in either species ($F_{1,20}$=0.073, P=0.790), nor either age class ($F_{2,20}$=0.297, P=0.747; Fig. 23). Apoptosis was also examined in individual nuclei of gracilis muscle sections using TUNEL labeling. In all cases, less than 1% of myocytes were associated with apoptotic nuclei (Fig. 24). No significant differences were apparent in comparisons of species ($F_{1,26}$=1.871, P=0.183) or age ($F_{1,20}$=0.869, P=0.360).

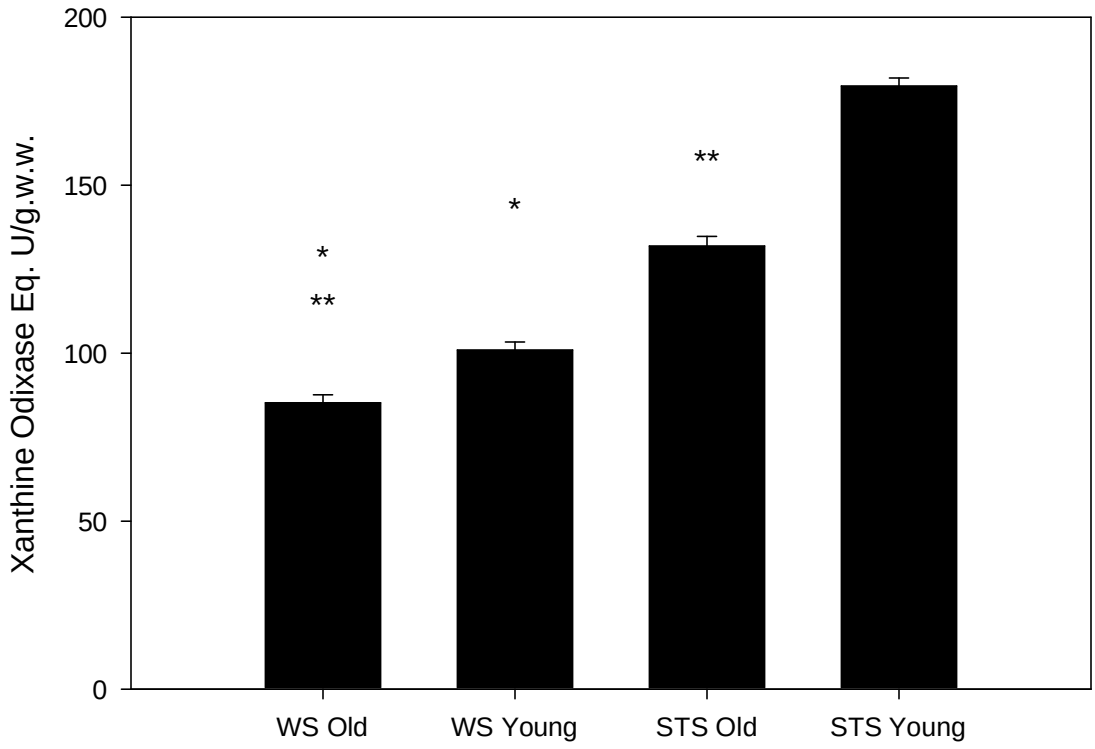

Fig. 22. Comparison of dihydroethidium oxidation (xanthine oxidase Eq. U/g.w.w.), in arbitrary units, in skeletal muscle homogenate from two species of shrew. Individuals of both the diving water shrew ('WS') and the terrestrial short-tailed shrew ('STS') were categorized as 'Old' or 'Young' as previously described (see Section 3). The single '*' denotes a significant (a=0.05) difference in the activity level of this enzyme between species, whereas the double '**' denotes a significant difference between age classes.

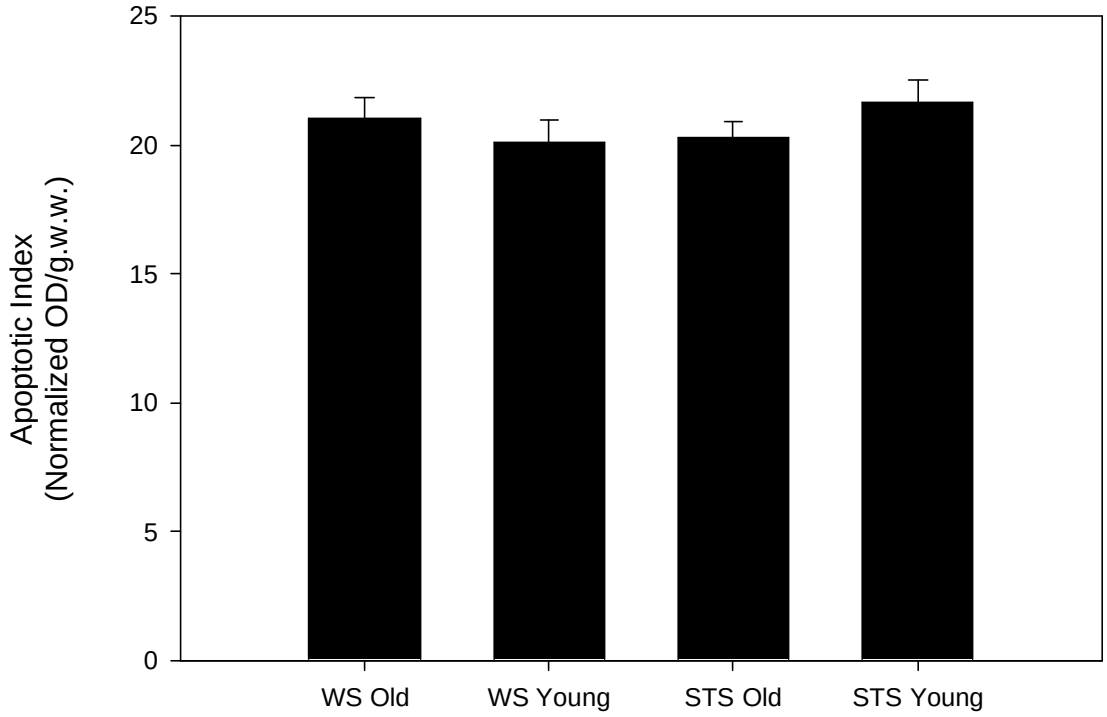

Fig. 23. Comparison of apoptotic indices in skeletal muscle homogenate from two species of shrew. Apoptotic index is measured in arbitrary optical density (OD) units per g.w.w. of fresh tissue, normalized to background values. Individuals of both the diving water shrew ('WS') and the terrestrial short-tailed shrew ('STS') were categorized as 'Old' or 'Young' as previously described (see Section 3). No significant differences were detected.

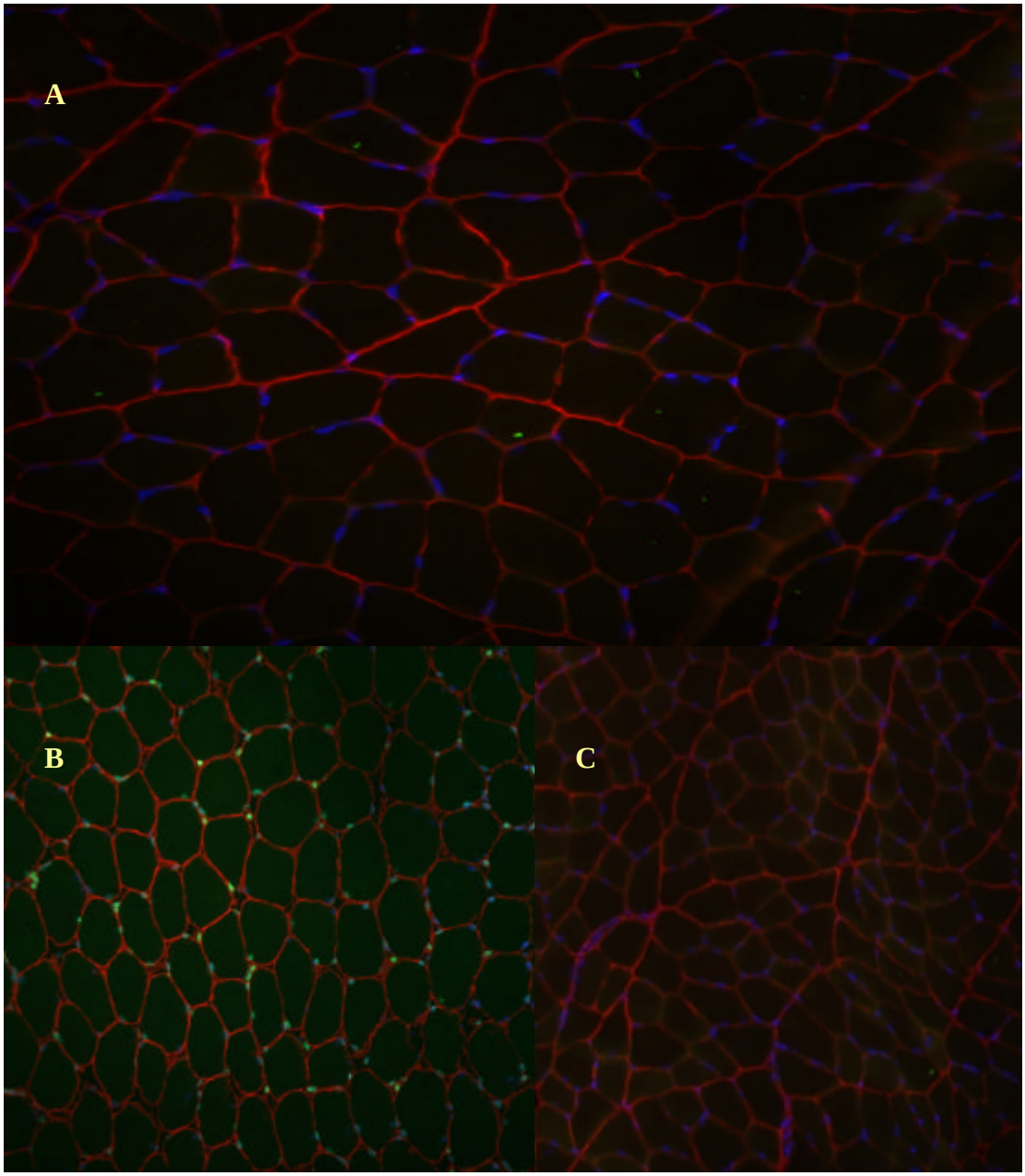

Fig. 24. Triply labeled gracilis muscle (7-9 um) of a representative water shrew. TUNEL-positive areas are labeled with green florescence, laminin with red, and all nuclei (DAPI) are labeled with blue florescence. A: representative section of gracilis muscle with triple label; B: positive TUNEL control; C: negative TUNEL control.

Discussion

Biochemical Properties of Aging Shrew Muscle

Aging in both species of shrew resulted in a slight non-significant decrease in both protein concentration and the activity of the citric acid cycle enzyme citrate synthase. In a study of muscle fiber type and exercise in rats, the only significant change in citrate synthase activity with age was a decline within the red gastrocnemius (type IIa) of the exercise groups (Lawler et al. 1993). Even in sedentary humans there is little difference in the activity of citrate synthase with advancing age, tending towards slight declines (Essén-Gustavsson and Borges 1986). In contrast citrate synthase does increase significantly in the muscle of thoroughbred horses with age (Ronéus et al. 1991). This is likely due to the collection of mixed-muscle biopsies. With advancing age, the biopsies collected in this study contained increased proportions of Type I and Type IIa and decreased portions of type IIb (Ronéus et al. 1991), all of which should increase the oxidative capacity and citrate synthase activity of general homogenate (Delp and Duan 1996).

From a statistical perspective, shrews do not entirely conform to the general redox profile expected with aging in small mammals. Muscle tissue collected from rats generally displays increased antioxidant levels with age (SOD, CAT, GPx; Ji et al. 1990), although as with citrate synthase there appears to be some fiber type specificity of these responses (Lawler et al.1993; Hollander et al. 2000). There was, in most cases, a slight elevation of antioxidant enzyme activities in shrews. However, for the case of GPx activity in particular, this change was minimal and not statistically significant.

While no significant changes in the activity of catalase were noted in shrews, there was a clear trend towards the increase of this value in water shrews. SOD was assayed for protein content rather than enzyme activity. When examined in rats, the recorded increase in the activity of Mn-SOD observed in older animals was the result of posttranslational modification, since the protein contents did not increase, and mRNA actually declined (Hollander et al. 2000). Increased activity of Cu,Zn-SOD was the result of translational and posttranslational controls, since an increase was observed in Cu,Zn-SOD protein content, but not mRNA (Hollander et al. 2000). The results of this study are in line with those findings, since an increase in the protein content of Cu,Zn-SOD was detected with age in both species, while no differences were detectable in the protein content of Mn-SOD.

When the literature is examined, it is clear that there is no general trend or consensus for the expected changes in skeletal muscle antioxidant capacity with age. This situation has been described by Beckman and Ames (1998) to be "a confusing assemblage of ambiguous trends". Despite the inconsistencies in which, or if any, antioxidant enzymes are increased with age, the measured rate of damage is consistently higher in aged muscle upon exposure to oxidative stress (Beckman and Ames 1998).

Lipid peroxidation increased with age in these two species of shrews, as was expected. Several studies of rats and mice also documented a consistent increase in the levels of lipid peroxidation detected in muscle of old animals (Lawler et al. 1993; Bejma and Ji 1999). Other indicators of oxidative stress in tissue are also increased with age in rodents (see Goto et al. 1999 for review). One corollary of the reported increase in

detectable oxidative stress in old rats is that old muscle shows more oxidative stress following exercise (Bejma and Ji 1999) and this in turn increases the acute and delayed onset levels of injury in old muscle (Zerba et al. 1990). By contrast, only total hydroperoxides were increased with age in the muscle of shrews. Levels of the reactive aldehyde 4-HNE, which is generated from lipid peroxidation, were significantly decreased in both species. This finding implies a reduction in exposure to oxidative stress with age in these species, since 4-HNE is particularly implicated in oxidative stress damage to muscle, due to its stability and ability to generate further oxidative stress events (Yang et al. 2003). The oxidation of dihydroxyethidine (DHE) was also significantly reduced with age in both shrew species. This assay measures the presence of superoxide radicals in the cytosol, since their presence oxidizes the DHE into the fluorescent product ethidium during a 10-min incubation at 37ºC. This measurement was taken from frozen homogenate, not freshly excised muscle, so it would not represent the outflow of superoxide from intact mitochondria, but rather the presence of superoxide in the cell at the point at which the muscle was frozen. From this measurement, one can infer a reduced mitochondrial superoxide outflow in old shrews, since muscles were collected after similar handling and anesthesia procedures for animals of all age classes. The indirect nature of this measurement could explain why the data are at odds with the general literature, since ROS production should increase in aged skeletal muscle (Meydani and Evans 1993; Bejma and Ji 1999). Taken together, these findings cast some doubt on the accumulation of oxidative damage in shrew muscle, as is predicted based on data from rats and mice. It is also possible however,

that the increased lipid peroxidation seen in this study is representative of the expected increase in oxidative stress with age, and that the declines in the other variables are the result of superior scavenging in shrews (especially the diving water shrew). Antioxidants such as glutathione-s-transferase catalyze the majority of 4-HNE metabolism by conjugating the aldehyde with GSH (Yang et al. 2003). Reduced degree of DHE oxidation (which represents ROS accumulation in the cell during anesthesia and muscle extraction) with age could as well be the end result of more effective cytosolic scavenging mechanisms.

As mentioned previously, muscles of different fiber types have different redox profiles with age, but this also occurs with exercise and other manipulations (Lawler et al. 1993; Hollander et al. 1999). In general, slow (Type I) fibers have higher antioxidant activity levels, followed by Type IIa and Type IIb (e.g., Lawler et al. 1993). This may be the protective result of an increased outflow of oxidation product in more oxidative fibers, but may result from other mechanisms. Muscles dominated by given fiber types are expected to share its general characteristics. Since shrew muscle homogenates are pooled collections of muscle from either forelimb or hindlimb, the data discussed here should represent average effects across several fiber types. It does appear, however, that shrew muscles lack type I fibers completely (Section 3; Savolainen and Vornanen 1995*a,b*; Peters et al. 1999; Jürgens 2002). Lower antioxidant (and oxidant) values are therefore expected in shrew muscles, in comparison to homogenates collected from type I rodent muscles, such as soleus. Shrew values should instead be comparable to those collected from rodent red fibers such as gastrocnemius and vastus lateralis.

There are several species differences in the data collected here compared to that of young rats. Citrate synthase activity was markedly higher in field-caught shrews versus laboratory rodents. The average activity of citrate synthase in the vastus lateralis of young rats was 8.2 $U \cdot gww^{-1}$ (Ji et al. 1990), whereas average values for hindlimb were 46.8 $U \cdot gww^{-1}$in short-tailed shrews, and 33 $U \cdot gww^{-1}$ in water shrews. Catalase activity in rats range from the average reported values of 3.5 $U \cdot gww^{-1}$ in soleus (Lawler et al. 2003) to 11.4 $U \cdot gww^{-1}$ in vastus (Li et al. 1990). In this study, average catalase activities were slightly higher in shrews, being 10.8 $U \cdot gww^{-1}$ for short-tailed shrews and 15.4 $U \cdot gww^{-1}$ for water shrews. GPx activity was 16.6 $U \cdot gww^{-1}$ in young rats (Ji et al 1990), while it was 28.9 $U \cdot gww^{-1}$ short-tailed shrews and 7.3 $U \cdot gww^{-1}$ for water shrews. Shrews had considerably higher total hydroperoxides, at 14 000 $nmol \cdot gww^{-1}$ (short-tailed shrews) and 7 000 $nmol \cdot gww^{-1}$ (water shrews), versus 1770 $nmol \cdot gww^{-1}$ reported in rats (Lawler et al. 2003).

Apoptosis, as measured both quantitatively (cell death ELISA) and qualitatively (TUNEL) was essentially absent in shrews. This finding is in stark contrast to those for laboratory species, in which apoptosis can increase by 50% in old rats (Dirks and Leeuwenburgh 2002). Apoptosis is speculated to be important in cell turnover both during and following exercise, which reduces the inflammatory process (Phaneuf and Leeuwenburgh 2001), and should preserve muscle function. On the other hand, apoptosis, which can be signaled by ROS, is involved in the fiber loss that accompanies muscle force reduction with age (Dirks and Leeuwenburgh 2002).

Adaptations in Redox System to Diving in Shrews

It is generally held that aquatic animals have elevated levels of antioxidants compared to terrestrial animals. This does not seem to be the case for diving versus non-diving shrews. Antioxidant capacity was generally higher in the short-tailed shrew versus the water shrew despite occupying similar habitats, aside from the aquatic component. Catalase activity appeared to be slightly higher in the diver, but this difference was not significant (P=0.076). On the other hand, the activity of GPx was over three times higher in the short-tailed shrew. No species differences were detected in the protein contents of the SOD enzymes. The general differences in antioxidant capacity between the two shrews may be related to the significantly higher levels of citrate synthase detected in the terrestrial species. It correlates to the higher levels of oxidative stress markers in the short-tailed shrew, such as total hydroperoxides (FOX), 4-HNE levels, and DHE oxidation. Yet, there were no species differences in apoptotic markers.

Larger bodied divers, such as seals, display the elevated antioxidant levels predicted for aquatic animals (Zenteno-Savín et al. 2002; Vázquez-Medina et al. 2006). While levels in ringed seals are generally higher than for non-aquatic control tissue, the results in skeletal muscle samples are the most ambiguous of all organs studied. While GPx levels in ringed seal were as expected, elevated versus pig controls, seal muscle had significantly lower activity of catalase (Zenteno-Savín et al. 2002). The redox age effects in the skeletal muscle of ringed seals also differ from other tissues (Zenteno-Savín et al. 2002).

It is difficult to make interspecies generalizations, based on the often conflicting literature, of redox changes with age in skeletal muscle. One generalization that holds is that diving mammals, which operate mainly within their ADL, have more oxidative muscle fibers. In fact, neither ringed, nor Weddell seals have any type IIb (fast glycolytic, equivalent to the make up of a rat's white gastrocnemius) fibers (Kanatous et al. 2002; Watson et al. 2003). Heterogeneous responses to in vitro oxidative stress exist in different types of fibers from the same heart (Suh et al. 2003). When type I, IIa and IIb muscle fibers were examined individually, there was a clear difference in antioxidant activities such that type I > type IIa > type IIb (Lawler et al. 1993). It is possible that the more accomplished diving mammals derive their increased antioxidant capacity from that increased proportion of oxidative muscle fibers.

My observations for shrews do not agree with the argument that antioxidant protection is derived from more oxidative muscle fibers. The low buffering capacity of muscle from water shrews (R.W. Gusztak, Unpubl. Obs.) indicates a high reliance on aerobic energy production during diving. Any species differences in type II fiber subtype would therefore suggest more oxidative fibers in water shrews. Perhaps the overall increased antioxidant and oxidant profile of short-tailed shrews is representative of some other aspect of the shrews' habitat. The short-tiled shrew compensates for the dietary lack of aquatic prey by digging to collect underground invertebrates. This foraging activity could increase fossorial activity, which in turn leads to hypercapnic and hypoxic stress. In fact, the anatomy of the short-tailed shrews' lung is indicative of extended time spent underground in dusty burrows (George et al. 1986). I postulate that

the tissue hypoxia encountered in the diving environment results in increased production of oxidative stress for water shrews. Perhaps the fossorial nature of the short-tailed shrew causes in a superior degree of hypoxia relative to the diver. This could explain the general trend in elevated oxidant and antioxidant levels in the terrestrial species.

There could be another component of muscle that would account for both the inconsistencies and declinations in antioxidant capacity in water shrews, and the reduction in oxidative stress and ROS markers. Evidence now suggests that in addition to the well-held view that myoglobin acts as an oxygen storage site, and a facilitator in oxygen diffusion, myoglobin may have direct antioxidant properties, at least in cardiac muscle (Flögel et al. 2004). Myoglobin appears to have direct peroxidase activity in the heart (Garry et al. 2003; Flögel et al. 2004). Myoglobin also acts as a scavenger of nitric oxide (NO), through the equation:

ferrous oxygenated Mb + NO = ferric oxidized Mb (metMb) + (NO_3) (14).

This reaction is thought to occur in a non-reversible manner due to the fact that the character of superoxide is assumed by oxymyoglobin (Ascenzi and Brunori 2001). Nitric oxide is a reactive nitrogen species (RNS) and produces downstream products such as peroxynitrate. RNS have been shown to reduce antioxidant enzyme activities in skeletal muscle, and therefore contribute to oxidative stress (Lawler and Song 2002). Elevated skeletal muscle myoglobin content is a hallmark of divers. As expected for divers, water shrews have higher myoglobin concentrations than short-tailed shrews

((R.W. Gusztak, Unpubl. Obs.; Stewart et al. 2005). Perhaps this component adds to the water shrews' protection against free radical stress.

Conclusions

Measurements collected from shrews in this study fall within the expected ranges for laboratory rodents in some cases, but are much elevated in others (i.e., citrate synthase activity). Total hydroperoxides were elevated in shrews versus rats, but corresponding increases in antioxidant capacity were inconsistent. In several ways shrews do not conform to expectations of the free radical theory of aging, which suggests an increase in oxidative stress within aged tissues, and a resultant increase in antioxidant levels. Baseline levels of lipid peroxidation are high, but the degree of elevation seen with age is not severe. Other examples of measured oxidative stress significantly decline with age in shrews. There tended to be slight increases in antioxidant enzymes with age, which would be expected in compensation for elevated oxidative damage, but these differences generally failed to be significant.

The lack of increase in oxidative stress markers, or the consistent significant increase in antioxidant activity in water shrews could be the result of several factors. First, water shrews have reduced ROS production because they do not tolerate hypoxia during diving. This seems impossible, considering that they do not likely tolerate anaerobic diving either. But, the ADL of water shrews is sufficient that muscle should become hypoxic without a reduction in diving metabolic rate. Short-tailed shrews, on the other hand are likely exposed to hypoxic tunnels. If lung oxygen extraction declines with age,

as it does in deer mice (Chappell et al. 2003), the severity of the resulting tissue hypoxia would increase with age in the terrestrial shrew.

Second, water shrews have higher myoglobin content in muscle than do short-tailed shrews. If myoglobin has direct antioxidant properties in muscle then oxidative stress might be reduced without the requirement of elevated antioxidant systems. This would occur independent of age, assuming that myoglobin content does not decline with age (Dolar et al. 1999; MacArthur et al. 2001).

Third, the life history of shrews may affect the resources allotted to oxidant defense. Perhaps due to the limited life span of these species, they do not divert resources into limiting oxidative stress. This would explain the elevation of FOX beyond that of rats. This might also explain the limited difference in oxidative stress markers, and in antioxidant defense detected with aging in either shrew species. In order to gain a fitness benefit, the shrews studied here would have to extend their lives to incorporate another breeding cycle. Since they already utilize multiple breeding cycles per season, that additional breeding cycle must occur in a following spring/summer. This requires at minimum a 20% increase in life span, and the expense of such an extension may make subsequent reproduction unfeasible. The bottom line may be that animals having only one or two reproductive seasons may not be good species in which to study constraints and tradeoffs in aging, because of the 'categorical' nature of such a tradeoff. Long-lived animals with many reproductive seasons are more likely to be faced with such tradeoffs.

In this study at least, the diving species did not display an overwhelming improvement in antioxidant defense of muscle, although they also did not show increased levels of oxidative stress markers. Neither are there differences in level of apoptosis in muscle from either species. While this study did not reveal any obvious adaptations of water shrews to defend against the oxidative stress insults associated with diving, it is also clear that they do not suffer from excessive oxidative damage to tissues.

5. SUMMARY AND CONCLUSIONS

Study Overview

This study was the first to demonstrate a change with age in the muscle extracellular space, and in the amount and type of muscle collagen in wild-caught animals. ECS was significantly elevated in old animals of both shrew species, and this corresponded to an increase in the extracellular collagen component of shrew muscle with age. Muscle samples were dominated by Type I collagen in all cases, and the ratio of collagen Type I: III increased significantly with age. This represents an increased proportion of the stiffer Type I collagen fibers and a reduced volume of more compliant Type III collagen. In fast twitch muscle, which relies on the compliance of Type III collagen for contractile speed, such age-related changes in the extracellular matrix could seriously impact performance.

Shrews in this study did not demonstrate the statistically consistent elevation of oxidative stress markers, and resultant increase in antioxidant capacity with age, which is predicted by the free radical theory of aging. On balance, the protective antioxidant defenses of the diving water shrew were not elevated with respect to the terrestrial short-tailed shrew. While this is unexpected based on the hypothesis that divers must defend muscle against the oxidative stress associated with dive-induced hypoxia, neither did the diving species display an elevated level of oxidative stress markers with respect to the non-diver. Levels of apoptosis were also similar between the species. This study therefore did not reveal any obvious adaptations of water shrews to defend against the oxidative stress insults associated with diving, yet it is also clear that they do not suffer

from excessive oxidative damage to tissues. I have suggested that this unexpected result might be due to: 1) water shrews becoming minimally hypoxic during diving, or short-tailed shrews becoming highly hypoxic as the result of a fossorial existence; 2) myoglobin content exerts direct antioxidant protective effects on water shrew muscle, and such effects are larger in the diver due to a higher muscle myoglobin content than in the non-diver; 3) the limited life span of both species of shrew equally depletes the need for limiting oxidative stress.

Based on physiological and behavioral data available, and the predictions generated from the data in Sections 3 and 4, a model was developed to predict the energetics of a foraging Weddell seal, and to determine how foraging is related to age. Among other things, the model predicts that the threshold of prey encounter rate for entering into a dive bout produces an optimal effect on energy gain if the threshold is slightly higher than the mean environmental prey encounter rate. With advancing age, the model predicts a declining net energy gain for the age paradigms Young > Old-Buoyancy > Old-ADL > Old- Muscle > Old-All, in that order. Such energetic differences between the age paradigms are exacerbated when good prey patches are scarce. An interesting concept addressed by this model is that behavioral plasticity may allow older animals to compensate for certain age-related performance constraints. It also demonstrates that plausible physiological and anatomical effects of age might have a large effect on foraging success, especially in areas of low prey density. Examinations of Weddell seals foraging in McMurdo Sound versus those foraging around White Island reveal that White Island seals are fatter (Castellini et al. 1984), which may suggest that

either prey depletion or increased competition occurs in McMurdo Sound. Weddell seals occupying the breeding colonies in Erebus Bay operate in a geographically constrained foraging area. This has been speculated to result in a regional prey depletion over time, and subsequently increased intraspecific foraging competition (Hindell et al. 2002), which would highlight any reduction in net energy gain resulting from aging. The possibility of compensation through behavioral plasticity, however, might explain the lack of apparent senescence in a species expected to be a prime candidate for such effects.

Diving Mammals as a Physiological Model

Divers offer a unique opportunity to investigate the physiological and ecological implications of aging in mammals. Divers can be regarded as central place foragers (i.e., animals which return with food to a central place; Orians and Pearson 1979), with this central place being the water surface (Houston and McNamara 1985). This represents an unusual connection between physiology and foraging ecology, and implies that the physiology of aging in such an animal is significant to our understanding of its ecology.

Application to Marine Mammal Ecology

Aging phenotypes may have additional severe ecological consequences in pinnipeds, since their unique life history (i.e., the requirement of solid substrate for reproduction) is associated with specific and elevated energetic demands relative to other marine mammals. Pinnipeds forage in open water in areas potentially distant from their

coastal reproductive grounds, and hunt prey at depth despite physiology that requires regular return to the surface. The resulting physiological demands may make pinnipeds more susceptible to fluctuations in natural and anthropogenic changes in both their food supply and the environment.

Recent population trends in several species of threatened marine birds and mammals indicate that, on the whole, these populations are "aging" (e.g., Holmes and York 2003). As population age structure is redefined in this way, older animals comprise greater proportions of both the reproductive population and the population overall. This aging trend has been documented in historically over-harvested populations as well as those threatened by environmental change. For example the population decline and slower-than-predicted recovery of the Steller sea lion, *Eumetopias jubatus*, seems related to a low juvenile recruitment into the breeding population (Calkins et al. 1999), due to female undernourishment and subsequent low birth rates (Pitcher et al. 1998). Furthermore, decreased fecundity and high juvenile and neonate mortality are likely impeding the recovery of North Atlantic right whale, *Eubalaena glacialis*, stocks (Knowlton et al. 1994). The result in this case is an aged population, in which juveniles comprise only 24.7- 31.1% of the known population, a percentage much lower than that observed in other mysticetes (Hamilton et al. 1998). Populations threatened by the growing strength and frequency of the El Niño Southern Oscillation are also faced with "aging". This stems from either a reduction in breeding success, in the case of the Galapagos penguin, *Spheniscus mendiculus* (Boersma 1998),

or juvenile survival, in the case of the Guadalupe fur seal, *Arctocephalus townsendi* (Hanni et al. 1997).

As previously mentioned, a unique link exists between physiology and ecology in these animals. In the examples listed above, older individuals experience the combined stressors of age as well as those affecting the population decline, and therefore, may be subject to age-related senescence not encountered within stable populations. Understanding the constraints facing old animals is important considering their presumably significant contribution to the reproductive output and health of their populations as a whole, making the question of senescence timely.

Sources of Variability

An issue encountered when analyzing samples was the individual variability of the wild-caught animals. This issue was not as problematic for morphological features, but there was a tremendous degree of inter-individual variability in enzyme activities and levels. In several cases, values recorded from animals of similar age class were more than double those recorded from others. This issue has also been noted in enzyme analyses for muscle samples of Weddell seals (Unpubl. Obs; S.B. Kanatous, personal communication). In the Weddell seal study, basic health and body condition information were collected in conjunction with the muscle biopsies, and there were no obvious concerns of animal health or sample collection procedure in samples that otherwise appeared to be outliers. Increased sample size is always helpful in dealing with such

inter-individual variability, and this may have improved the level of statistical significance in the results.

Another physiological aspect that was not considered in the scope of this project was gender. It is clear from data collected from Weddell seals (Unpubl. Obs.) that enzyme activity levels (including antioxidants) as well as levels of lipid peroxidation are significantly different between male and female seals of similar age class. Published studies involving both humans (Cavas 2005) and mice (Sanz et al. 2007) both postulate that the reduced oxidative stress markers observed in muscle samples collected from female subjects may be the result of direct antioxidant properties of estradiol.

Future Directions

This study could be expanded in several directions. For the shrew model, the production of ROS could be investigated within the mitochondria directly. This would enhance understanding of the adaptations of diving mammals to hypoxia. The investigation discussed here might also be pursued for the comparison of water shrews to other terrestrial species. For example, the arctic shrew (*Sorex arcticus*) is found in habitats near to water shrews, and is less fossorial in nature than the short-tailed shrew. Samples sizes could also be expanded to aid in dealing with the statistical variability.

Another obvious expansion of this study would be to examine populations of diving animals whose life spans are not constrained to one or two breeding seasons. Such animals may face larger aging “trade-offs” resulting from the somatic maintenance required to continue successful reproduction over several years.

Increased antioxidant capacity is a pattern observed when wild animals are exposed to environmental stress. For example, antioxidant levels are increased in aquatic animals (e.g., fish) in response to increased pollution loads (Winston 1991). Antioxidant levels are also elevated in arousing hibernators as well (Hermes-Lima and Zenteno-Savín 2002). If high antioxidant levels are consistently observed, it may represent a response to an increase in oxidative stress resulting from environmental change. Another possible continuation of this study would be to examine the relationships between oxidative stress, antioxidants and aging pathways in populations faced with environmental challenges such as pollution.

REFERENCES

Aebi, H. (1984). Catalase in vitro. *Meth. Enzymol.* **105**, 121-126.

Ainley, D.G., Ballard, G., Barton, K.J., Karl, B.J., Rau, G.H., Ribic, C.A. and Wilson, P.R. (2003). Spatial and temporal variation of diet within a presumed metapopulation of Adélie penguins. *The Condor* **105**, 95-106.

Ascenzi, P. and Brunori, M. (2001). Myoglobin: a pseudo-enzymatic scavenger of nitric oxide. *BAMBED* **29**, 183-185.

Barja, G. and Herrero, A. (2000) Oxidative damage to mitochondrial DNA is inversely related to maximum life span in the heart and brain of mammals. *FASEB J.* **14**, 312-318.

Beauchamp, C. and Fridovich, I. (1971). Superoxide dismutase: improved assays and an assay applicable to acrylamide gels. *Anal. Biochem.* **44**, 276-287.

Beauplet, G., Barbraud, C., Dabin, W., Küssener, C. and Guinet, C. (2006). Age-specific survival and reproductive performances in fur seals: evidence of senescence and individual quality. *Oikos* **112**, 430-441.

Becker, L.B., Vanden Hoek T.L., Shao, Z., Li, C. and Schumacker, P.T. (1999) Generation of superoxide in cardiomyocytes during ischemia before reperfusion. *Am. J. Physiol.* **277**, H2240-H2246.

Beckman, K.B. and Ames, B.N. (1998) The free radical theory of aging matures. *Physiol. Revs.* **78**:547-581.

Bejma, J., and Ji, L.L. (1999). Aging and acute exercise enhance free radical generation in rat skeletal muscle. *J. Appl. Physiol.* **87**, 465-470.

Beneski, J.T. Jr. and Stinson, D.W. (1987) Mammalian species: *sorex palustris*. *Am. Soc. Mammal.* **296**, 1-6.

Berrizbeitia, L.D., McGrath, L.B. and Klabunde, R.E. (2002) Oxygen modulation of superoxide radical injury in the Krebs-perfused, isolated rabbit heart. *J. Invest. Surg.* **15**, 251-257.

Bevan, R.M. and Butler, P.J. (1992) Cardiac output and blood flow distribution during swimming and voluntary diving of the tufted duck (*Aythya fuligula*). *J. Exp. Biol.* **168**, 199-217.

Boersma, P.D. (1998) Population trends of the Galápagos penguin impacts of El Niño and La Niña. *Condor* **100**, 245-253.

Bohr, V.A. and Anson, R.M. (1999) Mitochondrial DNA repair pathways. *J. Bioenerg. Biomembr.* **31**: 391-398.

Boveris, A. and Cadenas, E. (2000) Mitochondrial production of hydrogen peroxide regulation by nitric oxide and the role of ubisemiquinone. *IUBMB Life* **50**, 245-250.

Brooke, M.H. and Kaiser, K.K. (1970). Muscle fiber types: how many and what kind? *Arch. Neurol.* **23**, 369-379.

Brooks, G.A. and Faulkner, J.A. (1994). Skeletal-muscle weakness in old-age – underlying mechanisms. *Med. Sci. Sports Exerc.* **74**, 71-81.

Brooks, G.A., Fahey, T.D., White, T.P. White and Baldwin, K.M. (2000). *Exercise physiology: human bioenergetics and its applications, 3rd edition.* McGraw-Hill Co. Inc., NY.

Brunet-Rossinni, A.K. and Austad, S.N. (2004). Ageing studies on bats: a review. *Biogerontology* **5**, 211-222.

Burgeson, R.E. (1987). The collagens of skin. *Curr. Probl. Dermatol.* 17, 61–75.

Burns, J.M. (1999). The development of diving behavior in juvenile Weddell seals: pushing physiological limits in order to survive. *Can. J. Zool.* **77**, 737-747.

Burns, J.M. and Castellini, M.A. (1996). Physiological and behavioral determinants of the aerobic dive limit in Weddell seal (*Leptonychotes weddellii*) pups. *J. Comp. Physiol. B* **166**, 473-483.

Burns, J.M., Trumble, S.J., Castellini, M.A. and Testa, J.W. (1998). The diet of Weddell seals in McMurdo Sound, Antarctica as determined from scat collections and stable isotope analysis. *Polar Biol.* **19**, 272-282.

Butler, P.J. and Jones, D.R. (1997) Physiology of diving of birds and mammals. *Physiol. Revs.* **77**, 837-899.

Calder, W.A. (1969) Temperature relations and underwater endurance of the smallest homeothermic diver, the water shrew. *Comp Biochem Phsyiol* **30**, 1075-1082.

Calkins, D.G., McAllister, D.C., Pitcher, K.W. and Pendleton, G.W. (1999) Steller sea lion status and trend in Southeast Alaska: 1979-1997. *Mar. Mamm. Sci.* **15**, 462-477.

Carbone, C. and Houston, A.I. (1996). The optimal allocation of time over the dive cycle: an approach based on aerobic and anaerobic respiration. *Anim. Behav.* **51**, 1247-1255.

Carbone, C., De Leeuw, J.J. and Houston, A.I. (1996). Adjustments in the diving time budgets of tufted duck and pochard: is there evidence for a mix of metabolic pathways? *Anim. Behav.* **51**, 1257-1268.

Castellini, M.A., Davis, R.W., Davis, M. and Horning, M. (1984). Antarctic marine life under the McMurdo ice shelf at White Island: a link between nutrient influx and seal population. *Polar Biol*. **2**, 229-231.

Castellini, M.A., Kooyman, G.L. and Ponganis, P.J. (1992). Metabolic rates of freely diving Weddell seals: correlations with oxygen stores, swim velocity and diving durations. *J. Exp. Biol.* **165**, 181-194.

Cavas, L. (2005). Does underwater rugby stimulate the over-production of reactive oxygen species? *Cell. Biochem. Funct.* **23**, 59-63.

Chang, J. Knowlton, A.A. and Wasser, J.S. (2000) Expression of heat shock proteins in turtle and mammal hearts: relationship to anoxia tolerance. *Am. J. Physiol.* **78**, R209-R214.

Chappell, M.A., Rezende, E.L. and Hammond, K.A. (2003). Age and aerobic performance in deer mice. *J. Exp. Biol.* **206**, 1221-1231.

Clanton, T.L., Zuo, L. and Klawitter, P. (1999) Oxidants and skeletal muscle function physiologic and pathophysiologic implications. *Proc. Soc. Exp. Biol. Med.* **222,** 253-262.

Cornick, L.A. and Horning, M. (2003). A test of hypotheses based on optimal foraging considerations for a diving mammal using a novel experimental approach. *Can. J. Zool.* **81**, 1799-1807.

Crocker, D.E., Williams, J.D., Costa, D.P. and LeBoeuf, B.J. (2001) Maternal traits and reproductive effort in northern elephant seals. *Ecology* **82**, 3541-3555.

Davis, R.W. and Kanatous, S.B. (1999) Convective oxygen transport and tissue oxygen consumption in Weddell seals during aerobic dives. *J. Exp. Biol.* **202**, 1091-1113.

Davis, R.W., Catellini, M.A., Kooyman, G.L. and Maue, R. (1983) Renal glomerular filtration rate and hepatic blood flow during voluntary diving in Weddell seals. *Am. J. Physiol.* **245** , R743-R748.

Davis, R.W., Fuiman, L.A., Williams, T.M., Collier, S.O., Hagey, W.P., Kanatous, S.B., Kohin, S. and Horning, M. (1999). Hunting behavior of a marine mammal beneath the Antarctic fast ice. *Science* **283**, 993-996.

Davis, R.W., Polasek, L., Watson, R.W., Fuson, A., Williams, T.M. and Kanatous, S.B. (2004) The diving paradox: new insights in to the role of the dive response in air-breathing vertebrates. *Comp. Biochem. Physiol. A* **138**, 263-268.

Dawson, T.L., Gores, G.L., Nieminen, A.L., Herman, B. and Lemasters, J.J. (1993). Mitochondria as a source of reactive oxygen species during reductive stress in rat hepatocytes. *Am. J. Physiol.* **264**, C961-967.

Delp, M.D. and Duan, C. (1996). Composition and size if type I, IIa, IId/x, and IIb fibers and citrate synthase activity of rat muscle. *J. Appl. Physiol.* **80**, 261-270.

Dinenno, F.A., Jones, P.P., Seals, D.R. and Tanaka, H. (2000). Age-associated arterial wall thickening is related to elevations in sympathetic activity in healthy humans. *Am. J. Physiol.* **278**, H1205-H1210.

Dirks, A. and Leeuwenburgh, C. (2002). Apoptosis in skeletal muscle with aging. *Am. J. Physiol.* **282**, R519-R527.

Dolar, M.L.L., Suarez, P., Ponganis, P.J. and Kooyman, G.L. (1999) Myoglobin in pelagic small cetaceans. *J. Exp. Biol.* **202**, 227-236.

Dolber, P.C. and Spach, M.S. (1987). Picrosirius red staining of cardiac muscle following phosphomolybic acid treatment. *Stain Technol.* **62**, 23-26.

Edström, L. and Larsson, L. (1987) Effects of age on contractile and enzyme-histochemical properties of fast- and slow-twitch single motor units in the rat. *J. Physiol.* **392**, 129-45.

Elsner, R., Øyasæter S., Almaas, R. and Saugstad, O.D. (1998) Diving seals, ischemia-reperfusion and oxygen radicals. *Comp. Biochem. Physiol.* **199A**, 975-980.

Essén-Gustavsson, B. and Borges, O. (1986). Histochemical and metabolic characteristics of human skeletal muscle in relation to age. *Acta. Physiol. Scand.* **126**, 107-114.

Evans, W.J. (1995) What is sarcopenia? *J. Geronotol. A* **50 Spec No**, 5-8.

Fedak, M.A. and Thompson, D. (1993). Behavioural and physiological options in diving seals. *Symp. Zool. Soc. Lond.* **66**, 333-348.

Flaherty, J.T. and Weisfeldt, M.L. (1988) Reperfusion injury. *Free Rad. Biol. Med.* **5**, 409-419.

Flögel, U., Gödecke, A., Klotz, L. and Schrader, J. (2004). Role of myoglobin in the antioxidant defense of the heart. *FASEB J*. **18**, 1156-1158.

Flohé, L. and Günzler, W.A. (1894). Assays of glutathione peroxidase. *Meth. Enzymol.* **105**, 114-119.

Folkow, B. and Svanborg, A. (1993). Physiology of cardiovascular aging. *Physiol. Revs.* **73**, 725-764.

Fuiman, L.A. Davis, R.W. and Williams, T.M. (2002). Behavior of midwater fishes under the Antarctic ice: observations by a predator. *Marine Biol.* **140**, 815-822.

Fujise, Y., Hidaka, H., Tatsukawa, R. and Miyazaki, N. (1985). External measurements and organ weights of five Weddell seals (*Leptonychotes weddellii*) caught near Syowa station. *Jap. Fish. Bull*. **85**, 96-101.

Fulle, S., Protasi, F., Di Tano, G., Pietrangelo, T., Beltramin, A., Boncompagni, S., Vecchiet, L. and Fanò, G. (2004) The contribution of reactive oxygen species to sarcopenia and muscle aging. *Exp. Gerontol.* **39**, 17-24.

Garry, D.J., Kanatous, S.B. and Mammen, P.P.A. (2003). Emerging roles for myoglobin in the heart. *Trends Cardiovasc. Med.* **13**, 111-116.

Gilmour, K.M., Wilson, R.W. and Sloman, K.A. (2005). The integration of behaviour into comparative physiology. *Physiol. Biochem. Zool.* **78**, 669-678.

González, E., Messi, M.L., Zheng, Z. and Delbono, O. (2003) Insulin-like growth factor-1 prevents age-related decrease in specific force and intracellular Ca^{2+} in single intact muscle fibres from transgenic mice. *J. Physiol.* **552**, 833-844.

Gosselin, L.E., Martinez, D.A., Vailas, A.C. and Sieck, G.C. (1994). Passive length-force properties of senescent diaphragm: relationship with collagen characteristics. *J. Appl. Physiol.* **76,** 2680-2685.

Gosselin, L.E., Adams, A., Cotter, T.A., McCormick, R.J. and Thomas, D.P. (1998) Effect of exercise training on passive stiffness in locomotor skeletal muscle: role of extracellular matrix. *J. Appl. Physiol.* **85**, 1011-1016.

Goto, S., Nakamura, A., Radak, Z., Nakamoto, H., Takahashi, R., Yasuda, K., Sakurai, Y. and Ishii, N. (1999). Carbonylated proteins in aging and exercise: immunoblot approaches. *Mech. Ageing Dev.* **107**, 245-253.

Gottlieb, R. (2003) Cytochrome P450: major player in reperfusion injury. *Arch. Biochem. Biophys.* **420**, 262-267.

Goubel, F. and Marini, J.F. (1987). Fibre type transition and stiffness modification of soleus muscle of trained rats. *Pflügers Arch.* **410**, 321-325.

Guppy, M., Hill, R.D., Schneider, R.C., Qvist, J., Liggins, G.C., Zapol, W.M. and Hochachka, P.W. (1986). Microcomputer-assisted metabolic studies of voluntary diving of Weddell seals. *Am. J. Physiol.* **250**, R175-187.

Gusztak, R.W. and Campbell, K.L. (2004). Growth, development and maintenance of American water shrews (*Sorex palustris*) in captivity. *Mammal Study*. **29**, 65-72.

Guyton, G.P., Stanek, K.S., Schneider, R.C., Hochachka, P.W., Hurford, W.E., Zapol, D.G., Liggins, G.C. and Zapol, W.M. (1995) Myoglobin saturation in free-diving Weddell seals. *J. Appl. Physiol.* **79**, 1148-55.

Halasz, N.A., Elsner, R., Garvie, R.S. and Grotke, G.T. (1973). Renal recovery from ischemia: a comparative study of seal and dog kidneys. *Am. J. Physiol.* **227**, 1331-1335.

Hamilton, P.K., Knowlton, A.R., Marx, M.K. and Kraus, S.D. (1979). Age structure and longevity in North Atlantic right whales *Eubalaena glacialis* and their relation to reproduction. *Mar. Ecol. Prog. Ser.* **171**, 285-292.

Hanni, K.D., Long, D.J., Jones, R.E., Pyle, P. and Morgan, L.E. (1997) Sightings and strandings of Guadalupe fur seals in central and northern California, 1988-1995. *J. Mammal.* **78**, 684-690.

Harman, D. (1994). Aging: prospects for further increases in functional life span. *Age* **17**, 199-146.

Herbst, A., Pak, J.W., McKenzie, D., Bua, E., Bassiouni, M. and Aiken, J.M. (2007) Accumulation of mitochondrial DNA deletion mutations in aged muscle fibers: evidence for a causal role in muscle fiber loss. *J. Gerontol. A* **62**, 235-45.

Hermes-Lima, M. and Zenteno-Savín, T. (2002) Animal response to drastic changes in oxygen availability and physiological oxidative stress. *Comp. Biochem. Physiol.* **133C**, 537-556.

Hermes-Lima, M., Wilmore, W.G. and Storey, K.B. (1995). Quantification of lipid peroxidation in tissue extracts based on Fe(III) xylenol-orange complex formation. *Free Rad. Biol. Med.* **19**, 271-280.

Herrero, A. and Barja, G. (1997). Sites and mechanisms responsible for the low rate of free radical production of heart mitochondria in the long-lived pigeon. Mech*. Ageing Dev.* **98**, 95-11.

Herrero, A. and Barja, G. (1998). H_2O_2 production of heart mitochondria and aging rate are slower in canaries and parakeets than in mice: sites of free radical generation and mechanisms involved. *Mech. Ageing Dev.* **103**, 133-146.

Higami, Y. and Shimokawa, I. (2000). Apoptosis in the aging process. *Cell Tissue Res.* **301**, 125-132.

Hill, R.D., Schneider, R.C., Liggins, G.C., Shuette, A.H., Elliott, R.L., Guppy, M., Hochachka, P.W., Qvist, J., Falke, K.J. and Zapol, W.M. (1987). Heart rate and body temperature during free diving of Weddell seals. *Am. J. Physiol.* **253**, 344-351.

Hindell, M.A., Harcourt, R., Waas, J.R. and Thompson, D. (2002). Fine-scale three-dimensional spatial use by diving, lactating female Weddell seals *Leptonychotes weddellii*. *Mar. Ecol. Prog. Ser.* **242**, 275-284.

Hindle, A.G., McIntyre, I.W., Campbell, K.L. and MacArthur, R.A. (2003). The heat increment of feeding and its thermoregulatory implications in the short-tailed shrew (*Blarina brevicauda*). *Can. J. Zool.* **81**, 1445-1453.

Hindle, A.G., Horning, M., Mellish, J.E. and Lawler, J.M. (2007). Aging in a free-ranging pinniped population: structural changes in swimming muscle. *17th Biennial Conference of the Marine Mammal Society.* Cape Town, South Africa. Abstract.

Hollander, J., Bejma, J., Ookawara, T., Ohno, H. and Ji, L.L. (2000). Superoxide dismutase gene expression in skeletal muscle: fiber-specific effect of age. *Mech. Ageing Dev.* **116**, 33-45.

Holmes, E.E. and York, A.E. (2003) Using age structure to detect impacts on threatened populations: a case study with Steller sea lions. *Cons. Biol.* **17,** 1794-1806.

Holloszy, J.O., Chen, M., Cartee, G.D. and Young, J.C. (1991) Skeletal muscle atrophy in old rats: differential changes in the three fiber types. *Mech. Ageing Dev.* **60**, 199-213.

Horning, M. and Trillmich, F. (1997) Development of hemoglobin, hematocrit, and erythrocyte values in Galápagos fur seals. *Mar. Mamm. Sci.* **13**, 100-113.

Houston, A.I. and McNamara, J.M. (1985). A general theory of central place foraging for single-prey loaders. *Theor. Popul. Biol.* **28**, 233-262.

Houston, A.I. and Carbone, C. (1992). The optimal allocation of time during the diving cycle. *Behav. Ecol.* **3**, 255-265.

Ji, L.L., Dillon, D. and Wu, E. (1990). Alteration of antioxidant enzyme with aging in rat skeletal muscle and liver. *Am. J. Physiol.* **258**, R918-R923.

Julius, S., Amery, A., Whitlock, L. and Conway, J. (1967) Influence of age on hemodynamic response to exercise. *Circulation* **36**, 222-229.

Jürgens, K.D. (2002). Etruscan shrew muscle: the consequences of being small. *J. Exp. Biol.* **205**, 2161-2166.

Kanatous, S.B., DiMichele, L.V., Cowan, D.F. and Davis, R.W. (1999) High aerobic capacities in the skeletal muscles of pinnipeds: adaptations to diving hypoxia. *J. Appl. Physiol.* **86**, 1247-1256.

Kanatous, S.B., Davis, R.W., Watson, R., Polasek, L., Williams, T.M. and Mathieu-Costello, O. (2002) Aerobic capacities in the skeletal muscles of Weddell seals: key to longer dive durations? *J. Exp. Biol.* **205**, 3061-3068.

Kirkwood, T.B.L. and Austad, S.N. (2000) Why do we age? *Nature* **409**, 233-238.

Kjaer, M. (2004). Role of extracellular matrix in adaptation of tendon and skeletal muscle to mechanical loading. *Physiol. Rev.* **84**, 649-698.

Kleiber, M. (1975). *The Fire of Life*. Huntington, NY: Robert E. Krieger Publishing Co.

Klitgaard, H., Brunet, A., Maton, B., Lamaziere, C., Lesty, C. and Monod, H. (1989*a*). Morphological and biochemical changes in old rat muscles: Effect of increased use. *J. Appl. Physiol.* **67**, 1409-1417.

Klitgaard, H., Marc, R., Brunet, A., Vandewalle, H. and Monod, H. (1989*b*). Contractile properties of old rat muscles: Effect of increased use. *J. Appl. Physiol.* **67**, 1401-1408.

Knowlton, A.R., Kraus, S.D. and Kenney, R.D. (1994) Reproduction in North-Atlantic right whales (*Eubalaena glacialis*). *Can. J. Zool.* **72**, 1297-1305.

Kobzik, L., Reid, M.B., Bredt, D.S. and Stamler, J.S. (1994) Nitric oxide in skeletal muscle. *Nature* **372**, 546-548.

Kooyman, G.L., Wahrenbrock, E.A., Castellini, M.A., Davis, R.W. and Sinnett, E.E. (1980). Aerobic and anaerobic metabolism during voluntary diving in Weddell seals; evidence of preferred pathways from blood chemistry and behavior. *J. Comp. Physiol.* **138**, 335-346.

Kooyman, G.L., Castellini, M.A., Davis, R.W. and Maue, R.A. (1983). Aerobic diving limits of immature Weddell seals. *J. Comp. Physiol.* **151**, 171-174.

Kovanen, V. (1989). Effects of ageing and physical training on rat skeletal muscle. An experimental study on the properties of collagen, laminin, and fibre types in muscles serving different functions. *Acta Physiol. Scand.* **S577**, 1-56.

Kovanen, V. (2002). Intramuscular extracellular matrix: complex environment of muscle cells. *Exerc. Sport Sci. Rev.* **30**, 20-25.

Kovanen, V. and Suominen, H. (1989). Age- and training-related changes in the collagen metabolism of rat skeletal muscle. *Eur. J. Appl. Physiol. Occup. Physiol.* **58**, 765-772.

Kovanen V, Suominen H, and Heikkinen E. (1984). Mechanical properties of fast and slow skeletal muscle with special reference to collagen and endurance training. *J. Biomech.* 17, 725–735.

Kramer, D.L. (1988) The behavioral ecology of air breathing by aquatic animals. *Can. J. Zool.* **66**, 89-94.

Krebs, J.R., Ryna, J.C. and Charnov, E.L. (1974). Hunting by expectation or optimal foraging? A study of patch use in chickadees. *Anim. Behav.* **22**, 953-964.

Krivickas, L.S., Suh, D.W., Wilkins, J., Hughes, V.A., Roubenoff, R. and Frontera, W.R. (2001). Age- and gender-related differences in maximum shortening velocity of skeletal muscle fibers. *Am. J. Physiol. Med. Rehabil.* **80**, 447-455.

Kukreja, R.C. (2001) Essential role of oxygen radicals in delayed pharmacological preconditioning. *J. Molec. Cell. Cardio.* **33**, 1395-1398.

Larsson, L., Li, X.P. and Yu, F.S. (1997). Age-related changes in contractile properties and expression of myosin isoforms in single skeletal muscle cells. *Muscle Nerve* **falta volume**, S74-S78.

Lass, A., Sohal, B.H., Weindruch, R., Forster, J. and Sohal, M.J. (1998). Caloric restriction prevents age-assocaited accrual of oxidative damage to mouse skeletal muscle mitochondria. *Free Rad. Biol. Med.* **25**, 1089-1087.

Lawler, J.M. and Song, W. (2002). Specificity of antioxidant enzyme inhibition in skeletal muscle to reactive nitrogen species donors. *Biochem. Biophys. Res. Comm.* **294**, 1093-1100.

Lawler, J.M., Powers, S.K., Visser, T. Van Dijk, H., Kordus, M.J. and Ji, L.L. (1993). Acute exercise and skeletal muscle antioxidant and metabolic enzymes: effects of fiber type and age. *Am. J. Physiol.* **265**, Rl344-R1350.

Lawler, J.M., Song, W. and Demaree, S.R. (2003). Hindlimb unloading increases oxidative stress and disrupts antioxidant capacity in skeletal muscle. *Free Rad. Biol. Med.* **35**, 9-16.

Lee, H.C. and Wei, Y.H. (2001). Mitochondiral alterations, cellular response to oxidative stress and defective degradation of proteins in aging. *Biogerontology* **2**, 231-244.

Lee, J. and Alway, S.E. (1996). Adaptations of myonuclei to hypertrophy in patagialis muscle fibers from aged quail. *Mech. Ageing Dev.* **88**, 185-197.

Lowe, D.A., Surek, J.T., Thomas, D.D. and Thompson, L.V. (2001) Electron paramagnetic resonance reveals age-related myosin structural changes in rat skeletal muscle fibers. *Am. J. Physiol. Cell Phsyiol.* **280**, C540-547.

Lowe, D.A., Warren, G.L., Snow, L.M., Thompson, L.V. and Thomas, D.D. (2004). Muscle activity and aging affect myosin structural distribution and force generation in rat fibers. *J. Appl. Physiol.* **96**, 498-506.

MacArthur, R.A., Humphries, M.M., Fines, G.A. and Campbell, K.L. (2001) Body oxygenstores, aerobic dive limits, and the diving abilities of juvenile and adult muskrats (Ondatra zibethicus). *Physiol. Biochem. Zool.* **74**, 178-190.

Mackey, A.L., Donnelly, A.E., Turpeenniemi-Hujanen, T. and Roper, H.P. (2004). Skeletal muscle collagen content in humans after high-force eccentric contractions. *J. Appl. Physiol.* **97**, 197-203.

Marcell, T.J. (2003). Sarcopenia: Causes, consequences, and preventions. *J. Gerontol. A Biol. Sci. Med. Sci.* **58**, M911-M916.

Marshall, P., Williams, P.E. and Goldspink, G. (1989). Accumulation of collagen and altered fiber-type ratios as indicators of abnormal muscle gene expression in the mdx dystrophic mouse. *Muscle Nerve* **12**, 528-537.

Mathieu-Costello, O., Morales, S., Savolainen, J. and Varnanen, M. (2002). Fiber capillarization relative to mitochondrial volume in diaphragm of shrew. *J. Appl. Physiol.* **93**, 346-353.

Mays, P.K., Bishop, J.E., and Laurent, G.J. (1988). Age-related changes in the proportion of type I and III collagen. *Mech. Ageing Dev.* 45, 203–212.

McIntyre, I.W., Campbell, K.L. and MacArthur, R.A. (2002). Body oxygen stores, aerobic dive limits and diving behaiour of the star-nosed mole (*Condylura cristata*) and comparisons with non-aquatic talpids. *J. Exp. Biol.* **205**, 45-54.

Mecocci, P., Fanò, G., Fulle, S., MacGarvey, U., Shinobu, L., Polidori, M.C., Cherubini, A., Vecchiet, J., Senin, U. and Beal, M.F. (1999) Age-dependant increases in oxidative damage to DNA, lipids, and proteins in human skeletal muscle. *Free Radic. Biol. Med.* **26**, 303-308.

Meydani, M. and Evans, W.J. (1993). Free radicals, exercise, and aging. In: *Free Radicals in Aging.* Yu, B.P., ed, pp 183-204. Boca Raton, FL: CRC Press.

Miller, T.A., Lesniewski, L.A., Muller-Delp, J.M., Majors, A.K., Scalise, D. and Delp, M.D. (2001) Hindlimb unloading induces a collagen isoform shift in the soleus muscle of the rat. *Am. J. Phsyiol.* **281**, R1710-R1717.

Mohan, S. and Radha, E. (1980). Age-related changes in rat muscle collagen. *Gerontology* **26**, 61-67.

Moharaj, P., Wright, V. and Clanton, T.L. (1997) Tiron (1,2,Dihydroxybenzene-2,5-disulfate) inhibits diaphragmatic muscle fatigue. *Am. J. Respir. Crit. Care Med.* **155,** A923.

Mori, Y. (1998). The optimal patch use in divers: optimal time budget and the number of dive cycles during bout. *J. Theor. Biol.* **190**, 187-199.

Mori, Y. (2002). Optimal diving behaviour for foraging in relation to body size. *J. Evol. Biol.* **15**, 269-276.

Ogilvie, R.W. and Feedback, D.L. (1990). A metachromatic dye-ATPase method for the simultaneous identification of skeletal muscle fiber types I, IIA, IIB and IIC. *Stain Technol*. **65**, 231-241.

Orians, G.H. and Pearson, N.E. (1979). On the theory of central place foraging. In: *Analysis of Ecological systems.* (ed. D.J. Horn, R.D. Mitchell, and G.R. Stairs), pp 155-177. Columbus, OH: Ohio State Univ. Press.

Pansarasa, O., Felzani, G., Vecchiet, J. and Marzatico, F. (2002) Antioxidant pathways in human aged skeletal muscle: relationship with the distribution of type II fibers. *Exp. Gerontol.* **37**, 1069-1075.

Parsons, P.A. (2002) Life span: does the limit to survival depend upon metabolic efficiency under stress? *Biogerontology* **3**, 233-241.

Payne, A.M. and Delbono, O. (2004). Neurogensis of excitation-contraction uncoupling in aging skeletal muscle. *Exerc. Sport Sci. Rev.* **32**, 36-40.

Peters, T., Kubis, H.P., Wetzel, P., Sender, S., Asmussen, G., Fons, R. and Jurgens, K.D. (1999). Contraction parameters, myosin composition and metabolic enzymes of the skeletal muscles of the Etruscan shrew *Suncus etruscus* and of the common European white-toothed shrew *Crocidura russula* (Insectivora: Soricidae). *J. Exp. Biol.***202**, 2461-2473.

Phaneuf, S. and Leeuwenburgh, C. (2002). Cytochrome *c* release from mitochondria in the aging heart: a possible mechanism for apoptosis with age. *Am. J. Physiol.* **282**, R423-R430.

Pietschmann, M., Bartels, H. and Fons, R. (1982). Capillary supply of heart and skeletal muscle of small bats and non-flying mammals. *Resp. Physiol.* **50**, 267-282.

Pistorius, P.A. and Bester, M.N. (2002) A longitudinal study of senescence in a pinniped. *Can. J. Zool.* **80**, 395-401.

Pitcher, K.W., Calkins, D.G. and Pendleton, G.W. (1998). Reproductive performance of female Steller sea lions: an energetics-based reproductive strategy? *Can. J. Zool.* **76**, 2075-2083.

Pollack, M., Phaneuf, S., Dirks, A. and Leeuwenburgh, C. (2002). The role of apoptosis in the normal aging brain, skeletal muscle, and heart. *Ann. N.Y. Acad. Sci.* **959**, 93-107.

Ponganis, P.J., Kooyman, G.L., Castellini, M.A., Ponganis, E.P. and Ponganis, K.V. (1993). Muscle temperature and swim velocity profiles during diving in a Weddell seal, Leptonychotes weddellii. *J. Exp. Biol.* **183**, 341-348.

Pousson, M., Perot, C. and Goubel, F. (1991) Stiffness changes and fibre type transitions in rat soleus muscle produced by jumping training. *Pflügers Arch.* **419**, 127-130.

Prochniewicz, E., Thomas, D.D. and Thompson, L.V. (2005). Age-related decline in actomyosin function. *J. Gerontol. A Biol. Sci. Med. Sci.* **280**, C540-C547.

Reichmann, H. and Pette, D. (1982). A comparative microphotometric study of succinate dehydrogenase activity levels in type I, IIA and IIB fibres of mammalian and human muscles. *Histochem. Cell Biol.* **74**, 27-41.

Reid, M.B., Soji, T., Moody, M.R. and Entman, M.L. (1992) Reactive oxygen species in skeletal muscle II: extracellular release of free radicals. *J. Appl. Phsyiol.* **73**, 1805-1809.

Renault, V., Thornell, L.E., Butler-Browne, G. and Mouly, V. (2002) Human skeletal muscle satellite cells: aging, oxidative stress and the mitotic clock. *Exp. Gerontol.* **37**, 1229-1236.

Rivero, J.L.L., Galisteo, A.M., Agüera, E. and Miró, F. (1993). Skeletal muscle histochemistry in male and female Andalusian and Arabian horses of different ages. *Res. Vet. Sci.* **54**, 160-169.

Robertson, J.D., Chandra J., Gogvadze V. and Orrenius, S. (2001) Biological reactive intermediates and mechanisms of cell death. *Adv. Exp. Med. Biol.* **500**, 1-10.

Ronéus, M., Lindholm, A. and Asheim, A. (1991). Muscle characteristics in Thoroughbreds of different ages and sexes. *Equine Vet. J.* **23**, 207-210.

Ryan, M. and Ohlendieck, K. (2004). Excitation-contraction uncoupling and sarcopenia. *Basic Appl. Myol.* 14, 141-154.

Sanz, A., Hiona, A., Kujoth, G. C., Seo, A. Y., Hofer, T., Kouwenhoven, E., Kalani, R., Prolla, T. A., Barja, G. and Leeuwenburgh, C. (2007). Evaluation of sex

differences on mitochondrial bioenergetics and apoptosis in mice. *Exp. Geront.* **42**, 173-182.

Sastre, J., Pallardó, F.V. and Viña, J. (2000). Mitochondrial oxidative stress plays a key role in aging and apoptosis. *IUBMB Life* **49**, 427-435.

Sato, K., Mitani, Y., Cameron, M.F., Siniff, D.B. and Naito, Y. (2003). Factors affecting stroking patterns and body angle in diving Weddell seals under natural conditions. *J. Exp. Biol.* **206**, 1461-1470.

Savolainen, J. and Vornanen, M. (1995*a*). Myosin heavy chains in skeletal muscle of the common shrew (*Sorex araneus*): absence of slow isoform and transitions of fast isoform with ageing. *Acta Physiol. Scand.* **155**, 233-239.

Savolainen, J. and Vornanen, M. (1995*b*). Fiber types and myosin heavy chain composition in muscles of common shrew (*Sorex araneus*). *J. Exp. Zool.* **271**, 27-35.

Savolainen, J. and Vornanen, M. (1998). Muscle capillary supply in hind limb and diaphragm of the common shrew (*Sorex araneus*). *J. Comp. Physiol. B* **168**, 289-294.

Sharov, V.S., Dremina, E.S., Galeva, N.A., Williams, T.D. and Schoneich, C. (2006). Quantitative mapping of oxidation-sensitive cysteine residues in SERCA in vivo and in vitro by HPLC-electrospray-tandem MS: selective protein oxidation during biological aging. *Biochem. J.* **394**, 605-615.

Sohal, R.S. and Weindruch, R. (1996). Oxidative stress, caloric restriction, and aging. *Science* **273**, 59-63.

Srere, P.A. (1969). Citrate synthase. *Meth. Enzymol.* **13**, 3-11.

Stephenson, R. (2005). A theoretical analysis of diving performance in the Weddell seal (*Leptonychotes weddelli*). *Physiol. Biochem. Zool.* **78**, 782-800. 2005.

Stewart, J.M., Woods, A.K. and Blakely, J.A. (2005) Maximal enzyme activities, and myoglobin and glutathione concentrations in heart, liver and skeletal muscle of the Northern Short-tailed shrew (*Blarina brevicauda*; Insectivora: Soricidae). Comp. Biochem. Physiol., B **141**, 267-273.

Suh, J.H., Heath, S. and Hagen, T.M. (2003). Two subpopulations of Mitochondria in the aging rat heart display heterogenous levels of oxidative stress. *Free Rad. Biol. Med.* **35**, 1064-1072.

Supinsky, G., Nethery, D., Stofan, D. and DiMarco, A. (1999). Extracellular calcium modulates generation of reactive oxygen species by the contracting diaphragm. *J. Appl. Physiol.* **87**, 2177-2185.

Sweat, F., Puchtler, H. and Rosenthal, S.I. (1964). Sirius Red F3BA as a stain for connective tissue. *Arch. Pathol.* **78**, 69-72.

Thompson, L.V. (1999). Contractile properties and protein isoforms of single skeletal muscle fibers from 12-and 30-month-old Fisher 344 Brown Norway F1 hybrid rats. *Aging Clin. Exp. Res.* **11**, 109-118.

Thompson, D. and Fedak, M.A. (2001). How long should a dive last? a simple model of foraging decisions by breath-hold divers in a patchy environment. *Anim. Behav.* **61**, 287-296.

Tomonaga, M. (1977). Histochemical and ultrastructural changes in senile human skeletal muscle. *J. Am. Geriatr. Soc.* **25**, 125-131.

Troen, B.R. (2003) The biology of aging. *Mt Sinai J. Med.* **70**, 3-22.

Vanden Hoek, T.L., Li, C., Shao, Z., Shumacker, P.T. and Becker, L.B. (1997*a*) Significant levels of oxidants are generated by isolated cardiomyocytes during ischemia prior to reperfusion. *J. Molec. Cell. Cardiol.* **29**, 2571-2583.

Vanden Hoek, T.L., Shao, Z., Li, C. and Schumacker, P.T. (1997*b*) Mitochondrial electron transport can become a significant source of oxidative injury in cardiomyocytes. *J. Molec. Cell. Cardiol.* **29**, 2441-2450.

Vanden Hoek, T.L., Becker, L.B., Shao, Z., Li, C. and Schumacker, P.L. (1998) Reactive oxygen species released from mitochondria during brief hypoxia induce preconditioning in cardiomyocytes. *J. Biol. Chem.* **273**, 18092-18098.

Vázquez-Medina, J.P., Zenteno-Savi´n, T. and Elsner, R. (2006). Antioxidant enzymes in ringed seal tissues: potential protection against dive-associated ischemia/reperfusion. *Comp. Biochem. Physiol.* **142C**, 198-204.

Viner, R.I., Ferrington, D.A., Williams, T.D., Bigelow, D.J. and Schoneich, C. (1999). Protein modification during biological aging: selective tyrosine nitration of the SERCA2a isoform of the sarcoplasmic reticulum Ca^{2+}-ATPase in skeletal muscle. *Biochem. J.* **340**, 657-669.

Watson, R.R. Miller, T.A. and Davis, R.W. (2003) Immunohistochemical fiber typing of harbor seal skeletal muscle. *J. Exp. Biol.* **206**, 4105-4111.

Williams, P., Simpson, H., Kyberd, P., Kenwright, J. and Goldspink, G. (1999). Effect of rate of distraction on loss of range of joint movement, muscle stiffness, and intramuscular connective tissue content during surgical limb-lengthening: a study in rabbit. *Anat. Rec.* **255**, 78-83.

Williams, T.M., Davis, R.W., Fuiman, L.A., Francis, J., Le Boeuf, B.J., Horning M., Calambokidis, J. and Croll, D.A. (2000) Sink or swim: strategies for cost-efficient diving by marine mammals. *Science* **288**:133-136.

Williams, T.M., Haun, J., Davis, R.W., Fuiman, L.A. and Kohin, S. (2001). A killer appetite: metabolic consequences of carnivory in marine mammals. *Comp. Biochem. Physiol. A* **129**, 785-796.

Williams, T.M., Fuiman, L.A., Horning, M. and Davis, R.W. (2004). The cost of foraging by a marine predator, the Weddell seal *Leptonychotes weddellii*: pricing by the stroke. *J. Exp. Biol.* **207**, 973-982.

Winston, G.W. (1991). Oxidants and antioxidants in aquatic animals. *Comp. Biochem. Physiol.* **100C**, 173-176.

Yang, Y. Sharma, R., Sharma, A., Awasthi, S. and Awasthi, Y.C. (2003). Lipid peroxidation and cell cycle signaling: 4-hydrozynonenal, a key molecule in stress mediated signaling. *Acta Biochim. Pol.* **50**, 319-336.

Ydenburg, R.C. and Clark, C.W. (1989). Aerobiosis and anaerobiosis during diving by Western Grebes: an optimal foraging approach. *J. Theor. Biol.* **139**, 437-449.

Zenteno-Savín, T., Clayton-Hernández, E. and Elsner, R. (2002) Diving seals: are they a model for coping with oxidative stress? *Comp. Biochem. Physiol.* **133C,** 527-536.

Zerba, E., Komorowski T.E. and Faulkner, J.A. (1990). Free radical injury to skeletal muscles of young, adult, and old mice. *Am. J. Physiol.* **258**, C429-C435.

Zhong, S., Chen, C.N. and Thompson, L.V. (2007). Sarcopenia of ageing: functional, structural and biochemical alterations. *Rev. Bras. Fisioter.* **11**, 91-97.

APPENDIX A: REDOX EQUATIONS

Superoxide dismutase catalyzes the initial breakdown of the superoxide radical (e.g., CuZn-SOD)

$Cu^{2+} + O_2^{-}\cdot > Cu^{+} + O_2$

$Cu^{+} + O_2^{-}\cdot + 2H^{+} > Cu^{2+} + H_2O_2$

Net Reaction: $2\ O_2^{-}\cdot + 2H^{+} > H_2O_2 + O_2$

Catalase catalyzes the reaction:

$2\ H_2O_2 > 2\ H_2O + O_2$

*this is the basis of the spectrophotometric assay for catalase, where H_2O_2 depletion is measured directly.

Glutathione Peroxidase catalyzes the reaction:

$H_2O_2 + 2H^{+} > 2H_2O$

Glutathione Peroxidase activity is measured spectrophotometrically with the reaction:

Glutathione Peroxidase catalyzes,

$ROOH + 2GSH > GSSG + ROH + H_2O$

This solution is incubated, then Glutathione reductase is added to catalyze,

$GSSG + NADPH + H^{+} > 2\ GSH + NADP^{+}$

*NADPH depletion is monitored.

Citrate Synthase is measured via the reaction:

Citrate synthase catalyzes,

acetyl CoA + oxalacetate + H_2O > citrate + CoASH + H^{+}

mercaptide ion production is then measured,

CoASH + DTNB > mercaptide ion

Myoglobin may act as a direct antioxidant through the following equation:

ferrous oxygenated Mb + NO > ferric oxidized Mb (metMb) and nitrate (NO_3).

APPENDIX B: STELLA MODEL EQUATIONS

bout_dive_complete(t) = bout_dive_complete(t - dt) + (bout_count - bout_clear) * dt
INIT bout_dive_complete = 0

INFLOWS:
bout_count = IF prey_encounter_clear>= prey_threshold THEN 1 ELSE 0
OUTFLOWS:
bout_clear = IF prey_encounter_clear > 0 AND prey_encounter_clear < prey_threshold THEN bout_dive_complete ELSE 0

DAILY_DIVE(t) = DAILY_DIVE(t - dt) + (dive_clock_clear - daily_dive_clear) * dt
INIT DAILY_DIVE = 0

INFLOWS:
dive_clock_clear = IF surfacing = 1 THEN DIVE_CLOCK
ELSE 0
OUTFLOWS:
daily_dive_clear = IF minutes = 1440 THEN DAILY_DIVE ELSE 0

DAILY_ENERGY(t) = DAILY_ENERGY(t - dt) + (Egained - Eexpended) * dt
INIT DAILY_ENERGY = 0

INFLOWS:
Egained = IF minutes = 1440 THEN MIN (FISH*Caloric_value_fish , 301.709*(M^.7)) ELSE 0
OUTFLOWS:
Eexpended = IF minutes = 1440 THEN Ar+Aw ELSE 0

DAILY_SURFACE(t) = DAILY_SURFACE(t - dt) + (surface_clock_clear - daily_surface_clear) * dt
INIT DAILY_SURFACE = 720

INFLOWS:
surface_clock_clear = IF diving =1 THEN SURFACE_CLOCK
ELSE 0
OUTFLOWS:
daily_surface_clear = IF minutes = 1440 THEN DAILY_SURFACE ELSE 0

DIVE_CLOCK(t) = DIVE_CLOCK(t - dt) + (dive_minutes - dive_clock_clear) * dt
INIT DIVE_CLOCK = 0

INFLOWS:
dive_minutes = IF SUBMERGE = 1 THEN 1

```
        ELSE 0
OUTFLOWS:
        dive_clock_clear = IF surfacing = 1 THEN DIVE_CLOCK
        ELSE 0

Dive_Time(t) = Dive_Time(t - dt) + (dive_time_in - dive_time_clear) * dt
INIT Dive_Time = 0

INFLOWS:
        dive_time_in = IF diving = 1 THEN down
        ELSE 0
OUTFLOWS:
        dive_time_clear = IF surfacing = 1 THEN Dive_Time
        ELSE 0

FISH(t) = FISH(t - dt) + (fish_per_dive - fish_clear) * dt
INIT FISH = 0

INFLOWS:
        fish_per_dive = (IF capture = 1 AND down>2 THEN (down-2)*prey_probability
        ELSE 0)
OUTFLOWS:
        fish_clear = IF minutes = 1440 THEN FISH ELSE 0

M(t) = M(t - dt) + (growth) * dt
INIT M = 350

INFLOWS:
        growth = (Egained-Eexpended)/1000

Previous_Dive_TIme(t) = Previous_Dive_TIme(t - dt) + (dive_time_clear - dive_clear)
*dt
INIT Previous_Dive_TIme = 0

INFLOWS:
        dive_time_clear = IF surfacing = 1 THEN Dive_Time
        ELSE 0
OUTFLOWS:
        dive_clear = IF surfacing = 1 THEN Previous_Dive_TIme ELSE 0

prey_encounter(t) = prey_encounter(t - dt) + (prey_probability - prey_encounter_clear) *
dt
INIT prey_encounter = prey_probability
```

```
INFLOWS:
        prey_probability = IF diving =1 AND prey_encounter_delayed < prey_threshold
        THEN prey_filter
        ELSE
        (IF diving =1 AND prey_encounter_delayed >= prey_threshold
        THEN prey_encounter_delayed*.9
        ELSE 0)
OUTFLOWS:
        prey_encounter_clear = IF surfacing > 0 THEN prey_encounter
        ELSE 0

prey_encounter_delayed(t) = prey_encounter_delayed(t - dt) + (prey_encounter_clear -
prey_encounter_count_clear) * dt
INIT prey_encounter_delayed = prey_threshold

INFLOWS:
        prey_encounter_clear = IF surfacing > 0 THEN prey_encounter
        ELSE 0
OUTFLOWS:
        prey_encounter_count_clear = IF dive_clock_clear > 0 THEN
        prey_encounter_delayed ELSE 0

Prey_threshold_actual(t) = Prey_threshold_actual(t - dt) + (actual_prey_threshold -
PTA_clear) * dt
INIT Prey_threshold_actual = 0

INFLOWS:
        actual_prey_threshold = IF prey_probability >=prey_threshold AND
        bout_dive_complete=0 THEN prey_probability ELSE 0
OUTFLOWS:
        PTA_clear = IF prey_encounter < prey_threshold THEN Prey_threshold_actual
        ELSE 0

SUBMERGE(t) = SUBMERGE(t - dt) + (diving - surfacing) * dt
INIT SUBMERGE = 0

INFLOWS:
        diving = IF minutes < 720 THEN (IF SURFACE_CLOCK >= Surface_TIme
        THEN 1
        ELSE 0) ELSE 0
OUTFLOWS:
        surfacing = IF (count=1) THEN 0 ELSE (IF DIVE_CLOCK = Dive_Time
        THEN 1
        ELSE 0)
```

```
successful_dive_min(t) = successful_dive_min(t - dt) + (successful_minutes -
successful_minutes_clear) * dt
INIT successful_dive_min = 0

INFLOWS:
        successful_minutes = IF capture = 1 THEN down ELSE 0
OUTFLOWS:
        successful_minutes_clear = IF minutes = 1440 THEN successful_dive_min
        ELSE 0

SURFACE(t) = SURFACE(t - dt) + (surfacing - diving) * dt
INIT SURFACE = 1

INFLOWS:
        surfacing = IF (count=1) THEN 0 ELSE (IF DIVE_CLOCK = Dive_Time
        THEN 1
        ELSE 0)
OUTFLOWS:
        diving = IF minutes < 720 THEN (IF SURFACE_CLOCK >= Surface_TIme
        THEN 1
        ELSE 0) ELSE 0

SURFACE_CLOCK(t) = SURFACE_CLOCK(t - dt) + (surface_minutes -
surface_clock_clear) * dt
INIT SURFACE_CLOCK = 1

INFLOWS:
        surface_minutes = IF count = 1 THEN 0 ELSE (IF SURFACE = 1 THEN 1
        ELSE 0)
OUTFLOWS:
        surface_clock_clear = IF diving =1 THEN SURFACE_CLOCK
        ELSE 0

Surface_TIme(t) = Surface_TIme(t - dt) + (surface_time_in - Surface_TIme_clear) * dt
INIT Surface_TIme = 1

INFLOWS:
        surface_time_in = IF surfacing = 1 THEN up
        ELSE 0
OUTFLOWS:
        Surface_TIme_clear = IF diving = 1 THEN Surface_TIme
        ELSE 0
```

```
Adive = (16.19 + (12.08*(M^(-0.25))*(DAILY_DIVE*percent_success) +
(0.05*strokes))*M) + (9.98*(M^(-0.25))*(DAILY_DIVE*(1-
percent_success))+(0.04*strokes))*M

ADL = ROUND(23)

Af = .15*Egained

allometric_energy = 301.709*(M^.7)

Ar = (Adive*5.09 + Asurface*5.09)/1000

Asurface = (9.98*(M^(-0.25)))*DAILY_SURFACE*M

Au = (0.05*MAX(Egained,Ar))

Aw = Au+Af

blubber = 25

BMR = 16.01*(M^(-0.25))

Caloric_value_fish = 77.6249

capture = IF prey_probability*down >= 1 THEN 1 ELSE 0

Contractile_Props = 1

count = COUNTER(1,50000)

down = IF prey_probability >= prey_threshold AND bout_dive_complete = 0
        THEN ADL
        ELSE (IF prey_probability >= prey_threshold AND bout_dive_complete > 0
        THEN (IF ROUND(Previous_Dive_TIme*.9) > ROUND(ADL/2) THEN
        ROUND (Previous_Dive_TIme*.9) ELSE ROUND (ADL/2))
        ELSE ROUND(random (2,6)))

energy_index = IF allometric_energy = 0 THEN 0 ELSE Egained/allometric_energy

Index_Fatness = (22.5 + blubber)/67.4

minutes = COUNTER(1,1441)
```

```
percent_success = IF DAILY_DIVE = 0 THEN 0 ELSE
        successful_dive_min/DAILY_DIVE

prey_distribution = EXPRND (seed)

prey_filter = IF prey_distribution < 0 THEN 0
        ELSE (IF prey_distribution > 1 THEN 1
        ELSE prey_distribution)

prey_threshold = 0.3
seed = 0.3

strokes = IF Index_Fatness < 0.78
        THEN 50*DAILY_DIVE*Contractile_Props
        ELSE 60*DAILY_DIVE*Contractile_Props

up = IF Prey_threshold_actual < prey_threshold THEN
        (IF (ROUND (Dive_Time/d:s_ratio)) > 0 THEN ROUND (Dive_Time/d:s_ratio)
        ELSE 1) ELSE
        (IF (ROUND (Dive_Time/(50*Prey_threshold_actual/bout_dive_complete))) <
        ROUND (Dive_Time/d:s_ratio) THEN
        ROUND (Dive_Time/(50*Prey_threshold_actual/bout_dive_complete)) ELSE
        (IF (ROUND (Dive_Time/d:s_ratio)) > 0 THEN ROUND (Dive_Time/d:s_ratio)
        ELSE 1))

d:s_ratio = GRAPH(Index_Fatness)
        (0.65, 4.20), (0.663, 4.16), (0.676, 4.12), (0.689, 4.12), (0.703, 4.10), (0.716,
        4.06), (0.729, 3.86), (0.742, 3.66), (0.755, 3.42), (0.768, 3.10), (0.782, 2.80),
        (0.795, 2.56), (0.808, 2.27), (0.821, 2.06), (0.834, 1.90), (0.847, 1.82), (0.861,
        1.70), (0.874, 1.66), (0.887, 1.60), (0.9, 1.54)
```

APPENDIX C: SUMMARY OF RAW DATA

Table A-1: Identification and sample collection information from field-caught water shrews (WS) and short-tailed shrews (STS). Animals were collected during the summers of 2005 and 2006 in Manitoba, Canada.

ID	Age	Sex	Caught	Location	Initial Mass (g)	Euthanized
2005						
WS-01	Adult		27-Jul-05	downstream creek	14.03	23-Aug-05
WS-02	Adult		27-Jul-05	downstream creek	14.61	14-Aug-05
WS-03			27-Jul-05	Tulabi Falls	died	31-Jul-05
WS-04	Adult	female	27-Jul-05	Star Lake	14.46	13-Aug-05
WS-05	Juv	female	27-Jul-05	Star Lake	17.1	13-Aug-05
WS-06	Adult	male	27-Jul-05	Star Lake	13.15	15-Aug-05
WS-07	Adult		27-Jul-05	Star Lake	14.36	23-Aug-05
WS-08	Juv	female	27-Jul-05	Star Lake	13	12-Aug-05
WS-09	Juv	female	9-Aug-05	Caddy S basin	12.36	14-Aug-05
WS-10	Adult		9-Aug-05	Caddy S basin	14.75	14-Aug-05
WS-11	Juv	male	9-Aug-05	Caddy S basin	12.15	17-Aug-05
WS-12	Adult	male	9-Aug-05	Caddy S basin	13.53	17-Aug-05
WS-13	Juv	male	9-Aug-05	Caddy S basin	12.99	19-Aug-05
WS-14	Juv	male	9-Aug-05	Caddy S basin	14.34	19-Aug-05
WS-15	Juv	male	9-Aug-05	Caddy S basin	15.79	19-Aug-05
WS-16	Adult	male	9-Aug-05	Caddy S basin	14.98	23-Aug-05
2006						
WS-17	Adult	male	30-Jun-06	Star Lake	16.5	7-Jul-06
WS-18	Juv		1-Jul-06	Nopoming	15.65	7-Jul-06
WS-19	Juv		6-Jul-06	Point du Bois	12.79	26-Jul-06
WS-20	Juv		6-Jul-06	Point du Bois	11.71	27-Jul-06
2005						
STS-01			17-Aug-05	Caddy	died	
STS-02	Juv	male	27-Aug-05	Caddy	26.5	14-Aug-05
STS-03	Adult		28-Aug-05	Fort Whyte	21.5	14-Aug-05
STS-04	Adult	female	28-Aug-05	Fort Whyte	26.32	22-Aug-05
STS-05	Adult	male	8-Sep-05	Tannis	25.76	23-Aug-05
2006						
STS-06	Juv	male	29-Jul-06	Tannis	21.65	2-Aug-06
STS-07	Adult	female	30-Jul-06	Tannis	25.91	3-Aug-06
STS-10	Juv		2-Aug-06	Caddy	19.35	7-Aug-06
STS-11	Adult		2-Aug-06	Caddy	24.57	7-Aug-06
STS-12	Adult		2-Aug-06	Caddy	17.57	7-Aug-06
STS-13	Juv		2-Aug-06	Caddy	22.73	8-Aug-06
STS-14	Juv		2-Aug-06	Caddy	21	8-Aug-06
STS-15	Adult		2-Aug-06	Caddy	24.33	8-Aug-06
STS-16	Adult		2-Aug-06	Caddy	20.52	8-Aug-06

Table A-2: Protein concentrations of muscle homogenates ('H'indlimb and 'F'orelimb) assessed using the Bradford method. Data are presented for 1:25 and 1:50 dilutions of a 1:20 muscle homogenate.

ID	dilution 1:25		(redo)	**1:25 av protein**	dilution 1:50		(redo)	**1:50 av protein**	**1:20 homog. [protein]**
WS1H	0.865	0.865		**13.05**	0.583	0.567		**6.66**	**9.85**
WS2H	0.569	0.568		**3.11**	0.507	0.49		**1.53**	**2.32**
WS4H	0.799	0.716		**9.44**	0.661	0.641	0.603	**10.68**	**10.06**
WS5H	0.668	0.675		**6.56**	0.595	0.587	0.563	**7.10**	**6.83**
WS6H	0.541	0.545		**4.28**	0.516	0.476	0.472	**4.77**	**4.53**
WS7H	0.904	0.805		**15.02**	0.612	0.606	0.604	**13.00**	**14.01**
WS8H	0.871	0.742		**13.37**	0.696	0.585	0.627	**14.98**	**14.17**
WS9H	0.709	0.717		**10.14**	0.578	0.627	0.612	**12.89**	**11.52**
WS10H	0.576	0.562		**5.18**	0.523	0.501		**6.43**	**5.80**
WS11H	0.64	0.611	0.669	**7.63**	0.549	0.53		**8.32**	**7.98**
WS12H	0.735	0.673	0.742	**10.27**	0.545	0.548		**8.81**	**9.54**
WS13H	0.624	0.627		**7.13**	0.547	0.53		**8.26**	**7.69**
WS14H	0.736	0.717		**10.61**	0.606	0.615		**13.22**	**11.92**
WS15H	0.673	0.639		**8.18**	0.594	0.549		**10.53**	**9.36**
WS16H	0.713	0.703		**9.97**	0.556	0.592		**10.70**	**10.34**
WS17H	0.724	0.706		**10.21**	0.648	0.644		**15.67**	**12.94**
WS18H	0.615	0.606		**6.61**	0.546	0.543		**8.67**	**7.64**
WS19H	0.632	0.638		**7.46**	0.569	0.556		**9.91**	**8.68**
WS20H	0.649	0.656		**8.06**	0.662	0.643		**16.12**	**12.09**
WS1F	0.707	0.667	0.652	**6.69**	0.682	0.531	0.517	**6.77**	**6.73**
WS2F	0.644	0.592		**4.77**	0.497	0.489		**1.16**	**2.96**
WS4F	0.734	0.719		**8.40**	0.608	0.616		**9.14**	**8.77**
WS5F	0.652	0.647	0.642	**5.74**	0.559	0.536	0.534	**4.51**	**5.13**
WS6F	0.542	0.544		**4.28**	0.508	0.492		**5.60**	**4.94**
WS7F	0.681	0.72	0.678	**9.46**	0.558	0.571		**10.05**	**9.75**
WS8F	0.758	0.789	0.758	**12.05**	0.743	0.682	0.608	**17.85**	**14.95**
WS9F	0.569	0.559	0.521	**4.51**	0.478	0.483		**4.26**	**4.38**
WS10F	0.71	0.692		**9.73**	0.585	0.605		**12.15**	**10.94**
WS11F	0.554	0.569		**4.92**	0.511	0.506		**6.19**	**5.55**
WS12F	0.537	0.533		**4.01**	0.503	0.498		**5.63**	**4.82**
WS13F	0.687	0.676		**9.06**	0.554	0.548		**9.12**	**9.09**
WS14F	0.657	0.658		**8.23**	0.574	0.567		**10.46**	**9.35**
WS15F	0.666	0.645		**8.16**	0.577	0.57		**10.67**	**9.42**
WS16F	0.712	0.72		**10.25**	0.592	0.576		**11.39**	**10.82**
WS17F	0.627	0.599		**6.70**	0.585	0.562		**10.67**	**8.68**
WS18F	0.654	0.629		**7.68**	0.547	0.528		**8.19**	**7.93**
WS19F	0.65	0.649		**7.96**	0.542	0.532		**8.15**	**8.05**
WS20F	0.686	0.645		**8.51**	0.545	0.556		**9.08**	**8.79**

Table A-2: Continued

ID	dilution 1:25		(redo)	**1:25 av protein**	dilution 1:50		(redo)	**1:50 av protein**	**1:20 homog. [protein]**
STS2H	0.77	0.81	0.756	**10.15**	0.589	0.604		**8.1**	**9.12**
STS3H	0.616	0.64		**5.10**					**5.10**
STS4H	0.734	0.704		**8.15**	0.598	0.602		**8.33**	**8.24**
STS5H	0.699	0.681		**7.18**	0.659	0.617		**10.88**	**9.03**
STS6H	0.695	0.704		**9.68**	0.676	0.671		**17.57**	**13.62**
STS7H	0.685	0.677		**9.04**	0.609	0.615	0.585	**12.70**	**10.87**
STS8H	0.662	0.671		**8.54**	0.538	0.548		**8.57**	**8.55**
STS9H	0.658	0.676		**8.56**	0.575	.2		**10.32**	**9.44**
STS10H	0.69	0.681		**9.20**	0.566	0.549		**9.57**	**9.38**
STS11H	0.74	0.743		**11.13**	0.623	0.557	0.611	**12.29**	**11.71**
STS12H	0.665	0.643		**8.11**	0.55	0.542		**8.77**	**8.44**
STS13H	0.67	0.65		**8.32**	0.635	0.628		**14.67**	**11.49**
STS14H	0.696	0.675		**9.20**	0.575	0.573		**10.70**	**9.95**
STS15H	0.653	0.638		**7.82**	0.549	0.553		**9.12**	**8.47**
STS16H	0.581	0.576		**5.51**	0.534	0.514		**7.26**	**6.38**
STS2F	0.555	0.518	0.648	**3.28**	0.513	0.558		**4.01**	**3.65**
STS3F	0.622	0.752	0.68	**7.00**	0.568	0.542	0.542	**5.02**	**6.01**
STS4F	0.701	0.757		**8.49**	0.503	0.518		**2.33**	**5.41**
STS5F	0.677	0.757		**8.09**	0.628	0.567		**8.16**	**8.13**
STS6F	0.617	0.619		**6.87**	0.533	0.535		**7.94**	**7.41**
STS7F	0.651	0.687		**8.63**	0.64	0.631		**14.94**	**11.79**
STS8F	0.664	0.662		**8.42**	0.601	0.594		**12.32**	**10.37**
STS9F	0.739	0.776		**11.68**	0.708	0.654	0.701	**18.54**	**15.11**
STS10F	0.656	0.629		**7.71**	0.552	0.531		**8.46**	**8.09**
STS11F	0.701	0.67		**9.20**	0.594	0.6		**12.29**	**10.74**
STS12F	0.653	0.652		**8.06**	0.587	0.566		**10.88**	**9.47**
STS13F	0.657	0.655		**8.18**	0.58	0.58		**11.12**	**9.65**
STS14F	0.578	0.573		**5.40**	0.515	0.517		**6.70**	**6.05**
STS15F	0.688	0.649		**8.61**	0.569	0.563		**10.15**	**9.38**
STS16F	0.634	0.624		**7.25**	0.508	0.534		**7.05**	**7.15**

Table A-3: Histology data collected from the gracilis of water shrews and short-tailed shrews, sectioned at 7-9 µm. The data are presented over a consistent size of the viewing field, and include number of cells and average size, size of the extracellular space (ECS), percent collagen area, as well as area occupied by the types of collagen. Ratios are presented for the areas occupied by collagen and muscle, as well as collagen subtypes. The percentage of myocyte identified by TUNEL as having any apoptotic nuclei is also presented.

ID	Cells	av. cell size	ECS	% area	collagen: muscle	Type I area	Type III area	I: III	apoptotic myocytes
		μm^2	μm^2			μm^2	μm^2		%
WS 01	41	1876	66932	15.6	348.0	28737	3452	8.3	0.48
WS 02	116	731	59080	12.5	718.9	30368	11489	2.6	0.20
WS 04	81	959	66199	32.3	1413.6	13700	5260	2.6	0.50
WS 05	139	770	36848	12.6	684.5				0.20
WS 06	97	1006	46265	20.7	864.7	25596	3152	8.1	0.47
WS 07	98	706	74686	21.4	1271.7	12196	7086	1.7	0.44
WS 08	150	638	48120	11.3	742.4	26907	15539	1.7	0.00
WS 09	96	1050	43036	22.6	901.8	36007	15876	2.3	0.48
WS 10	101	603	82971	10.3	717.4	27130	6367	4.3	0.11
WS 11	112	683	67374	11.0	678.8	22823	12502	1.8	0.36
WS 12	90	877	64929	24.4	1169.2	29299	9074	3.2	0.55
WS 13	130	695	53470	14.6	882.1	28148	13453	2.1	0.33
WS 14	104	730	67946	10.9	629.3				0.13
WS 15	106	815	57487	8.4	434.1	28089	13752	2.0	0.00
WS 16	99	1024	42455	27.8	1139.3	25389	11084	2.3	0.07
WS 17	68	1548	38610	16.7	453.5	16605	3100	5.4	0.97
WS 18	88	985	57150	9.8	419.2	17817	11392	1.6	0.80
WS 19	109	695	68040	13.9	838.3	27062	13052	2.1	0.00
WS 20	80	1233	45197	8.0	272.6	21568	13151	1.6	0.00
STS 02	113	731	61276	18.4	1056.2	42558	9606	4.4	0.17
STS 04	157	558	56190	24.7	1857.2	38764	8480	4.6	0.00
STS 05	91	840	67412	11.0	548.6	26908	7566	3.6	0.00
STS 06	102	789	63357	18.0	955.4	26680	11830	2.3	0.13
STS 07	112	580	78918	19.6	1417.2	36598	11918	3.1	0.10
STS 08	122	870	37718	14.5	696.8	43083	20561	2.1	0.87
STS 09	146	737	36242	7.4	421.6	20393	13279	1.5	0.00
STS 10	132	667	55758	6.3	399.1	13640	15587	0.9	0.07
STS 11	142	524	69441	18.1	1452.5	39175	4007	9.8	0.50
STS 14	130	888	28435	15.6	736.1	21186	8076	2.6	0.04
STS 15	106	657	74164.1	18.0	1151.2	33010	8979	3.7	0.20

Table A-4: Biochemistry of muscle homogenates collected from water shrews and short-tailed shrews. Activities were measured for the enzymes citrate synthase (CS), catalase (CAT) and glutathione Peroxidase (GPx). Oxidation of the fluorescent probe dihydroethidium (DHE) was also measured, along with total hydroperoxides (FOX assay) and an ELISA to detect apoptotic cell death.

ID	CS	CAT	GPx	DHE	FOX	ELISA
WS1H	36.22		8.04	68.02	33.89	
WS2H	15.61		14.27		24.15	
WS4H	27.89	30.78	8.44	86.19	20.95	22.9
WS5H	27.22	8.00	12.06	140.35	10.61	
WS6H	18.59	42.49	11.35	89.24	15.61	
WS7H	36.93	8.28	6.53		7.07	21
WS8H	32.43	23.55	6.73	89.06	3.60	18.8
WS9H	34.55	5.91	7.94	70.41	5.87	8.5
WS10H	13.17	46.40	10.81	67.54	7.14	
WS11H	28.44			119.23	4.07	
WS12H					10.91	
WS13H			4.52	59.41	8.61	23.9
WS14H	36.09	26.56	10.75		4.80	19.8
WS15H	24.26	26.80	4.22	125.49	4.67	25.9
WS16H	36.42	22.86	3.82	64.19	8.27	18.5
WS17H	41.63	6.60	9.24	136.13	13.61	21.7
WS18H	32.68	9.27	6.43	121.80	11.87	23.1
WS19H	34.49	7.36	8.04		8.41	22
WS20H	42.08		4.82		8.27	18.7
WS1F	31.87	7.33	9.65	58.93	5.60	0.4
WS2F	16.66		16.68		23.61	0.1
WS4F	33.11			54.14	31.62	
WS5F				62.28	17.61	
WS6F	15.06		11.76	96.02	18.14	0.2
WS7F	35.06		7.74	86.67	25.22	1
WS8F		13.59		69.93	27.62	0.2
WS9F	20.03				5.74	
WS10F				97.74	13.88	
WS11F	22.33	13.73	9.14	58.93	2.67	
WS12F	18.47	19.14			12.27	
WS13F			10.45	49.36	12.41	
WS14F	35.90		7.34	88.58	27.75	9.8
WS15F	31.98		6.23	89.06	8.81	5.7
WS16F	37.32		5.43	91.93	16.01	16.2
WS17F	32.10		2.41	165.75	20.55	13.9
WS18F	32.81		6.43		10.94	19.4
WS19F	34.42	9.50	8.04	145.17	13.34	21.4
WS20F	38.80	9.03	7.44	161.58	22.95	14.1

Table A-4: Continued

ID	CS	CAT	GPx	DHE	FOX	ELISA
STS2H	40.93	26.57	43.81	211.76	16.28	25
STS3H	16.86	6.13	26.73		27.62	23.2
STS4H	33.73	24.69	39.79	143.22	14.94	17.9
STS5H	35.19	25.73	30.35	70.90	42.56	22.5
STS6H	41.76	7.54	28.54	173.35	20.15	17.9
STS7H	45.94	14.45	30.35	166.58	13.34	19.3
STS8H	43.81	7.34	27.13	161.47	7.34	21.2
STS9H	51.99		27.33	181.29	8.54	23.5
STS10H	51.92	6.20	23.11		15.08	20.7
STS11H	47.80	7.11	22.91		12.81	18.3
STS12H	46.39	8.53	29.94	123.92	6.27	19.5
STS13H	52.56	6.09	23.31		12.67	
STS14H	44.91		25.92	170.34	17.88	
STS15H	44.39		37.38	151.04	20.68	21.3
STS16H		9.59	23.40	136.54	12.07	
STS2F	47.82		41.80	114.80	28.02	
STS3F	42.55			56.06	17.88	
STS4F	36.37			103.41	20.35	
STS5F	32.81	6.65	24.52	139.40	46.96	16.8
STS6F	34.55		28.94	138.21	35.89	18
STS7F	50.25	6.45	29.54		27.75	19.8
STS8F	46.90	8.89	30.55		16.81	23.3
STS9F	32.68	5.30	30.55	153.65	11.07	19.1
STS10F	51.92	8.46	16.68		13.88	19.3
STS11F	49.80		28.54	173.99	13.74	20.5
STS12F	47.48	7.93	29.94	139.05	16.01	
STS13F	49.24	6.95	23.31	181.29	11.34	19.7
STS14F	44.91	9.10	25.92		12.41	
STS15F	46.39	9.27	33.16	153.65	15.21	18.2
STS16F	42.21		32.96	156.57	12.94	20.1

Table A-5: Relative protein contents collected from Western blots of superoxide dismutase (CuZn SOD, Mn SOD) and 4-hydroxynenal (4-HNE) conducted for water shrews and short-tailed shrews.

ID	CuZn SOD	Mn SOD	4-HNE	CuZn SOD	Mn SOD	4-HNE
		Hindlimb			***Forelimb***	
WS1		35.2	11.5	53.6	17.5	12.6
WS2	134.0		11.2		18.8	
WS4		25.6	10.4	46.0	12.8	10.6
WS5	15.7		16.2	43.2	24.1	7.7
WS6		31.1			27.2	
WS7	66.2	14.2	9.4	141.5	9.4	5.3
WS8			9.1	40.0	27.8	
WS9	31.6	25.5	14.0	44.5	26.5	9.8
WS10	46.8	48.5	6.6	41.5	20.6	5.0
WS11	29.4	19.9	13.5	38.2	20.7	10.5
WS12		42.4	10.3			20.1
WS13	69.7	36.5	35.5	64.4	22.0	10.0
WS14	49.1	14.7	12.0	45.4	33.3	7.3
WS15	34.6	30.6	10.1	41.3	18.4	6.1
WS16	94.4	41.6			18.7	10.7
WS17	76.6	55.3			12.9	10.9
WS18		22.1	14.2	106.3		8.7
WS19		24.1			22.9	
WS20		28.9	15.3	49.9		10.8
STS2	23.1	38.3	14.3	48.6	46.6	28.2
STS3		22.1	15.3	49.5	34.2	23.1
STS4	27.5	7.1	10.7	23.4	10.7	19.3
STS5	62.3	11.4	11.6	53.1	39.8	17.6
STS6	56.2			84.7		21.1
STS7	120.8	21.2	13.5	103.1	43.0	15.5
STS8	46.5	26.1	24.7	62.9	18.1	35.3
STS9	86.8	27.2	18.2	72.2	12.2	12.3
STS10	25.2	17.8	32.1	74.7	30.0	10.2
STS11	104.4	48.4	22.3	62.9	11.7	14.2
STS12	54.6	28.3	15.8	101.9	20.0	16.4
STS13	84.6	41.3	24.8	22.1	8.0	13.0
STS14	21.3		18.6	56.9		19.1
STS15		15.8	17.9	81.1	24.2	17.8
STS16	168.5		10.8	61.7		37.0

VITA

Name: Allyson Gayle Hindle

Address: Marine Biology Department, Texas A&M University at Galveston, 5007 Avenue U, Galveston, TX, 77551

Email address: allyson.hindle@gmail.com

Education: B.S. (Hons.) Zoology, University of Manitoba, Winnipeg, 2000.
M.S. Zoology, University of Manitoba, Winnipeg, 2002.
Ph.D. Wildlife and Fisheries Sciences, Texas A&M University, 2007.